

Targeting Undruggable Oncoprotein Epitopes with Protein Catalyzed Capture Agents

Thesis by
Ryan Kenneth Henning

In Partial Fulfillment of the Requirements for
the degree of
Doctor of Philosophy

The logo for the California Institute of Technology (Caltech), featuring the word "Caltech" in a bold, orange, sans-serif font.

CALIFORNIA INSTITUTE OF TECHNOLOGY
Pasadena, California

2017
(Defended June 13, 2016)

© 2016

Ryan Kenneth Henning
ORCID: 0000-0002-3783-2455

ACKNOWLEDGEMENTS

I would like to start by thanking my advisor, Prof. Jim Heath, for taking me into his group. I am extremely grateful for the opportunities I had to work on such amazing projects throughout my graduate career. Jim, you are phenomenal at identifying interesting problems and addressing them in new and creative ways. It is truly inspiring to have been in such a vibrant scientific atmosphere and I am certain that I am leaving as a better scientist than when I arrived. And of course thanks for being such a great provider!

I must also thank the members of my thesis committee. I could not have asked for a better committee chair than Prof. David Tirrell. You were always extremely thoughtful and supportive during my committee meetings. I also thank you for the encouragement and support when I attempted to use BONCAT early on in my project. That taught me not to shy away from trying to combine different technologies or do new things. I thank Prof. Ray Deshaies for teaching me about PROTACs. I still think that is one of the coolest concepts in science today and it wouldn't exist if not for you. I was also inspired during all of our discussions to see how much you truly love science. I thank Prof. Andre Hoelz for being a constant source of energy and excitement. Thank you for allowing me to work in your lab and squeeze in on the Aktas! I'm glad I had a front row seat to watch the science unfold in your group. I'm also glad you were the first Caltech professor I met!

Next I have to thank the past and present members of the Heath lab. A special thanks to the capture agent folks who were great friends and colleagues over the years. Thanks to Dr. Steve Millward for taking me under his wing when I first joined the lab. I have to thank Dr. Samir

Das and Dr. Arundhati Nag for being such great mentors to me and everyone else in the subgroup. Joey Varghese was always a great colleague, collaborator, and friend. Thanks for being so patient with me in the early days of when I was still getting the hang of things. I also want to extend a big thanks to Dr. Jessica Pfeilsticker, Dr. Kaycie Deyle, Dr. Aiko Umeda, Blake Farrow, JingXin Liang, Dr. David Bunck, Dr. Ashwin Ram, Amy McCarthy, and Baoqing Zhou for all the whiskey hours, happy hours, coffee breaks and other fun times we had together.

I am similarly indebted to those in the others subgroups as well. Dr. Alex Sutherland, Dr. Young Shik Shin, Dr. Peter Agbo, Dr. Ann Cheung, Marilena Dimotsantou, Dr. Suresh Poovathingal – you are all great friends and colleagues who have helped me get through grad school and life in more ways than you know. And to all the others - Dr. Habib Ahmad, Dr. John Nagarah, Dr. Kiwook Hwang, Dr. Jing Zhou, Dr. Jing Yu, Dr. Min Xue, Dr. Jun Wang, Dr. Nataly Kravchenko-Balasha, Dr. Jen-kan Yu, Dr. Slobodan Mitrovic, Dr. Alex Xu, Jungwoo Kim, Elizabeth Holman Yapeng Su – you’ve all influenced me for the better in one way or another and for that I thank you.

I also want to give a shout out to all the awesome summer students I worked with over the years – Grace Tang, Kevin Tang, Erica Leung, Mary Boyajian, Rachel Ng, Joseph Oh, Emma Winson, and John Heath – you all helped make each summer fun and exciting for me and I wish you the best with the bright futures you have ahead of you. And last but not least from the lab I’d like to thank Elyse Garlock, Katrine Museth, and Kevin Kan for going above and beyond to make the lab a better place for all of us.

Finally I would like to thank my life-long friends and family. Mark and Jayne Hitman, thank you for the immovable love and support you've had for me for so long. Dan Krauth, thanks for being a brother to me for all these years. Johnny Goodman, thanks for all the good times. Dr. Minshu Yu, thanks for being my sensei. Dr. Geoffrey Kim, I'll never forget our fun times in lab. Jason and Jonathan Cole, you guys are the best cousins I could have ever dreamed. And to my parents and siblings, Loxley, Irma, Jenny, Kathy and Sean, I love you guys, thanks for everything and I hope I've made you guys proud. Lastly, I have to thank Sophia for being my favorite niece ever!

ABSTRACT

The protein catalyzed capture (PCC) agent platform provides a new strategy to develop peptide-based ligands for difficult protein targets. This approach utilizes the target-guided *in situ* click reaction to allow the protein of interest to assemble its own binder. Developing a PCC agent begins with an epitope targeting strategy to develop anchor candidates against a specific region of interest on the target protein. This approach has been used to target diverse epitopes including unstructured hydrophobic regions, allosteric enzyme sites, and single amino acid point mutations. The process can then be iterated to expand a monoligand into a multiligand binder with affinity and selectivity that rivals monoclonal antibodies.

One disease-associated protein of particular importance is the serine/threonine kinase Akt. Akt is a key regulator of signal transduction pathways and is implicated in many disease such as cancer, diabetes, and neurodegeneration. Several ligands for Akt have been developed recently with the PCC agent screening approach. PCC agents now exist that can alter Akt enzymatic activity, detect its position in the cell, identify mutations within the protein, and even cause its destruction within the cell. The first part of this thesis summarizes the prior efforts to develop PCC agents against Akt and then describes new applications for these reagents while the latter part describes efforts to develop new PCC agents against another interesting target.

Chapter 1 provides a summary of the technology and describes how it has been utilized thus far. Chapter 2 describes how a PCC agent was used as an imaging probe capable of detecting Akt membrane localization. Chapter 3 provides several examples of the modularity of PCC agents and demonstrates how they can be used to influence a target protein in cells. A pair of allosteric

Akt modulators were functionalized with a cell penetrating peptide for cellular delivery and were subsequently used to activate or inhibit Akt enzymatic activity. PCC agents can also be used as a targeting moiety to deliver a specific signal to a protein. When functionalized with a degradation tag the Akt-binding capture agents caused the protein to be degraded. This provides another demonstration of the usefulness of Proteolysis Targeting Chimeric Molecules, or PROTACs, in destroying disease-associated proteins. Finally, Chapter 4 describes the development of PCC agents against the oncoprotein K-Ras^{G12D} and how these molecules can be used to target this protein in new ways.

PUBLISHED CONTENT AND CONTRIBUTIONS

- (1) Millward, S.W., Henning, R.K., Kwong, G.A., Pitram, S., Agnew, H.D., Deyle, K.M., Nag, A., Hein, J., Lee, S.S., Lim, J., et al. (2011). Iterative in Situ Click Chemistry Assembles a Branched Capture Agent and Allosteric Inhibitor for Akt1. *J. Am. Chem. Soc.* *133*, 18280–18288. doi: 10.1021/ja2064389.

This study was conceived of and primarily led by Dr. Steven Millward. All authors contributed to designing experiments, conducting experiments, analyzing the data, and/or writing the manuscript. Ryan Henning conceived of the imaging experiments, synthesized the necessary compounds, performed the experiments, acquired the data, analyzed the data, and contributed to writing the manuscript.

- (2) Henning, R.K., Varghese, J.O., Das, S., Nag, A., Tang, G., Tang, K., Sutherland, A.M., and Heath, J.R. (2016). Degradation of Akt using protein-catalyzed capture agents. *J. Pept. Sci.* *22*, 196–200. doi: 10.1002/psc.2858.

This study was conceived of and led jointly by Ryan Henning and Dr. Joseph Varghese. All authors contributed to designing experiments, conducting experiments, analyzing the data, and/or writing the manuscript. Ryan Henning contributed to the synthesis, purification, and characterization of the compounds reported here. Ryan also conducted several of the experiments, analyzed the data, and co-wrote the manuscript.

TABLE OF CONTENTS

Acknowledgements.....	iii
Abstract	vi
Published Content and Contributions.....	viii
Table of Contents.....	ix
List of Figures	x
List of Tables	xii
Nomenclature.....	xiii
Chapter I: Protein Catalyzed Capture as an Alternative Strategy for Developing Diagnostic and Therapeutic Reagents.....	1
1.1 Introduction	1
1.2 Protein Catalyzed Capture Agents	4
1.3 References	9
Chapter II: Protein Catalyzed Capture Agents as Imaging Probes to Visualize Akt Subcellular Localization	12
2.1 Summary of Contributions.....	12
2.2 Introduction	13
2.3 Results and Discussion	15
2.4 Conclusion	16
2.5 Materials and Methods	16
2.6 Figures	20
2.7 References	24
Chapter III: Activation, Inhibition and Degradation of Akt.....	26
3.1 Summary of Contributions.....	26
3.2 Introduction	27
3.3 Results and Discussion.....	28
3.4 Conclusion	32
3.5 Materials and Methods.....	32
3.6 Figures	42
3.7 References	53
Chapter IV: Discovery of the First Selective Ligands Against the Mutant Oncoprotein K-Ras ^{G12D}	58
4.1 Summary of Contributions.....	58
4.2 Introduction	59
4.3 Results and Discussion.....	60
4.4 Conclusion	64
4.5 Materials and Methods.....	65
4.6 Figures	73
4.7 References	87
Appendix A: Supplementary Information for Chapter 4.....	89

LIST OF FIGURES

<i>Number</i>	<i>Page</i>
2.1	Chemical structure of fluorescent Akt biligand 20
2.2	Imaging Akt membrane localization with fluorescent biligand..... 21
2.3	Structure of fluorescent Akt triligand 22
2.4	Imaging Akt with fluorescent triligand PCC agent..... 23
3.1	Exploiting the modularity of Akt-activating PCC agent tri_a 42
3.2	tri_a activates Akt in cells 43
3.3	Structure of Akt-inhibiting CPP-tri_i 44
3.4	CPP-tri_i inhibits Akt in cells 45
3.5	PCC agent-induced degradation of Akt..... 46
3.6	Structure of CPP-tri_a 47
3.7	Structure of CPP-tri_a-FL 48
3.8	Structure of CPP-tri_a-PR..... 49
3.9	Structure of CPP-tri_i-PR 50
3.10	Reaction scheme for synthesizing cyclooctyne-containing tri_i 51
3.11	Reaction scheme for synthesizing CPP-tri_i 52
4.1	Structure of K-Ras synthetic epitopes 73
4.2	Structure of the macrocyclic peptide library 74
4.3	Layout of the K-Ras epitope-targeted PCC agent screen 75
4.4	Single point ELISA of hit peptides against K-Ras ^{G12D} 77
4.5	Characterization of hit 7b1 78
4.6	Single point ELISA of second generation hits against K-Ras ^{G12D} 80
4.7	Characterization of hit 7b10..... 81
4.8	7b10 alanine scan 82
4.9	Characterization of hit 7b5..... 83
4.10	Structure of 7b5-Hif PROTAC 84
4.11	Structure of 7b5-Hif-TAT PROTAC..... 85

4.12	7b5 PROTACs induce proteasomal degradation of K-Ras ^{G12D}	86
A1	Structure and characterization of wild type K-Ras fragment.....	90
A2	Structure and characterization of G12D K-Ras fragment.....	91
A3	Structure and characterization of hit 1: NDETY	92
A4	Structure and characterization of hit 2: PSEEG	93
A5	Structure and characterization of hit 3: SEEGG	94
A6	Structure and characterization of hit 5: YEQGE.....	95
A7	Structure and characterization of hit 6: YGEQE.....	96
A8	Structure and characterization of hit 7: LRGDR.....	97
A9	Structure and characterization of hit 8: QEKPP.....	98
A10	Structure and characterization of hit 9: ELTFG.....	99
A11	Structure and characterization of peptide 7b1	100
A12	Structure and characterization of peptide 7b2	101
A13	Structure and characterization of peptide 7b3	102
A14	Structure and characterization of peptide 7b4	103
A15	Structure and characterization of peptide 7b5	104
A16	Structure and characterization of peptide 7b6	105
A17	Structure and characterization of peptide 7b7	106
A18	Structure and characterization of peptide 7b8	107
A19	Structure and characterization of peptide 7b9	108
A20	Structure and characterization of peptide 7b10.....	109
A21	Structure and characterization of peptide 7b11.....	110
A22	Structure and characterization of peptide 7b12.....	111

LIST OF TABLES

<i>Number</i>		<i>Page</i>
4.1	Hit sequences from K-Ras ^{G12D} epitope-targeted anchor screen.....	76
4.2	Sequence of second generation hits designed from hit 7b1	79

NOMENCLATURE

Ahx. 6-aminohexanoic acid

Az4. L-azidolysine

CPP. Cell penetrating peptide

DIEA. N,N-Diisopropylethylamine

EGF. Epidermal growth factor

ELISA. Enzyme-linked immunosorbent assay

Gnf. 4-guanidine phenylalanine

HPLC. High Performance Liquid Chromatography

ICC. Immunocytochemical

MALDI-TOF MS. Matrix-assisted laser desorption/ionization time-of-flight mass spectrometry

OBOC. One-bead-one-compound

PCC. Protein catalyzed capture

PEG. Polyethylene glycol

PHD. Pleckstrin homology domain

PIP3. Phosphatidylinositol (3,4,5)-trisphosphate

Pra. Propargylglycine

PROTAC. Proteolysis targeting chimeric molecule

SPPS. Solid phase peptide synthesis

SynEp. Synthetic epitope

Chapter 1

PROTEIN CATALYZED CAPTURE AGENTS AS AN ALTERNATIVE PLATFORM FOR DEVELOPING DIAGNOSTICS AND THERAPEUTIC REAGENTS

1.1 Introduction

There is a great need to develop high-affinity protein binding reagents. As proteins serve as the functional output of the genetic code it is crucial that new ligands are developed to advance our basic understanding of biological processes. Development of such ligands can help elucidate protein functions, diagnose disease, and develop novel therapeutics. Such efforts are thus necessary to continue advancing the field of personalized medicine.

The current standard reagents for protein binding assays are antibodies.¹ Antibodies are large, typically 150 kDa, Y-shaped proteins that are normally created by the immune system to help combat disease.² Researchers have used antibodies as tools for studying proteins for several decades. Antibodies have also proven useful as diagnostic reagents for detecting biomarkers such as human chorionic gonadotropin (hCG) in home pregnancy tests or the cancer-associated antigen Prostate-specific antigen (PSA).³ Additionally, antibodies are also a very useful class of therapeutic molecules to treat disease. For instance, the anti-inflammatory medication Humira is a monoclonal antibody against the pro-inflammatory signal TNF alpha and this molecule is used to treat myriad autoimmune diseases.⁴ However, while antibodies have become invaluable tools for basic research, diagnostics, and therapeutics, they do have several limitations that include lack of

reproducibility, instability, and poor bioavailability. Antibodies often suffer from batch to batch variability due to the biological nature of their production.⁵ They are often produced in immunized animals and the same animal will produce multiple antibodies against the same antigen. Complicating matters further is the fact that the same animal will produce different mixtures of antibodies after each immunization with the same antigen. In addition, if an antibody source, whether an animal or cell line, is lost then the corresponding antibody will also be difficult to reproduce — because research antibodies are often poorly characterized it is more likely that the antibody will be lost forever.⁶ Moreover, antibodies can also suffer from instability. As with any protein, antibodies are subject to thermal denaturation, aggregation, and proteolytic degradation.⁷ Therapeutic antibodies are also known to be susceptible to oxidation which can abrogate the desired binding properties and effectiveness of the treatment.⁸ Finally, due to their relatively large size therapeutic antibodies are thought to be limited to extracellular targets.⁹ While therapeutic antibodies have been very successful against soluble proteins and extracellular membrane receptors a large number of important therapeutic targets are intracellular proteins that are inaccessible to this type of drug – membrane and secreted proteins only account for about one third of the approximately 20,000 proteins in the human proteome.¹⁰ While antibodies are immensely useful for basic research, diagnostics, and therapeutics, complementary methods are still needed to develop protein-binding reagents.

Another useful class of reagents for studying and perturbing protein functions are small molecules. Small molecules are low molecular weight (typically <500 daltons) organic compounds that often have interesting biological properties. Small molecules are widely

used to modulate protein function through either activation or inhibition of the enzymatic activity of specific target proteins.¹¹ These compounds can thus have dramatic effects on biological systems, depending on the protein target. By enabling the specific activation or inhibition of a given target small molecules can be useful probes for elucidating enzyme functions in cells.¹¹ In addition, the relatively small size and hydrophobicity of many small molecules enable diffusion across biological membranes to reach intracellular targets — small molecules thus make up the majority of drugs.¹² However, while small molecules have been developed against myriad enzymes they are typically limited to this class of protein, yet enzymes only represent a small portion of the proteome. They are often restricted to binding in small hydrophobic pockets of proteins and these pockets are most often found in enzymes where a substrate will bind prior to its transformation. Small molecule inhibitors can therefore outcompete the natural substrate for the active site and inhibit the enzyme's catalytic activity.¹³ It has proven difficult to target non-enzymatic disease-associated targets such as transcription factors or protein-protein interactions because these proteins often lack hydrophobic pockets for small molecules to bind.¹⁴ Therefore, targeting certain disease-associated targets will require alternative approaches to both antibodies and small molecules.

While antibodies and small molecules differ in their chemical properties and uses, one class of molecule that can potentially combine the advantageous properties of these two groups is peptides.¹⁵ Antibodies are very useful because of their relatively high affinity and specificity for their corresponding antigen. While antibodies are 150 kDa macromolecules only a small portion of the structure is responsible for antigen recognition. The majority of

diversity found in an antibody variable regions is located in the single CDR-H3 loop,¹⁶ and the average size of this loop is 15 amino acid residues¹⁷ – peptides thus represent promising antibody replacements. Additionally, peptides also have similarities to small molecules. The major strength of small molecules (bioavailability) is thought to arise in large part from their size and peptides can also be small enough to diffuse into cells and tissues. Indeed, over 60 therapeutic peptides have been approved to date with approximately 140 additional peptide drugs in clinical trials.¹⁸ The recent success of peptide medicines demonstrates that these molecules can potentially combine the favorable properties of antibodies and small molecules to develop new probes, diagnostics, and therapeutic reagents. One emerging class of useful peptides is protein catalyzed capture agents, which will be the focus of this thesis.

1.2 Protein Catalyzed Capture Agents

Protein catalyzed capture (PCC) agent technology is an emerging screening platform that enables the identification of high-affinity peptide ligands against a protein of interest. The screening approach is based on the iterative *in situ* click chemistry reaction that allows a target of interest to identify its own high-affinity, multiligand binder.

A key component of this screening platform is the *in situ* click reaction between an azide and alkyne. This reaction was first developed by the Sharpless group as a target-guided method to identify potent, small molecule enzyme inhibitors.¹⁹ In their initial study the Sharpless group identified a small molecule inhibitor that could be divided into two fragments and each fragment was expanded into a small molecule library – one library was

functionalized with an azide and the other with an alkyne. Both libraries were then simultaneously incubated with the target protein and only the library elements that bound the protein adjacent to one another in the proper orientation could undergo the Huisgen 1,3-dipolar cycloaddition reaction to create a new inhibitor. The resulting inhibitor was more potent than either library element alone. The protein thus serves as a scaffold to properly align the molecules and assemble its own “best fit” inhibitor.

In the Heath group at Caltech we have been working to generalize the *in situ* click screening approach and have made several improvements. First, a novel one-bead-one-compound macrocyclic peptide library that presents either an azide or alkyne has been developed.²⁰ The library is easily synthesized via solid phase peptide synthesis using standard methods. The synthesis begins by making the linear library consisting of Pra-X₁X₂X₃X₄X₅-Az4 (where Pra = Propargylglycine and Az4 = Azidolysine) followed by a copper catalyzed azide-alkyne cycloaddition to close the macrocycle through the Pra and Az4 side chains. The variable region, X₁-X₅, is composed of the 18 naturally occurring amino acids (excluding Cys and Met) and yields more than 1.8x10⁶ possible sequences. Unnatural amino acids can also be incorporated into the library increasing the potential diversity even more. The variable region is also sequenceable by Edman degradation. This allows facile identification of hit sequences.

Secondly, our PCC agent screening platform utilizes a chemical epitope targeting strategy to home in on a specific region of the protein of interest.^{21,22} The epitope of interest can be chemically synthesized with the addition of a Pra or Az4 click group and a biotin affinity

handle. This new synthetic epitope (SynEp) can then be screened against a macrocyclic library containing the opposite click group and hit sequences are identified with a streptavidin-reporter conjugate. Only the library peptides that bind to the SynEp will undergo the click reaction. While most small molecule probes are limited to targeting hydrophobic binding pockets, our epitope targeting strategy allows us to potentially target any site on a protein surface. Thus far we have targeted unstructured hydrophobic regions,²¹ single amino acid point mutations,²² and allosteric enzymatic sites.²³

Additionally, a third major advance has been to iterate the *in situ* click screens to develop multiligand binders that are much improved over monoligands.^{23,24} After the initial epitope targeting screen the hit sequences are tested for binding to the full-length protein. After multiple rounds of binding assays a consensus sequence, typically called the anchor peptide, is chosen to improve upon with subsequent screens. As with the SynEp in the anchor screen, the anchor peptide is synthesized with a click group and biotin handle and incubated with the target protein in the presence of a library. Similar to the original *in situ* click study, the click reaction is catalyzed by the formation of a ternary complex between the anchor peptide, target protein, and the appropriate library element. The hit secondary ligands can then be combined with the anchor peptide to provide a series of biligand candidates. Typically, the biligands will show increased affinity and selectivity for the target protein compared to the anchor peptide. Once a consensus biligand is identified after multiple rounds testing the process can be iterated once again to develop a triligand peptide with further improved binding properties. These major advances have greatly improved the

in situ click screening approach and provide a promising strategy for the development of high-affinity protein ligands.

The subsequent chapters of this thesis will describe the development of PCC agents against cancer-associated targets and new applications of this technology. One target of particular interest is the human protein Akt. Akt is a serine/threonine protein kinase with three closely related isoforms (Akt1-3) and is involved in cellular processes such as glucose metabolism, apoptosis, and cell proliferation.^{25,26} Aberrant Akt signaling is implicated in diabetes and in many cancers, making it an attractive drug and diagnostic target.²⁷ This protein was thus chosen as a model target for PCC agent platform development. Several PCC agents were developed against the various domains of Akt – including the kinase domain, pleckstrin homology domain and the C-terminal hydrophobic motif – and the screening platform was greatly improved in the process. Chapter 2 describes the use of Akt-targeted PCC agents as antibody replacements in immunofluorescent imaging experiments. Akt is known to localize to the cell membrane upon cell stimulation and fluorescent PCC agents were able to visualize the membrane localization. A second set of PCC agents developed against the C-terminal domain of Akt demonstrated allosteric activation and inhibition of the protein's enzymatic activity. Chapter 3 describes the functionalization of the allosteric Akt modulators with a cell penetrating peptide for cellular uptake in order to control Akt's enzymatic activity in live cells.

Also in Chapter 3 is the introduction of chemical degradation tags to PCC agents. An exciting new paradigm in drug discovery is the ability to induce protein degradation with

proteolysis targeting chimeric molecules, or PROTACs. A PROTAC is a heterobifunctional molecule that can form a ternary complex between a target protein and an E3 ubiquitin ligase by covalently linking existing ligands for each.²⁸ When added to cells the PROTAC-induced association of the target protein with the E3 ligase results in ubiquitination and degradation of the target. The C-terminal Akt PCC agents were functionalized with a degradation tag and shown to induce degradation of Akt in cells.

Another exciting advance in PCC agent technology is the ability to target single amino acid point mutations on protein surfaces. Genetic mutation is often a key step in tumorigenesis, and selectively inhibiting the resultant mutant proteins is an attractive therapeutic strategy. The Akt1 gene was found to have a single point mutation (glutamic acid to lysine at position 17) in certain types of cancers.²⁹ The E17K mutation of Akt is found in the pleckstrin homology domain and activates the protein by increasing its membrane association and thus activating the downstream signaling pathway. The PCC agent epitope targeting strategy was recently used to develop a capture agent that was selective for the oncogenic mutation and could inhibit Akt membrane localization. This new strategy opens the possibility of targeting other mutated oncoproteins. The oncoprotein K-Ras is another attractive target that is known to be a major driver in many human cancers. Finally, Chapter 4 of this thesis details efforts to target the oncoprotein K-Ras^{G12D} with the PCC agent screening platform.

1.3 References

1. Binz, H. K. & Plückthun, A. Engineered proteins as specific binding reagents. *Curr. Opin. Biotechnol.* **16**, 459–469 (2005).
2. Woof, J. M. & Burton, D. R. Human antibody–Fc receptor interactions illuminated by crystal structures. *Nat. Rev. Immunol.* **4**, 89–99 (2004).
3. Stenman, U.-H. Biomarker development, from bench to bedside. *Crit. Rev. Clin. Lab. Sci.* **53**, 69–86 (2016).
4. Lapadula, G. *et al.* Adalimumab in the treatment of immune-mediated diseases. *Int. J. Immunopathol. Pharmacol.* **27**, 33–48 (2014).
5. Marx, V. Finding the right antibody for the job. *Nat. Methods* **10**, 703–707 (2013).
6. Bradbury, A. & Plückthun, A. Reproducibility: Standardize antibodies used in research. *Nature* **518**, 27–29 (2015).
7. Wang, W., Singh, S., Zeng, D. L., King, K. & Nema, S. Antibody structure, instability, and formulation. *J. Pharm. Sci.* **96**, 1–26 (2007).
8. Torosantucci, R., Schöneich, C. & Jiskoot, W. Oxidation of therapeutic proteins and peptides: structural and biological consequences. *Pharm. Res.* **31**, 541–553 (2014).
9. Baker, M. Upping the ante on antibodies. *Nat. Biotechnol.* **23**, 1065–1072 (2005).
10. Uhlén, M. *et al.* Tissue-based map of the human proteome. *Science* **347**, 1260419 (2015).
11. Schreiber, S. L. *et al.* Advancing Biological Understanding and Therapeutics Discovery with Small-Molecule Probes. *Cell* **161**, 1252–1265 (2015).

12. Lipinski, C. A., Lombardo, F., Dominy, B. W. & Feeney, P. J. Experimental and computational approaches to estimate solubility and permeability in drug discovery and development settings. *Adv. Drug Deliv. Rev.* **23**, 3–25 (1997).
13. Hopkins, A. L. & Groom, C. R. The druggable genome. *Nat. Rev. Drug Discov.* **1**, 727–730 (2002).
14. Johnson, D. K. & Karanicolas, J. Druggable Protein Interaction Sites Are More Predisposed to Surface Pocket Formation than the Rest of the Protein Surface. *PLOS Comput Biol* **9**, e1002951 (2013).
15. Craik, D. J., Fairlie, D. P., Liras, S. & Price, D. The Future of Peptide-based Drugs. *Chem. Biol. Drug Des.* **81**, 136–147 (2013).
16. Xu, J. L. & Davis, M. M. Diversity in the CDR3 region of V(H) is sufficient for most antibody specificities. *Immunity* **13**, 37–45 (2000).
17. Zemlin, M. *et al.* Expressed murine and human CDR-H3 intervals of equal length exhibit distinct repertoires that differ in their amino acid composition and predicted range of structures. *J. Mol. Biol.* **334**, 733–749 (2003).
18. Fosgerau, K. & Hoffmann, T. Peptide therapeutics: current status and future directions. *Drug Discov. Today* **20**, 122–128 (2015).
19. Lewis, W. G. *et al.* Click Chemistry In Situ: Acetylcholinesterase as a Reaction Vessel for the Selective Assembly of a Femtomolar Inhibitor from an Array of Building Blocks. *Angew. Chem.* **114**, 1095–1099 (2002).
20. Das, S. *et al.* A General Synthetic Approach for Designing Epitope Targeted Macrocyclic Peptide Ligands. *Angew. Chem. Int. Ed.* **54**, 13219–13224 (2015).

21. Nag, A. *et al.* A Chemical Epitope-Targeting Strategy for Protein Capture Agents: The Serine 474 Epitope of the Kinase Akt2. *Angew. Chem. Int. Ed.* **52**, 13975–13979 (2013).
22. Deyle, K. M. *et al.* A protein-targeting strategy used to develop a selective inhibitor of the E17K point mutation in the PH domain of Akt1. *Nat. Chem.* **7**, 455–462 (2015).
23. Millward, S. W. *et al.* Iterative in Situ Click Chemistry Assembles a Branched Capture Agent and Allosteric Inhibitor for Akt1. *J. Am. Chem. Soc.* **133**, 18280–18288 (2011).
24. Agnew, H. D. *et al.* Iterative In Situ Click Chemistry Creates Antibody-like Protein-Capture Agents. *Angew. Chem. Int. Ed.* **48**, 4944–4948 (2009).
25. Engelman, J. A. Targeting PI3K signalling in cancer: opportunities, challenges and limitations. *Nat. Rev. Cancer* **9**, 550–562 (2009).
26. Manning, B. D. & Cantley, L. C. AKT/PKB Signaling: Navigating Downstream. *Cell* **129**, 1261–1274 (2007).
27. Lawlor, M. A. & Alessi, D. R. PKB/Akt a key mediator of cell proliferation, survival and insulin responses? *J. Cell Sci.* **114**, 2903–2910 (2001).
28. Toure, M. & Crews, C. M. Small-Molecule PROTACS: New Approaches to Protein Degradation. *Angew. Chem. Int. Ed.* n/a–n/a (2016). doi:10.1002/anie.201507978
29. Carpten, J. D. *et al.* A transforming mutation in the pleckstrin homology domain of AKT1 in cancer. *Nature* **448**, 439–444 (2007).

*Chapter 2***PROTEIN CATALYZED CAPTURE AGENTS AS IMAGING PROBES
TO VISUALIZE AKT SUBCELLULAR LOCALIZATION****2.1 Summary of Contributions**

Parts of the contents of this chapter are adapted with permission from:

- (1) Millward, S.W., Henning, R.K., Kwong, G.A., Pitram, S., Agnew, H.D., Deyle, K.M., Nag, A., Hein, J., Lee, S.S., Lim, J., et al. (2011). Iterative in Situ Click Chemistry Assembles a Branched Capture Agent and Allosteric Inhibitor for Akt1. *J. Am. Chem. Soc.* *133*, 18280–18288.

This work was conducted in collaboration with Dr. Steven Millward. Steve led the study and carried out the majority of the experiments to identify and characterize the PCC agents reported here. I conceived of the imaging experiments, synthesized the necessary compounds, cultured the cells, and acquired the images. I also helped analyze the data and write the manuscript. The initial work is summarized and only the original data that I generated is included in this chapter.

2.2 Introduction

A critical bottleneck in the transition from a potential cancer biomarker to a clinical diagnostic tool is the availability of high-affinity, high-selectivity molecular entities to recognize and capture biomarkers from complex biological mixtures. Almost all current platforms employ antibodies as capture agents despite their high cost, poor stability,^{1,2} and the batch-to-batch variability that often characterizes biologicals. Many antibodies are poorly characterized, and reports have called into question the high specificity that is a perceived hallmark of antibodies.^{3,4} Emerging protein capture agent approaches, such as phage display peptides⁵ or nucleic acid aptamers, can potentially represent a powerful alternative to antibodies for certain diagnostic arrays.^{6,7} However, the challenge of finding a general and robust approach to produce protein capture agents that match the performance of monoclonal antibodies remains daunting. A high quality monoclonal antibody possesses a low-nanomolar affinity and high target specificity. An ideal antibody replacement would be synthetically facile, be stable to a range of thermal and chemical conditions, and display high affinity and specificity for the target of interest.

Iterative *in situ* click chemistry was used to develop a high-specificity, branched, triligand protein catalyzed capture (PCC) agent for the Akt kinase. Akt is a critical molecular router that mediates cellular signal transduction from the plasma membrane (cytokine receptors, GPCRs) to downstream effector molecules that control cell growth, apoptosis, and translation.⁸ Akt overexpression and/or hyperactivation has been observed in numerous cancer types.⁹ Such ubiquitous and aberrant Akt activity has made Akt a target for cancer

diagnostics and therapeutics.¹⁰ For developing a PCC agent against Akt, a novel screening strategy was developed. One can take advantage of the fact that an *in situ* click screen, in which an anchor ligand and protein target are screened against a large one-bead-one-compound (OBOC) library, will selectively generate triazole-linked products on the hit beads. The presence of on-bead clicked product is thus taken to be the signature of a hit bead, leading to the concept of a product screen. Such a product screen was utilized to increase the affinity and selectivity of the final multiligand PCC agent.

The Akt-binding PCC agent was developed by first identifying an anchor ligand. The initial anchor peptide was discovered by incubating the expressed kinase domain of Akt1 with a linear OBOC peptide library. The hit peptides were identified by probing the OBOC library for beads to which the protein was bound using Akt-specific antibodies. The consensus anchor sequence was identified as H₂N-Az8-VFYRLGY-CONH₂ (where Az8 is an unnatural amino acid with a side chain containing an eight carbon linker and a terminal azide) and the anchor showed a modest affinity of 25 μM. To increase the affinity of the anchor, a biligand branch was selected through a sequence of target and product screens. For these screens, the anchor peptide was modified with a C-terminal biotin for use in the product screen and incubated with an alkyne-containing, linear OBOC peptide library in the presence of the target protein. The most promising secondary ligand was identified as Pra-FWFLRG-CONH₂ and the resultant biligand showed an affinity of 338 nM. For triligand development, the *in situ* click screen was then iterated to identify a third ligand. The sequence of the tertiary ligand of the final branched PCC agent was RHERI and the K_d of the final triligand was 200 nM. In order to test the utility of the PCC agent as a drop-in replacement for antibodies it

was employed in immunofluorescent imaging experiments. Fluorescent versions of the biligand and triligand were synthesized and used to stain cells in order to monitor the subcellular localization of Akt.

2.3 Results and Discussion

To explore the biological applications of PCC agents, we asked if these compounds can be used as labeling agents in immunofluorescent imaging experiments. To address this question, fluorescent Akt biligand and triligand (Figures 2.1 and 2.3) were synthesized and used to stain fixed and permeabilized OVCAR3 cells and compared with a fluorescein-labeled anti-Akt monoclonal antibody. Previous studies have shown that Akt2 is overexpressed in the OVCAR3 ovarian cancer cell line, and so we utilized this cell line as an experimental platform for the immunocytochemical experiments (ICC).¹¹ When cellular receptor tyrosine kinases are activated, Akt is known to localize to the inner leaflet of the plasma membrane through binding of its pleckstrin homology domain (PHD) to phosphatidylinositol (3,4,5)-triphosphate (PIP₃).¹² Thus, we sought to visualize Akt membrane localization by imaging OVCAR3 cells stimulated with EGF and/or Insulin. When cells were stained with the fluorescent biligand the effect was visible, but it was not as profound (Figure 2.2) — this may be due to some of the off-target binding in the biligand. We also later found that the best images were obtained when cells were stimulated with both EGF and insulin, while the biligand images were acquired after stimulation with EGF alone. When imaging with the fluorescent triligand (Figure 2.3), which has much improved specificity over the biligand, AKT membrane localization was much more apparent (Figure 2.4). These results

demonstrate the ability of PCCs to selectively bind their targets in complex cellular environments.

2.4 Conclusion

The ultimate test of a protein capture agent is whether or not it can be used to detect its cognate protein from a biologically relevant sample. Visualization of Akt membrane localization in the complex cellular milieu corroborates the *in vitro* biochemical data and confirms that the PCC agent screening platform is a viable approach to develop protein binders with high affinity and selectivity. In addition, fluorescence imaging has become a standard benchmark for PCC agent performance in subsequent studies.¹³⁻¹⁵

2.5 Materials and Methods

Peptide Synthesis

In general, peptides were synthesized using standard SPPS protocols either manually or on a Titan 357 automated peptide synthesizer (Aapptec). Briefly, Fmoc resins were swelled in NMP and deprotected with 20% piperidine. Per coupling reaction, 4 equivalents of Fmoc-amino acid, 3.9 equivalents of HATU, and 12 equivalents of DIEA were added (equivalents relative to loading capacity of the resin). Couplings proceeded for 30-45 minutes. Azido amino acids were added at 2 equivalents relative to the resin loading capacity. The N-termini were acetylated with 20 equivalents of acetic anhydride and 10 equivalents of DIEA. In cases where use of Azido- amino acid Az8 produced a mixture of two diastereomers, the diastereomers were purified as a single product unless otherwise noted.

Synthesis of Fluorescein-biligand

The anchor peptide VFYRLGY-CONH₂ was synthesized on Rink Amide resin (Anaspec). Following addition of Az8, the resin was washed with NMP and set aside (Fmoc-Az8-VFYRLGY-CONH₂). In parallel the secondary ligand (Pra-FWFLRG-CONH₂) was synthesized on Sieber amide resin. After Fmoc deprotection the fluorescein derivative 6-[Fluorescein-5(6)-carboxamido]hexanoic acid (Sigma) was then conjugated to the amino terminus of the secondary peptide using 1.2 equivalents of fluorescein, 1.1 equivalents of HATU and 3 equivalents of DIEA and incubated at room temperature for 30 minutes. The peptide was cleaved by adding 4.5 mL 2% TFA in CH₂Cl₂ and incubating for 5 minutes. The TFA was quenched by filtration into 225 μ L DIEA. The cleavage was repeated five times, the filtrates were combined, and the solvent removed by rotary evaporation. The protected fluorescent secondary peptide was then purified by C18 RP-HPLC with a dH₂O:CH₃CN (0.1% TFA) gradient. The product was confirmed by MALDI-TOF MS. The secondary peptide was coupled to the anchor peptide via copper catalyzed azide-alkyne cycloaddition by addition of 1 equivalent of anchor peptide with 2 equivalents of fluorescent secondary peptide, 4 equivalents of CuI, and 6 equivalents of Ascorbic Acid. The reaction proceeded for 18 hours at room temperature followed by washing in NMP and copper chelation solution. The N-terminal Fmoc group was removed in 20% piperidine. 8 equivalents of 5-hexynoic acid (Sigma), 7 equivalents of HATU, and 24 equivalents of DIEA were added in NMP and the reaction was allowed to proceed at room temperature for 2 hr. After washing with NMP, the 5HA-Fluorescent-Biligand was cleaved from the resin in 95:5:5 TFA:dH₂O:TES and precipitated in diethyl ether. The product was

purified by RP-HPLC as a mixture of diastereomers and analyzed by MALDI-TOF mass spectrometry (Expected $[M+H]^+ = 2612.00$, Observed $[M+H]^+ = 2612.78$).

Synthesis of Fluorescein-triligand

For the synthesis of the fluorescent triligand, the biligand was synthesized as described above without the addition of the fluorescent dye. The tertiary peptide Az8-RHERI-CONH₂ was synthesized on Rink Amide resin as described. Following deprotection of the N-terminal Fmoc group, the resin-bound tertiary peptide was reacted with 1.2 equivalents of 6-[Fluorescein-5(6)-carboxamido]hexanoic acid (Sigma), 1.1 equivalents of HATU, and 3 equivalents of DIEA at room temperature for 30 minutes. Following cleavage from resin, C18 RP-HPLC purification and MALDI-TOF verification of the product, the fluorescein-labeled tertiary peptide was coupled to 5HA-Biligand-Bio via copper catalyzed azide-alkyne cycloaddition by addition of 1 equivalent of fluorescein-labeled tertiary peptide to 1.15 equivalents of 5HA-Biligand-Bio, and 3 equivalents of TBTA in the presence of 10 mM CuI and 30 mM L-ascorbic acid in 4:1 NMP:water. The reaction proceeded for 24 hours at room temperature. The fluorescent triligand was purified by RP-HPLC and analyzed by MALDI-TOF MS: Expected $[M+H]^+ = 3841.0$, Observed $[M+H]^+ = 3840.8$.

Immunofluorescence Microscopy

OVCAR3 cells were grown on poly-lysine coated cover slips, then serum starved for 1 hr. The cells were then treated with either 400 ng/mL EGF (Sigma) or 20 µg/mL insulin (Sigma) or untreated for 10 minutes. Cells were then fixed with 10% formaldehyde for 10 min at 37 °C, washed with PBS, permeabilized by incubating with 0.1% Triton X-100 for

5 min at room temperature, and blocked with 5% goat serum. Permeabilized cells were stained with either a fluorescein-conjugated Pan Akt antibody (R&D Systems IC2055F, 10 $\mu\text{g}/\text{mL}$) overnight, 1 μM fluorescein conjugated biligand for 1 hour, or 100 nM fluorescein-triligand for 1 hr. Images were acquired using a Zeiss Pascal 5 Laser Scanning Microscope (Caltech Biological Imaging Center).

2.6 Figures

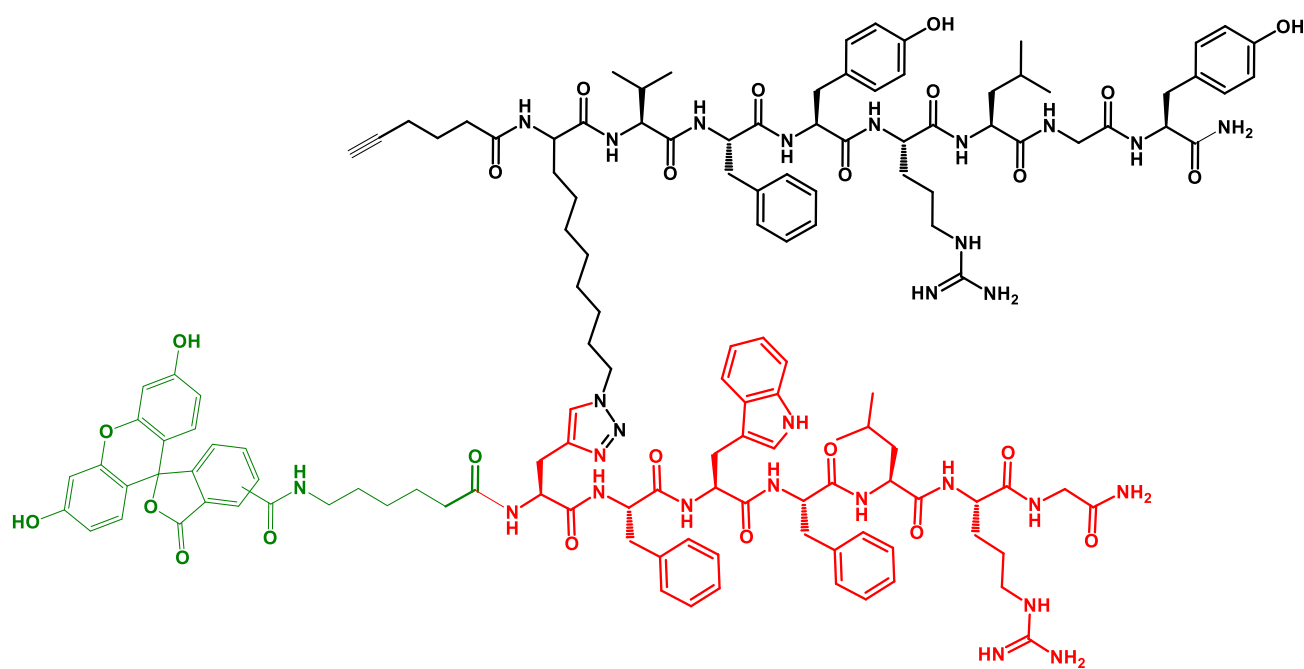


Figure 2.1 – Chemical structure of fluorescent Akt biligand

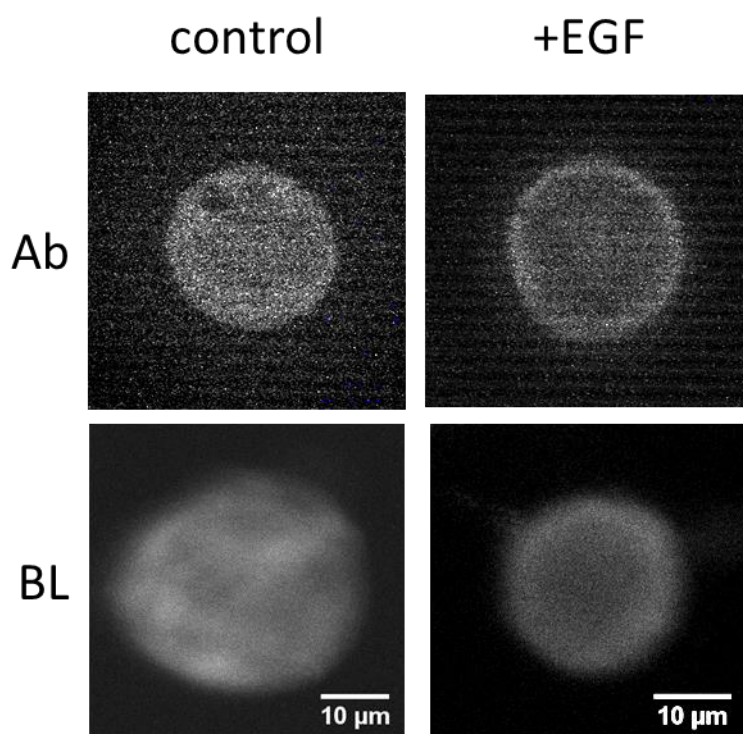


Figure 2.2 – Imaging Akt membrane localization with fluorescent biligand. OVCAR3 cells stimulated with or without EGF and stained with a fluorescent anti-AKT antibody (Ab) or the AKT biligand (BL).

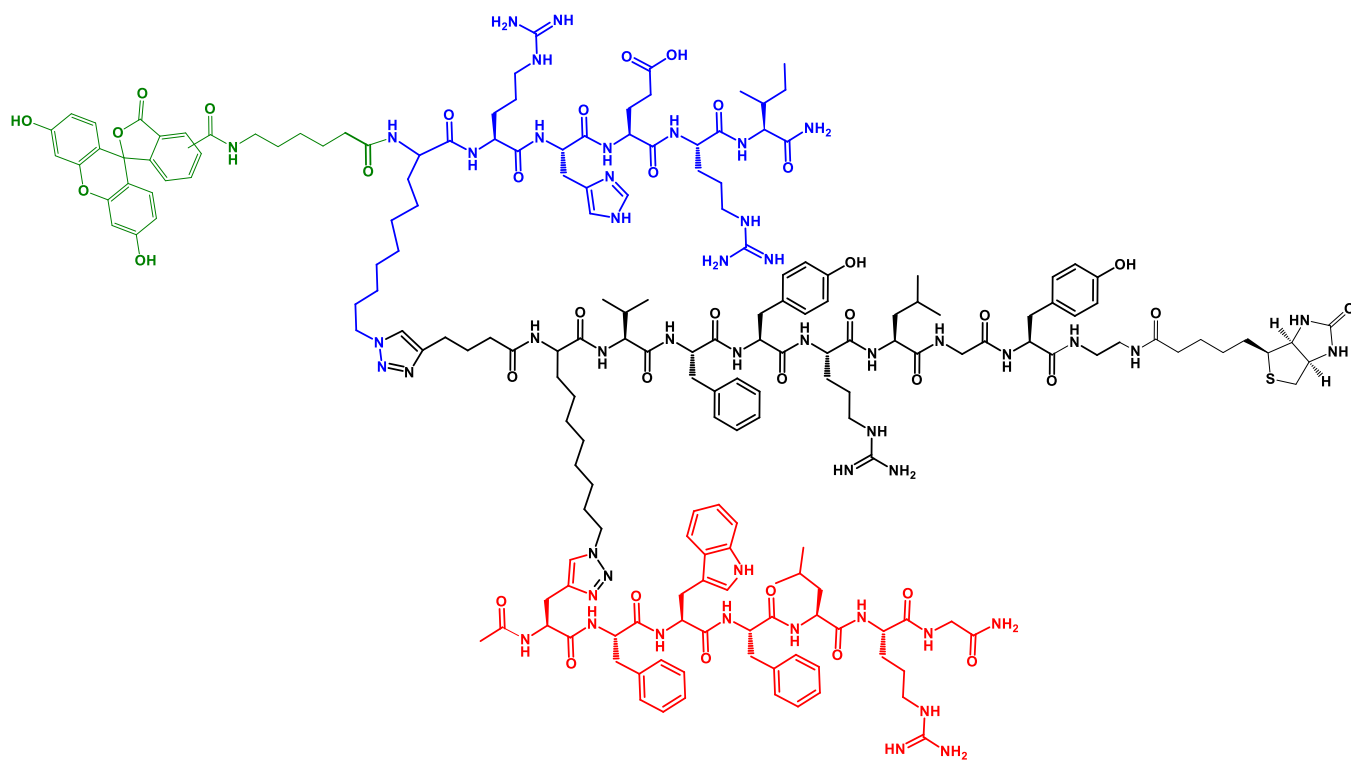


Figure 2.3 – Structure of fluorescent Akt triligand

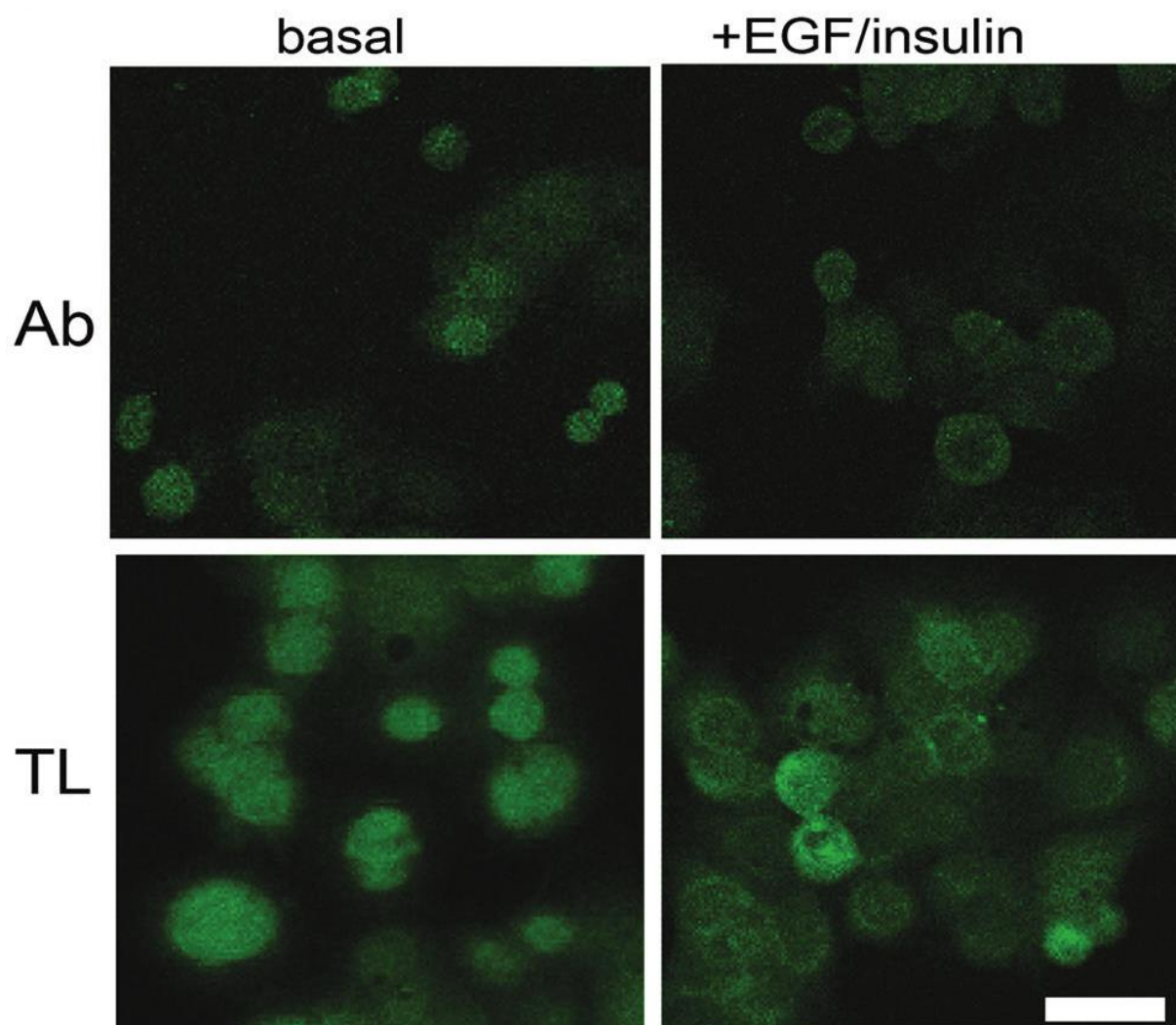


Figure 2.4 – Imaging Akt with fluorescent triligand PCC agent. Immunofluorescent images of Akt in fixed OVCAR3 cells stained with either a fluorescein-conjugated anti-Akt antibody (Ab) or a fluorescein-conjugated triligand (TL). Each imaging agent distinguishes cytoplasmic or membrane-bound Akt in unstimulated or EGF+insulin-treated cells, respectively. Contrast is enhanced equally in all images, but the fluorescence images of the triligand stained cells were achieved at a 3-fold lower excitation laser intensity relative to the (much dimmer) antibody-stained cells. Scale bar = 100 μ m.

2.7 References

1. Borrebaeck, C. A. Antibodies in diagnostics - from immunoassays to protein chips. *Immunol. Today* **21**, 379–382 (2000).
2. Kodadek, T., Reddy, M. M., Olivos, H. J., Bachhawat-Sikder, K. & Alluri, P. G. Synthetic molecules as antibody replacements. *Acc. Chem. Res.* **37**, 711–718 (2004).
3. Kijanka, G. *et al.* Rapid characterization of binding specificity and cross-reactivity of antibodies using recombinant human protein arrays. *J. Immunol. Methods* **340**, 132–137 (2009).
4. Michaud, G. A. *et al.* Analyzing antibody specificity with whole proteome microarrays. *Nat. Biotechnol.* **21**, 1509–1512 (2003).
5. Smith, G. P. & Petrenko, V. A. Phage Display. *Chem. Rev.* **97**, 391–410 (1997).
6. Gold, L. *et al.* Aptamer-based multiplexed proteomic technology for biomarker discovery. *PloS One* **5**, e15004 (2010).
7. Ostroff, R. M. *et al.* Unlocking biomarker discovery: large scale application of aptamer proteomic technology for early detection of lung cancer. *PloS One* **5**, e15003 (2010).
8. Vivanco, I. & Sawyers, C. L. The phosphatidylinositol 3-Kinase AKT pathway in human cancer. *Nat. Rev. Cancer* **2**, 489–501 (2002).
9. Altomare, D. A. & Testa, J. R. Perturbations of the AKT signaling pathway in human cancer. *Oncogene* **24**, 7455–7464 (2005).
10. Garcia-Echeverria, C. & Sellers, W. R. Drug discovery approaches targeting the PI3K/Akt pathway in cancer. *Oncogene* **27**, 5511–5526 (2008).

11. Yang, L. *et al.* Akt/protein kinase B signaling inhibitor-2, a selective small molecule inhibitor of Akt signaling with antitumor activity in cancer cells overexpressing Akt. *Cancer Res.* **64**, 4394–4399 (2004).
12. Lasserre, R. *et al.* Raft nanodomains contribute to Akt/PKB plasma membrane recruitment and activation. *Nat. Chem. Biol.* **4**, 538–547 (2008).
13. Deyle, K. M. *et al.* A protein-targeting strategy used to develop a selective inhibitor of the E17K point mutation in the PH domain of Akt1. *Nat. Chem.* **7**, 455–462 (2015).
14. Farrow, B. *et al.* Epitope Targeting of Tertiary Protein Structure Enables Target-Guided Synthesis of a Potent In-Cell Inhibitor of Botulinum Neurotoxin. *Angew. Chem. Int. Ed.* **54**, 7114–7119 (2015).
15. Henning, R. K. *et al.* Degradation of Akt using protein-catalyzed capture agents. *J. Pept. Sci.* **22**, 196–200 (2016).

ACTIVATION, INHIBITION, AND DEGRADATION OF AKT USING PROTEIN CATALYZED CAPTURE AGENTS

3.1 Summary of Contributions

Adapted with permission from:

- (1) Henning, R.K., Varghese, J.O., Das, S., Nag, A., Tang, G., Tang, K., Sutherland, A.M., and Heath, J.R. (2016). Degradation of Akt using protein-catalyzed capture agents. *J. Pept. Sci.* 22, 196–200.

This work was performed in close collaboration between Dr. Joseph Varghese and myself as indicated in our co-first authorship on resultant publication from our efforts. In the early stages of the project Joey optimized several reactions that were necessary for synthesizing the PCC agents used in the study, such as the TAT cleavage reaction. Together we worked closely to synthesize, purify, and characterize the compounds reported and we also collaborated while conducting several of the assays. My unique contribution was the incorporation of the degradation tag for PROTAC development.

3.2 Introduction

Protein-catalyzed capture (PCC) agents are a class of ligands that are built using *in situ* click chemistry¹ to allow a protein of interest to select its own high-affinity binders.² These synthetic peptides have some similarities to monoclonal antibodies, but are a fraction of the size and can exhibit a high level of stability.³ A recent advance of this technology permits the targeted development of a PCC against a specific epitope of a given protein.^{4,5} Unlike the case for small molecule ligands, the generalized PCC epitope targeting strategy does not rely on the presence of a hydrophobic binding pocket. This opens up several non-traditional approaches towards altering enzymatic activity, including the targeting of sites that can allosterically influence that activity⁶ or by disrupting protein-activator associations.⁷ A second possibility is simply to use the synthetic flexibility of the PCC agent as a selective targeting moiety for labeling the target with a molecular signal, such as a degradation signal, as is used for the case of proteolysis targeting chimeric molecules (PROTACs). Here, we explore the use of a pair of epitope-targeted PCC agents developed against an allosteric site of Akt2 for in-cell allosteric activation, inhibition, and degradation of Akt.

We previously reported the development of a pair of PCC agents targeting the C-terminal hydrophobic motif of Akt2 that includes the Ser474 residue.⁵ Phosphorylation of Akt at Ser474 leads to allosteric activation of Akt and increases the kinase activity tenfold.⁸ We therefore hypothesized that targeting the Ser474 site could lead to compounds that influence Akt kinase activity. We increased the interaction footprint of the initial epitope-

targeted 5-mer peptide ligand with Akt2 by expanding it into two distinct triligands through *in situ* click chemistry screens. The two PCC agent triligands, **tri_a** and **tri_i**, developed from the same epitope-targeted the anchor peptide, were shown to activate and inhibit Akt enzymatic activity respectively, in *in vitro* kinase assays.⁵

Although specific peptides (typically macrocycles) have been designed for cell entry,⁹ the **tri_a** and **tri_i** PCC agents are branched structures consisting of linear branches, and so do not naturally enter into live cells. A common approach for cellular delivery of peptides is to append a cell penetrating peptide (CPP),¹⁰ and that is the route we choose here. CPP-labeled **tri_a** was found to penetrate into live cells. The influence of the CPP-labeled compounds on in-cell kinase activity and on cellular proliferation were then explored in two cancer cell lines. We next modified the two triligands to present a HIF-1 α degradation signal and explored the capacity of these compounds to promote in-cell Akt degradation.

3.3 Results and Discussion

We conjugated the PCC agents to the HIV TAT peptide, which is a CPP that efficiently penetrates cell membranes via endocytosis, and allows CPP-bound molecules to enter cells.¹¹ Figure 3.1A shows the structure of TAT-conjugated **tri_a**, where the TAT sequence is separated from the capture agent by two PEG spacers placed on either side of a protected-lysine residue. This permits further functionalization as desired during the solid phase peptide synthesis via the lysine ϵ -amino group (adding a dye, signaling peptide, etc.). To validate cellular uptake, we treated U87 cells with fluorescein-labeled **tri_a** (**CPP-tri_a-FL**, Figure 3.1B and Figure 3.7) and acquired simultaneous fluorescence and transmission

images. U87 cells are particularly useful for imaging because they grow in a uniform monolayer.¹² We found that the **CPP-tri_a-FL** is able to efficiently penetrate the cell membrane and enter the cells. No fluorescence signals were detected outside the cells, and the uniform distribution of the fluorescence through the cell cytoplasm suggests that the PCCs were released into the cells (rather than completely trapped within endosomes).

We next performed functional assays to confirm that the *in vitro* effects translate into live cells. The enzymatic activity of Akt can be monitored by measuring the phosphorylated level of its direct substrate, glycogen synthase kinase 3 beta (GSK-3 β).¹³ SKOV3 ovarian cancer cells were dosed with TAT-coupled **tri_a** (**CPP-tri_a**, Figures 3.1A and Figure 3.6) for various times. Following cell lysis, the relative levels of various proteins were measured via western blotting (Figure 3.2A). Both untreated cells and EGF-stimulated cells were used as controls. The level of phospho(p)-GSK-3 β was seen to increase after 1 h of treatment, decrease over the next few hours, and finally increase once more – perhaps alluding to a feedback mechanism in the cell. The initial increase in the p-GSK-3 β level indicates that the capture agent is binding Akt and stimulating its enzymatic activity in cells. The p-Akt level initially increases and then steadily decreases over time. Notably, EGF-stimulated cells display a large increase in p-Akt, but the corresponding level of p-GSK-3 β in EGF-stimulated cells is still lower than the initial levels in cells treated with **CPP-tri_a**.

We next performed an XTT cell proliferation assay to determine if Akt activation by **CPP-tri_a** stimulates cell proliferation.¹⁴ Dehydrogenase enzymes in live cells reduce XTT

tetrazolium salt to a vividly colored formazan dye that can be used to quantify the number of viable cells.^{15,16} We found that **CPP-tri_a** affected both OVCAR3 and SKOV3 cell lines (Figure 3.2B). Interestingly, for both cell lines, a sharp increase in proliferation after 24 h is followed by a steady decrease over a few days – once more suggesting a possible feedback mechanism. Eventually, after several days of treatment, cellular proliferation falls back to baseline levels for SKVO3 cells while OVCAR3 cells are inhibited relative to the untreated control. An initial increase in cell number after treatment with **CPP-tri_a** is consistent with previous studies showing that Akt activation promotes cell cycle progression during the G1 and G2 phases of the cell cycle.^{17,18} Additionally, activated Akt is known to inhibit the pro-apoptotic bad protein,^{19,20} as well as the FoxO and Myc family of proteins.^{21,22} Such enhanced cell proliferation can be used in beneficial ways. Many pathological disorders are associated with aberrant cell death signaling, including various neurodegenerative diseases.²³ Akt activation was recently shown to prevent neuronal cell death.²⁴ Thus, an Akt activator might prove useful as a tool to probe the Akt signaling pathway and to help develop potential therapeutics for disease-associated apoptosis abnormalities. In any case, these results further corroborate the *in vitro* data that **tri_a** directly activates Akt.

Similarly, the TAT-modified **tri_i** (**CPP-tri_i**, Figure 3.3) inhibits phosphorylation of GSK-3 β and reduces cancer cell viability (Figure 3.4). SKOV3 cells were treated with 50 μ M **CPP-tri_i** for various times, lysed simultaneously, and analyzed by western blot (Figure 3.4A). Cells treated with **tri_i** show less phospho-GSK-3 β than untreated or EGF stimulated cells over the entire 24 hour time course. Similar to **CPP-tri_a**, **CPP-tri_i**

inhibition of Akt appears to be independent of Akt phosphorylation at Ser473. Additionally, **CPP-tri_i** also inhibits cell proliferation. SKOV3 and OVCAR3 cells each show an initial drop in cell viability upon treatment with **CPP-tri_i**, with values remaining consistently lower than untreated cells for 5 days (Figure 3.4B). The results from the XTT assays are consistent with the expected phenotypic outcome of Akt inhibition.

Proteolysis targeting chimeric molecules represent an example of using cellular signals to control levels of specific proteins.^{25,26} In particular, PROTACs utilize the quality control machinery of the cell by artificially labeling proteins for proteasomal degradation. We sought to create Akt PROTACs by encoding a peptide ligand for the E3 ubiquitin ligase von Hippel Lindau protein directly into the CPP-labeled PCC agents.²⁷ The peptide represents the von Hippel Lindau binding site from hypoxia-inducible factor (HIF-1 α) protein.

When OVCAR3 cells were treated with **CPP-tri_a-PR** over a variable time period up to 24 h Akt levels diminished. After 30 min of treatment, a relative decrease in Akt level was measurable, with a continuing decrease that reached a nadir after 4 h (Figure 3.5A). Similarly, **CPP-tri_i** was also modified into a PROTAC (**CPP-tri_i-PR**, Figure 3.9) and effectively removed Akt from cells, with a slightly slower time constant (Figure 3.5B). We also observed a dose-dependent decrease in Akt upon treatment with the **CPP-tri_a-PR** and determined an EC₅₀ degradation constant of $128 \pm 19 \mu\text{M}$ (Figure 3.5C).

3.4 Conclusion

Previous PROTACs have been developed by adding a degradation signal to a modified protein ligand²⁸ or previously discovered inhibitors.^{29,30} Here, we report that epitope-targeted PCC agents can be modified into PROTACs to direct synthetic degradation to specific proteins in cells. We also show an Akt activator and inhibitor can both serve as PROTACs (Figure 3.5), indicating that ubiquitination and degradation of this protein can be induced regardless of the activation state of the protein. Targeting proteins for enzymatic destruction is an attractive alternative to developing traditional small molecule inhibitors, especially for proteins (such as Akt) that are difficult to inhibit with traditional methods.³¹

The principle concept reported here is the use of an epitope-targeted PCC as simply a vehicle for directing PROTAC-initiated degradation to a specific target. A limitation of this approach, as reported, is that the PCCs are not intrinsically cell penetrant, and so were modified with a CPP for the in-cell assays. We have recently reported on epitope-targeted macrocyclic PCC agents,⁴ and such peptide architectures have been modified for both cell permeability^{9,32,33} and other desired pharmacokinetic properties.³⁴ Other promising proteolysis tags include members of the IMiD family, such as thalidomide, which is a drug with a rich history.³⁵ In 2010, it was discovered that thalidomide targets the E3 ubiquitin ligase member cereblon.³⁶ Related examples of cereblon-targeted degradation include the use of pomalidomide³⁷ and phthalimide³⁸ for PROTAC development.

3.5 Materials and Methods

Solid phase peptide synthesis general protocol:

Peptides were synthesized on Rink Amide MBHA, Biotin Novatag, and Sieber Amide resin either manually, on a Liberty1 Microwave Peptide Synthesizer (CEM), or on a Titan 357 Automatic Peptide Synthesizer (AAPPTec). Peptide coupling reactions were done in NMP with 2 equivalents of amino acid, 2 equivalents of HATU and 6 equivalents of N,N-Diisopropylethylamine (Sigma). For removal of N α -Fmoc protecting groups, a solution of 20% piperidine in NMP was used.

Acylation

The resin was treated twice for ten minutes with a solution of anhydrous acetic anhydride and DIEA in NMP (acetic anhydride: DIEA: Peptide; 40:20:1) at room temperature. Excess reagent was removed by washing five times successively with NMP.

Cleavage of side chain protected peptides

The peptides were synthesized on Sieber Amide resin and cleaved by washing three times for one minute with 1% TFA/DCM, and finally washed with DCM. The acidic peptide solution was neutralized using 2 equivalents of DIEA followed by removal of the solvent by rotary evaporation. The remaining semisolid was dissolved in filtered DMSO, HPLC grade acetonitrile, and double distilled water, and purified via HPLC.

Cleavage of side chain deprotected Biotin Linker peptide

The peptides were synthesized on Biotin Novatag resin. The dried resin was then treated with a TFA cleavage solution of 95% TFA, 2.5% H₂O, and 2.5% triethylsilane for two hours at room temperature. The cleavage solution was filtered to remove the resin and added dropwise to an ice-cooled solution of diethyl ether.

Cleavage of TAT-containing peptides

TAT-containing peptides were synthesized on Rink Amide MBHA resin. The dried resin was then incubated with a TFA cleavage solution of 80% TFA, 10% thioanisole, 5% H₂O, 5% triethylsilane for 3 hours at room temperature. The cleavage solution was filtered to remove the resin and added dropwise to a cooled solution of diethyl ether.

HPLC purification of peptides

All peptides were purified using a preparative or semi-preparative scale HPLC with a C18 reverse phase column. A gradient of double distilled water and HPLC grade acetonitrile and 0.1% TFA was used for all purifications.

Protocol for on-bead copper (Cu) catalyzed azide alkyne cycloaddition (CuAAC) click reaction

On-bead Cu catalyzed click reactions were performed with the azide on bead and the alkyne in solution. The resin was treated with 2 equivalents of the relevant alkyne, 1.5

equivalents of CuI (Sigma), and 2.5 equivalents of ascorbic acid (Sigma), in a solution of 20% piperidine in DMF. The reaction was performed overnight at room temperature. Excess copper was removed from the resin by washing with a Cu chelating solution (5% (w/v) sodium diethyl dithiocarbamate, 5% (v/v) DIEA in DMF).

Removal of Dde protecting group

For removal of Dde protecting groups, resin-bound peptide was washed with a solution of 2% hydrazine in DMF three times for ten minutes.

Mass spectrometry analysis

All intermediate and final peptides were analyzed via MALDI-TOF-MS using a Voyager DE-PRO MALDI TOF-MS system (Applied Biosystems). Peptides were dissolved in 50:50 water/acetonitrile with 0.1% trifluoroacetic acid at a final concentration of 10 pmol/ μ L. 1 μ L of the peptide sample was then added to 10 μ L of a saturated solution of MALDI matrix, either α -cyano-4-hydroxycinnamic acid or Sinapinic Acid, in 50:50 water/acetonitrile with 0.1% trifluoroacetic acid and analyzed via MALDI-TOF MS.

Synthesis of CPP-tri_a

For the synthesis of the N-terminal triligand the HIV-TAT sequence H₂N-GRKKRRQRRRPPQQ-CONH₂ was synthesized on rink amide MBHA resin using

standard SPPS conditions. Fmoc-PEG₅-COOH was then coupled to the N-terminus of the resin-bound TAT peptide with 1.5 equivalents of PEG₅, 1.5 equivalents of HATU and 4.5 equivalents of DIEA. Following the PEG₅ coupling and subsequent Fmoc deprotection Fmoc-Lysine(Dde)-OH was then coupled using standard conditions. After the Lys(Dde) coupling and deprotection a second PEG₅ group was added. The N-terminal triligand was then synthesized on the resin bound PEG₅-Lys(Dde)-PEG₅-TAT peptide as previously reported.⁵ The Dde group was then removed and the peptide was either cleaved/deprotected and purified for assays or further modified at the epsilon amino group of the lysine side chain at the linker region. The TAT-conjugated triligands were cleaved from the resin in 80:10:5:5 TFA:thioanisole:TES:H₂O for 2.5 hours. Expected [M+H]⁺ = 6047.1, Observed [M+H]⁺ = 6049.9. The molecular structure of **CPP-tri_a** is shown in Figure 3.6

Synthesis of fluorescently labeled CPP-tri_a

To resin-bound N-terminal triligand described above, 5-Carboxyfluorescein was coupled to the epsilon amino group of the lysine side chain at the linker region. The coupling reaction was performed with 1:1.5:1.5:4.5 ratios of peptide:5-Carboxyfluorescein:HATU:DIEA. The peptide was then cleaved and purified with the same conditions as the unlabeled N-terminal triligand. MALDI-TOF MS: Expected [M+H]⁺ = 6405.4, Observed [M+H]⁺ = 6408.7. The molecular structure of **CPP-tri_a-FL** is shown in Figure 3.7.

Synthesis of CPP-tri_a-PR with HIF-1 α degradation signal

To resin-bound N-terminal triligand previously described, 6-aminohexanoic acid(Ahx) followed by the HIF-1 α degradation peptide ALAPYIP were coupled to the epsilon amino group of the lysine side chain at the linker region using standard SPPS conditions. The peptide was then cleaved and purified with the same conditions as the unlabeled N-terminal triligand. MALDI-TOF MS: Expected $[M+H]^+ = 6886.1$, Observed $[M+H]^+ = 6885$. The molecular structure of CPP-tri_a-PR is shown in Figure 3.8.

Synthesis of CPP-tri_i inhibiting triligand

Unlabeled C-terminal triligand was synthesized as previously reported.⁵ Fmoc-PEG₂-COOH was then coupled to the N-terminus of the resin-bound peptide with molar ratios of 1:1.5:1.5:4.5 peptide:PEG₂:HATU:DIEA. Ahx followed by cysteine were then coupled using standard conditions and 5-carboxyfluorescein was coupled as before resulting in compound **1**. Fluorescent C-terminal triligand was then cleaved with 95:2.5:2.5 TFA:H₂O:TES and HPLC purified. The observed MALDI-TOF MS $[M+H]^+ = 4001.6$, which is +4 amu from expected $[M+H]^+ = 3997.6$, most likely due to oxidation of tryptophan to kynurenine³⁹ – tryptophan oxidation is a known artifact in MS of peptides.⁴⁰

Dibenzocyclooctyne-maleimide (Sigma) was then coupled to the cysteine thiol group as reported⁴¹ to yield cyclooctyne C-terminal triligand **2** (Figure 3.10). The crude mixture was

then HPLC purified and a single peak at 495 nm (Fluorescein λ_{max}) was collected corresponding to compound 2.

Azide-containing TAT peptide 3 was synthesized using standard conditions and Fmoc-PEG₂-COOH was coupled as before followed by addition of 5-azidopentanoic acid using standard coupling conditions. Resin-bound 3 was then cleaved and purified with conditions mentioned above. Peptides 2 and 3 were then clicked together as reported⁴¹ resulting in C-terminal triligand 4 (Figure 3.11). The crude mixture was then injected onto a semiprep C18 reverse phase HPLC column and new peak appeared that was distinct from the HPLC traces of compounds 2 and 3 alone, corresponding to peptide 4. Peptide 2 elutes from the analytical HPLC beginning around 18 minutes and TAT peptide 3 begins eluting around 8 minutes. After the strain-promoted click reaction peptide 4 elutes after approximately 11 minutes. MALDI-TOF MS: Expected $[M+H]^+ = 6582.6$, Observed $[M+H]^+ = 6599.1$. The +16 difference is likely due to oxidation of the peptide in the MALDI-TOF.

Synthesis of CPP-tri_i-PR with HIF-1 α degradation signal

Resin-bound HIV-TAT peptide H₂N-PEG₅-Lys(Dde)-PEG₅-GRKKRRQRRRPPQQ-CONH₂ was synthesized as described above. The C-terminal triligand was then synthesized onto the TAT peptide as before. The ϵ -amino group of the Lys(Dde) in the linker region was then deprotected and the degradation sequence Ahx-ALAPYIP was added by SPPS as

with the N-terminal triligand. $[M+H]^+ = 6641.81$, Observed $[M+H]^+ = 6641.89$. The molecular structure of **CPP-tri_i-PR** is shown in Figure 3.9.

Cell Culture

All cell lines were purchased from American Type Culture collection Q4 (Manassas, VA, USA). U87 (ATCC number HTB14), OVCAR3 (ATCC number HTB161), and SKOV3 (ATCC number HTB77) cells were cultured under conditions specified by the provider.

Fluorescence Microscopy

Cells were seeded onto chambered cover glass slides (Sigma-Aldrich, St. Louis, MO, USA) and allowed to attach overnight. The following day, cells were serum starved and treated with fluorescent capture agent. Live cells were then imaged using a Zeiss (Oberkochen, Germany) LSM5 Exciter microscope in the Caltech Biological Imaging Center.

Immunoblotting

Western blots were performed according to standard protocols. Briefly, cells were lysed with cell lysis buffer (Cell Signaling Technology) containing protease and phosphatase inhibitors (Cell Signaling Technology). Cell lysates were quantified with a Bradford protein assay (Thermo Scientific, Waltham, MA, USA) and prepared for gel electrophoresis in Laemmli sample buffer and reducing agent. Twenty micrograms of cell lysate were added to precast polyacrylamide gels (Bio-Rad Laboratories, Inc., Hercules, CA, USA), and proteins were separated by electrophoresis followed by transfer to PVDF

membrane. Membranes were then blocked and probed with primary antibodies followed by horseradish peroxidase-conjugated secondary antibodies. The bands were visualized via a chemiluminescent substrate (Thermo Scientific). The following antibodies were used according to manufacturer protocol: p-GSK3 β (Cell Signaling, 9323), GSK3 β (Cell Signaling, 12456), AKT (Cell Signaling, 4691), p-AKT (S473) (Cell Signaling, 4060), Actin (Cell Signaling, 8456), and HRP-linked Anti-rabbit IgG (Cell Signaling, 7074).

Cell Proliferation Assay

Cell viability kit II (XTT) assay was purchased from Cell Signaling Technology (#9095) and used according to manufacturer protocol. Briefly, 1×10^4 cells per well were seeded in a 96-well plate. The following day, cells were serum starved and treated with PCC agent. Following treatment, XTT was added to the media, and after 1 h, the absorbance at 450nm was measured.

In-cell ELISA Assay

In-cell ELISA kits were purchased from Thermo Scientific (#62215) and used according to manufacturer protocol. Briefly, 1×10^4 cells were seeded in 384-well plates and allowed to attach overnight. The following day, cells were serum starved and treated with capture agent. Following capture agent treatment, cells were fixed, permeabilized, blocked, and then stained with primary and HRP-conjugated secondary antibody and developed with colorimetric peroxidase substrate. The absorbance was measured at 450 nm to quantify the protein. Cells were then incubated with Janus Green whole-cell stain, and the absorbance

was measured at 615 nm to quantify relative number of cells per well. The Akt signal was then normalized to the relative cell number for each well to determine the Akt/cell.

3.6 Figures

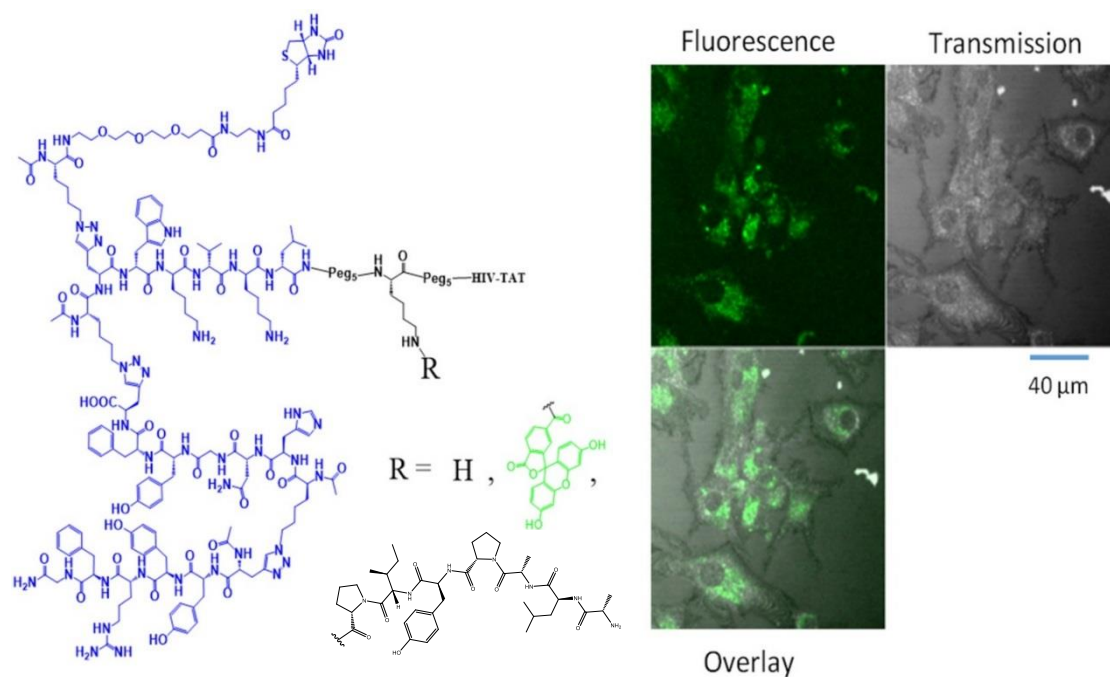


Figure 3.1 – Exploiting the modularity of Akt-activating PCC agent *tri_a*. (A) Structure of Akt-activating N-terminal triligand, ***tri_a***. The lysine residue between the PEG spacers can be further functionalized with fluorescein or the degradation-inducing Hif-1 α peptide. Complete structures are shown in the subsequent figures. R = H is referred to as **CPP-*tri_a***, R = fluorescein is **CPP-*tri_a*-FL**, and R = ALAPYIP (Hif-1 α degradation peptide) is **CPP-*tri_a*-PR**. (B) Live-cell confocal images of the fluorescein-labeled capture agent **CPP-*tri_a*-FL** delivered into U87 cells.

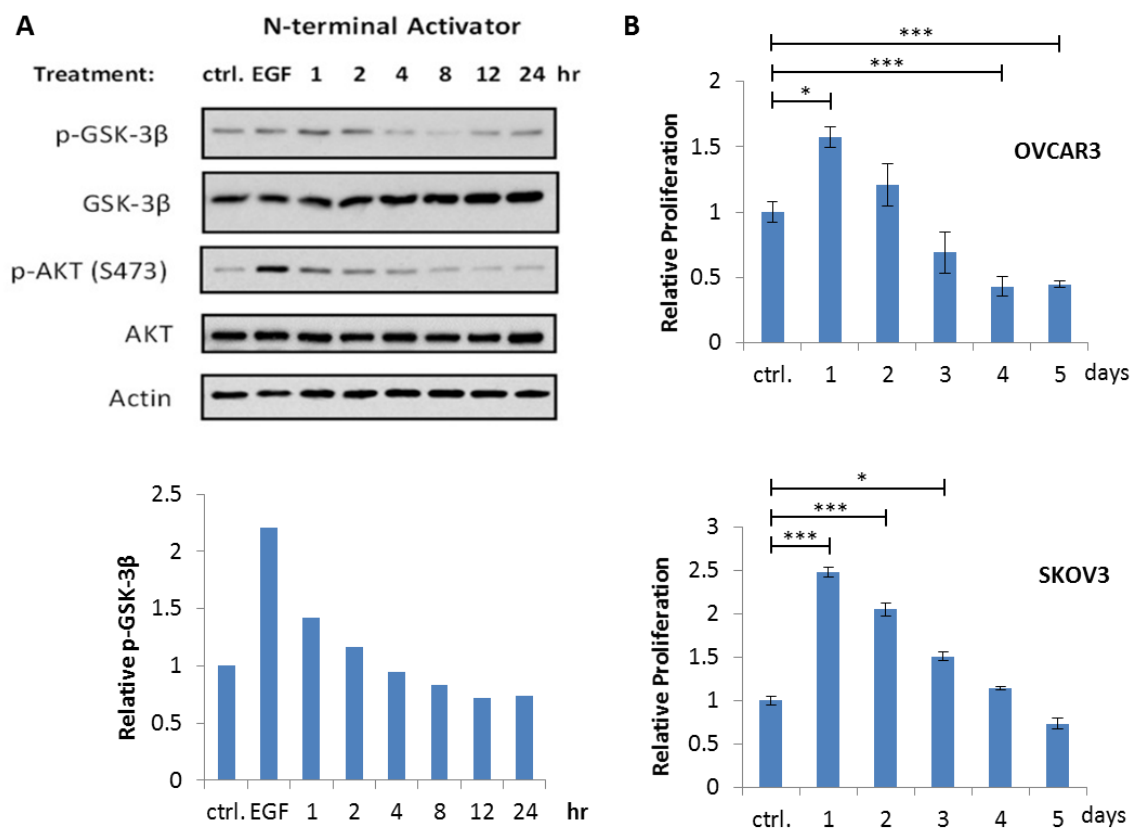


Figure 3.2 - tri_a activates Akt in cells. (A) Western blots of SKOV3 cells treated with 50 μ M CPP-tri_a. Densitometry was performed on the p-GSK-3 β blot, and the relative intensities were plotted on the bar graph below the blotting assays. (B) XTT cell proliferation assay results from OVCAR3 and SKOV3 cells treated with 50 μ M CPP-tri_a for times varying from 1 to 5 days. A student's t-test was used to determine significant differences where * = p-value \leq 0.05 and *** = p-value \leq 0.01.

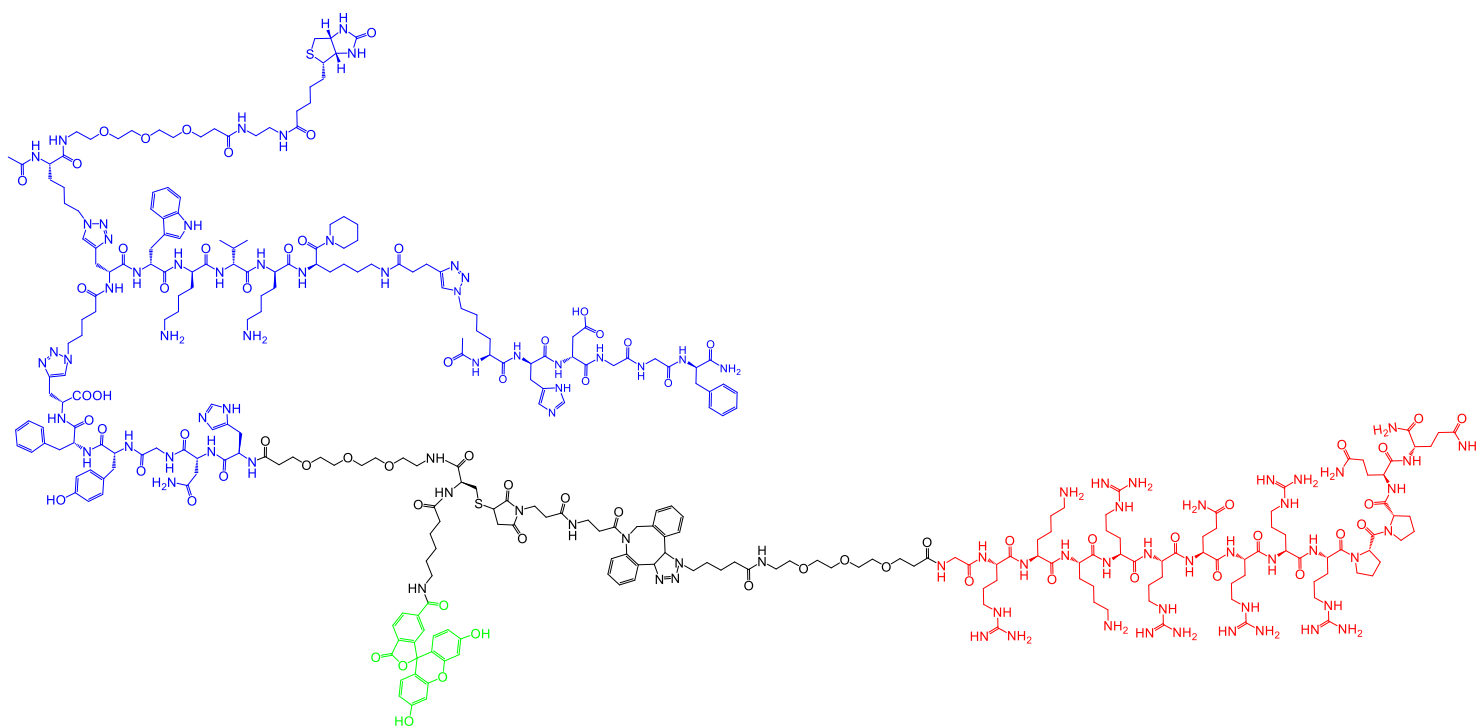


Figure 3.3 - Structure of Akt-inhibiting CPP-tri_i

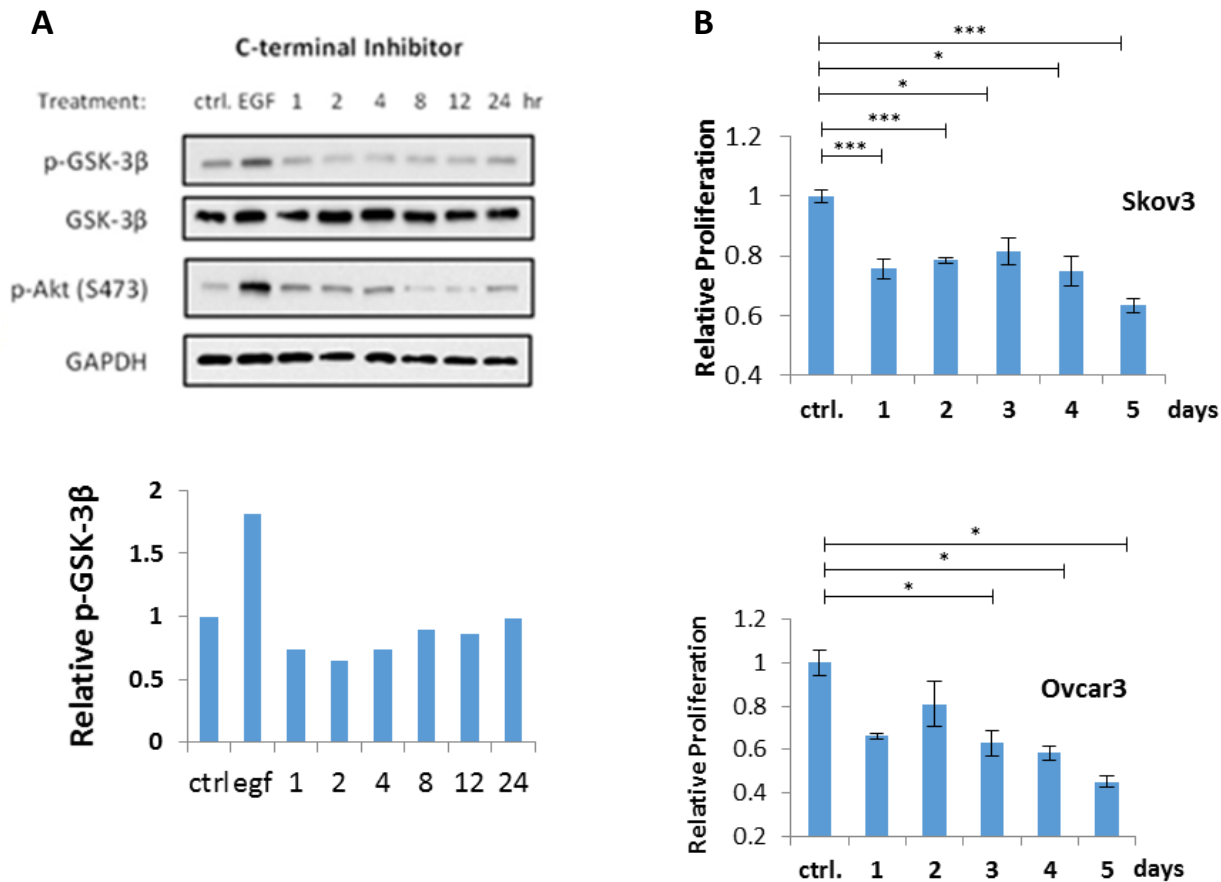


Figure 3.4 – CPP-tri_i inhibits Akt in cells. (A) Western blots of SKOV3 cells treated with 50 μ M CPP-tri_i. Cells were treated for various times and compared with 100 ng/mL EGF stimulation and an untreated control. Densitometry was performed on the p-GSK-3 β blot and the relative intensities were plotted on the graph below. (B) XTT results from OVCAR and SKOV3 cells treated with 50 μ M CPP-tri_i for 1-5 days. Each point shows a decrease in relative proliferation compared to the control. A student's t-test was used to determine significant differences where * = p-value \leq 0.05 and *** = p-value \leq 0.01.

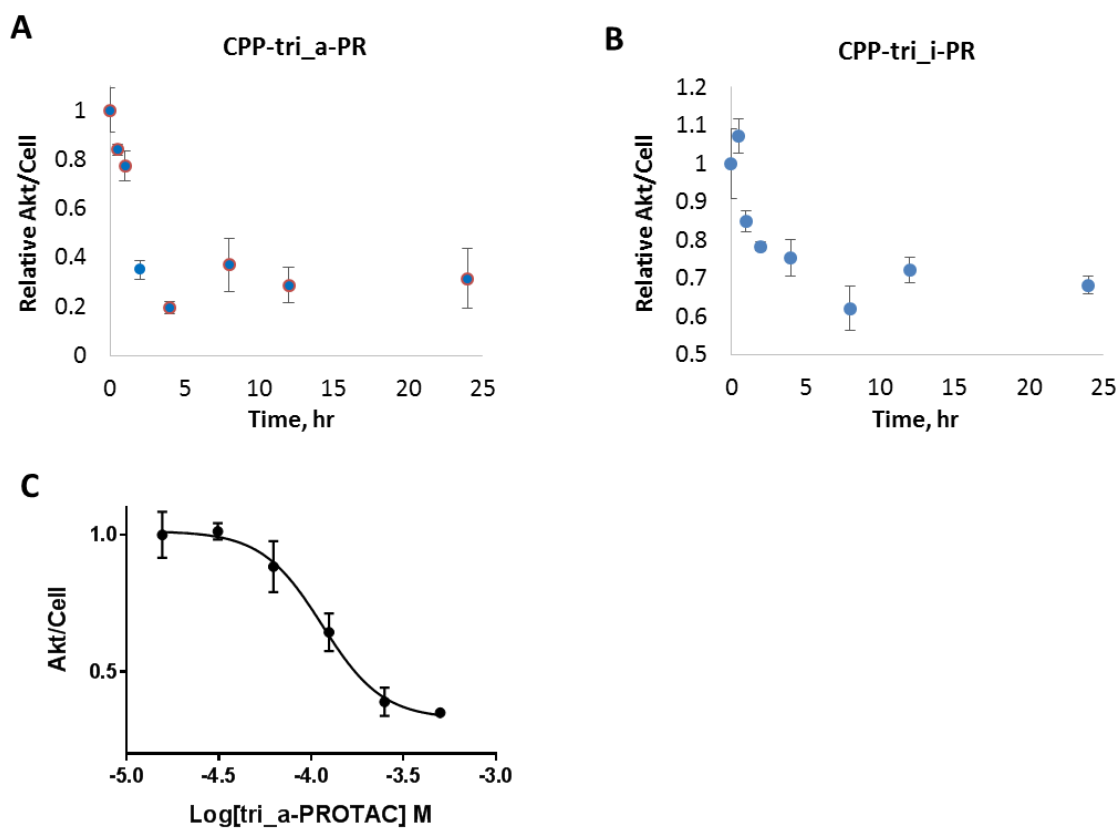


Figure 3.5 – PCC agent-induced degradation of Akt (A) In-cell ELISA measurement of Akt in OVCAR3 cells treated with **CPP-tri_a-PR** for various times. (B) In-cell ELISA measurement of Akt in OVCAR3 cells after treatment with 100 μ M **tri_i-PR** for various times. (C) In-cell ELISA measurement of Akt after 4 hour treatment at variable **CPP-tri_a-PR** doses. Results show dose-dependent degradation of Akt with an EC_{50} value of $128 \pm 19 \mu$ M

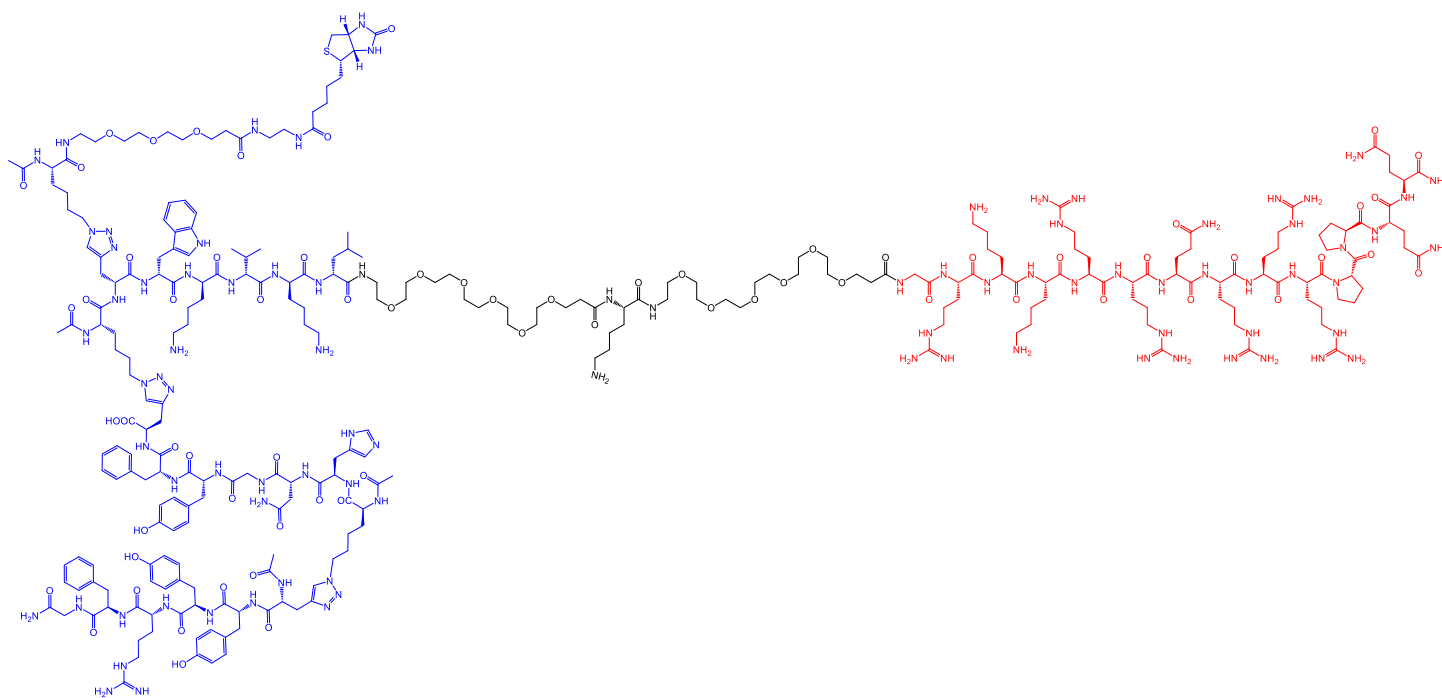


Figure 3.6 - Structure of CPP-tri_a

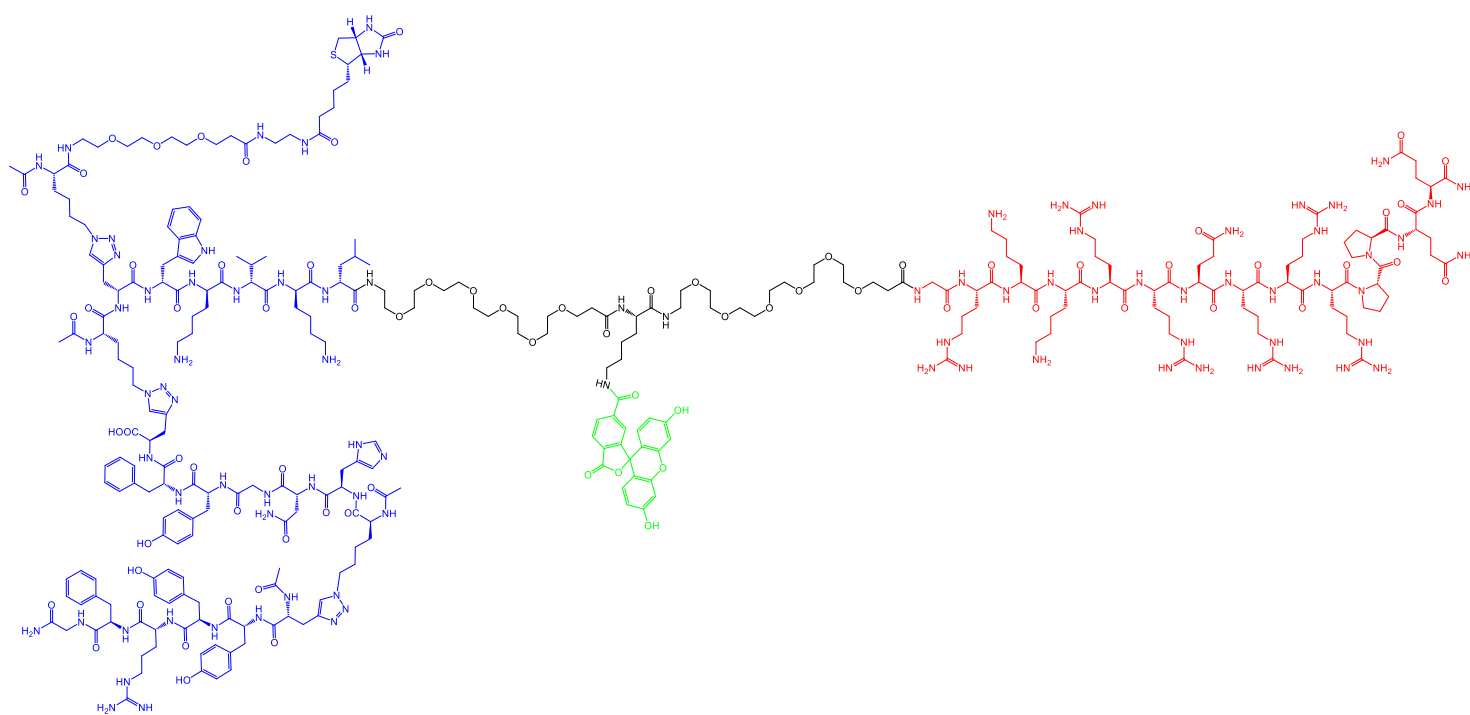


Figure 3.7 - Structure of CPP-tri_a-FL

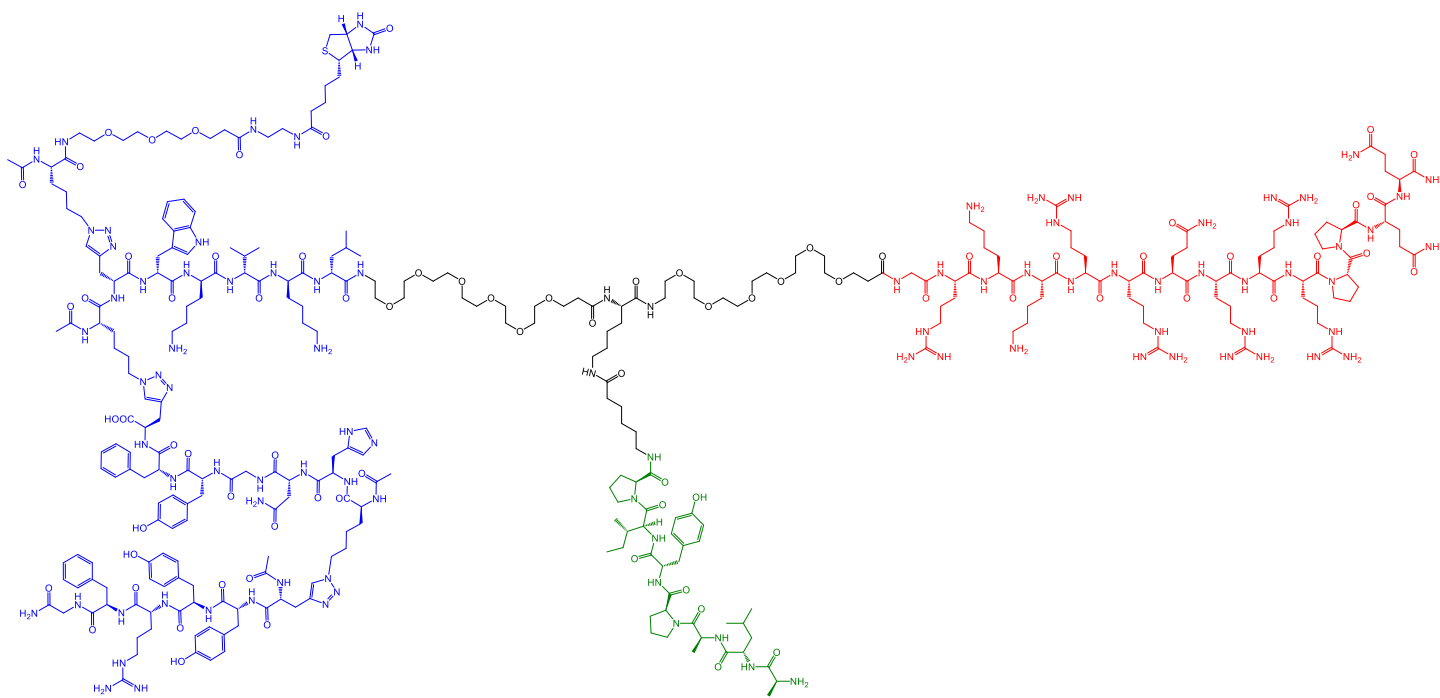


Figure 3.8 - Structure of the CPP-tri_a-PR

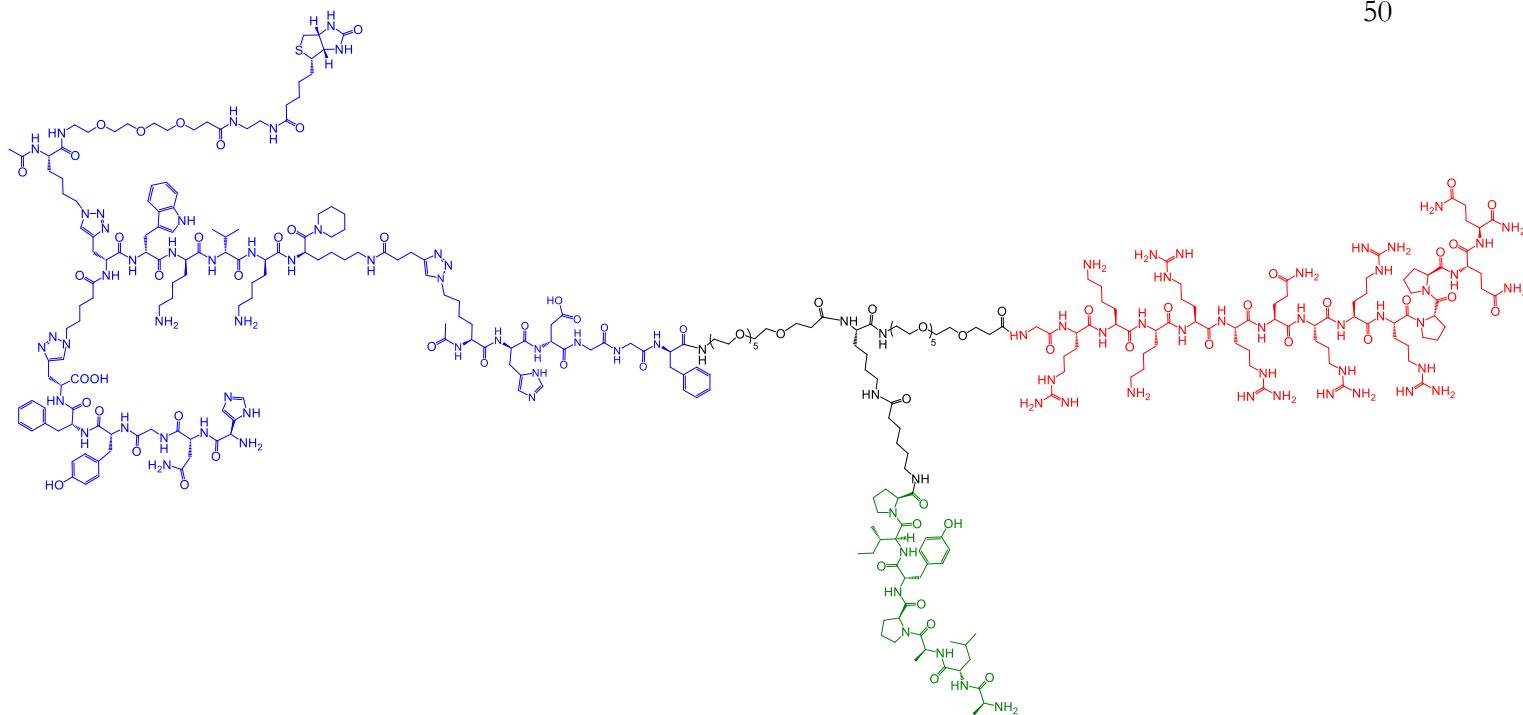


Figure 3.9 - Structure of CPP-tri_i-PR

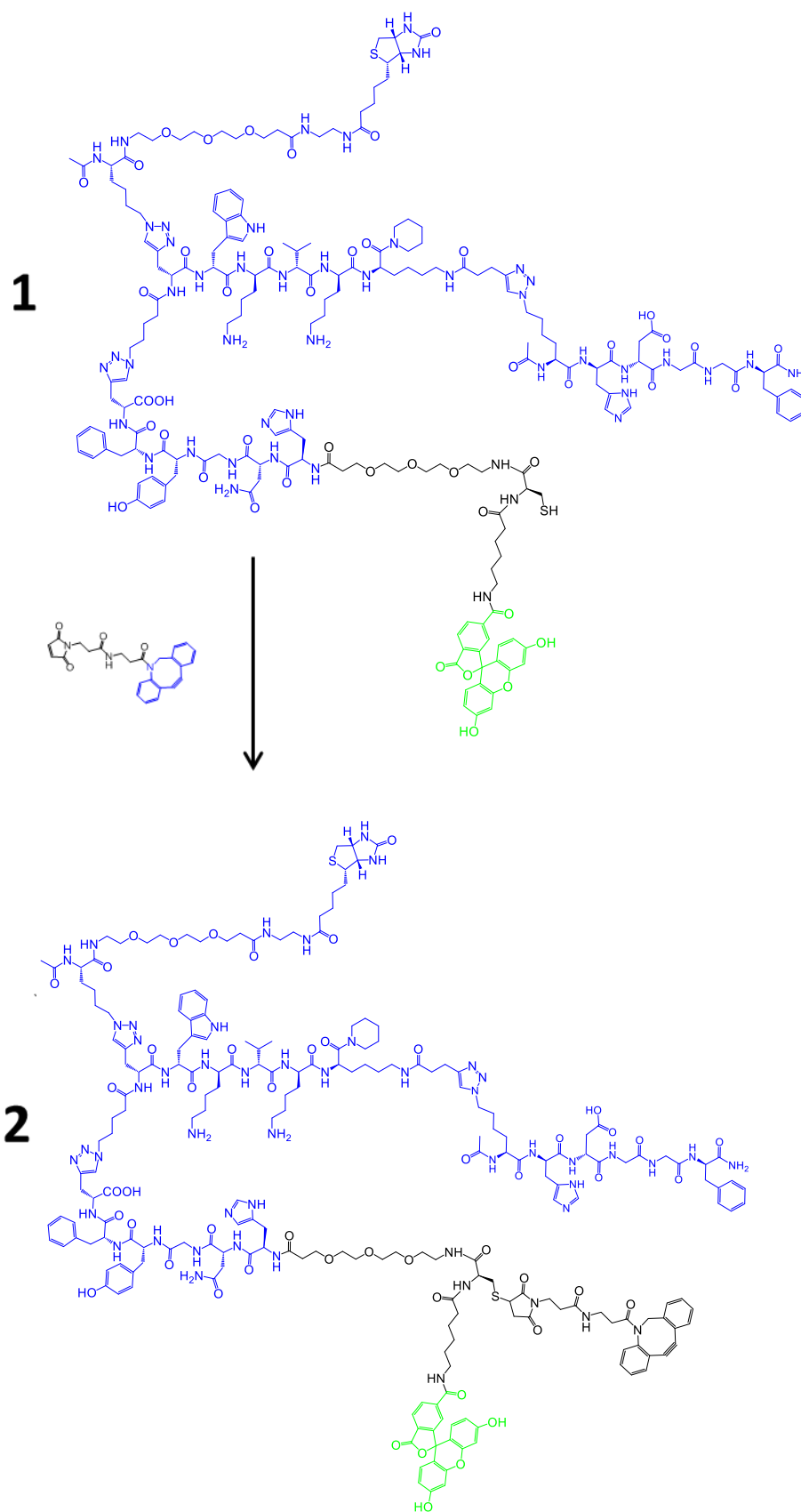
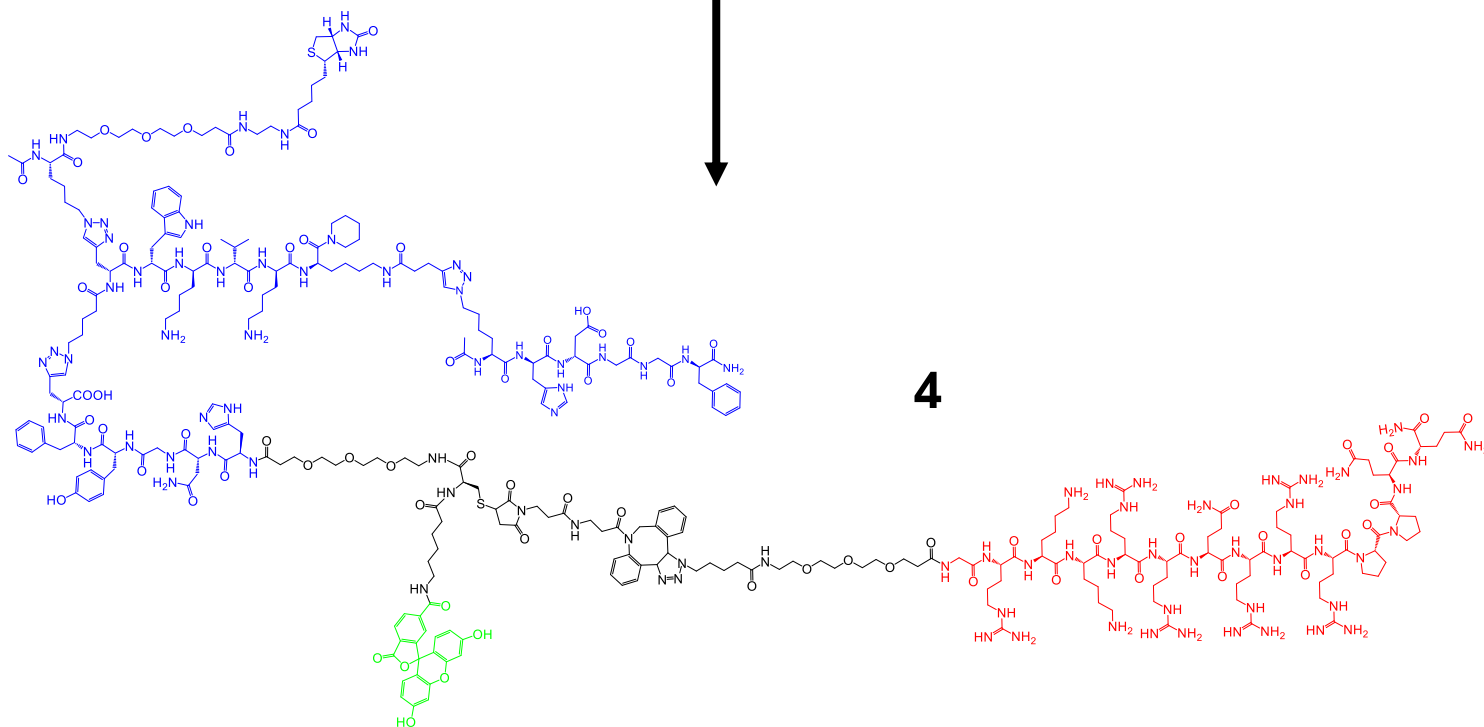
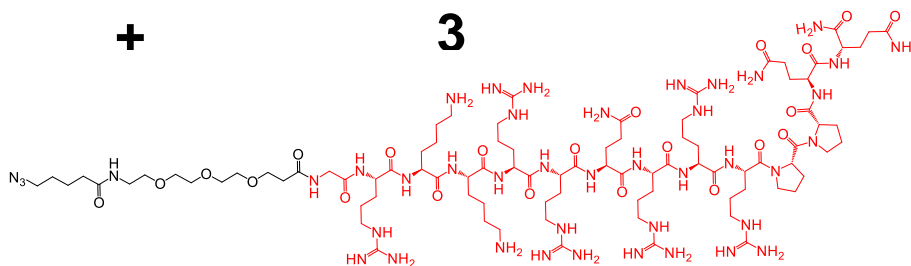


Figure 3.10 – Reaction scheme for synthesizing cyclooctyne-containing tri_i. The C-terminal triligand was synthesized with a cyclooctyne via thiol-maleimide conjugation for copper-free click chemistry.

2

+

3**4**

synthesized with via copper-free click chemistry by reacting the cyclooctyne-containing C-terminal triligand with azide-containing TAT peptide.

3.7 References

1. Lewis, W. G. *et al.* Click Chemistry In Situ: Acetylcholinesterase as a Reaction Vessel for the Selective Assembly of a Femtomolar Inhibitor from an Array of Building Blocks. *Angew. Chem.* **114**, 1095–1099 (2002).
2. Agnew, H. D. *et al.* Iterative In Situ Click Chemistry Creates Antibody-like Protein-Capture Agents. *Angew. Chem. Int. Ed.* **48**, 4944–4948 (2009).
3. Pfeilsticker, J. A. *et al.* A Cocktail of Thermally Stable, Chemically Synthesized Capture Agents for the Efficient Detection of Anti-Gp41 Antibodies from Human Sera. *PLoS ONE* **8**, e76224 (2013).
4. Das, S. *et al.* A General Synthetic Approach for Designing Epitope Targeted Macrocyclic Peptide Ligands. *Angew. Chem. Int. Ed.* **54**, 13219–13224 (2015).
5. Nag, A. *et al.* A Chemical Epitope-Targeting Strategy for Protein Capture Agents: The Serine 474 Epitope of the Kinase Akt2. *Angew. Chem. Int. Ed.* **52**, 13975–13979 (2013).
6. Millward, S. W. *et al.* Iterative in Situ Click Chemistry Assembles a Branched Capture Agent and Allosteric Inhibitor for Akt1. *J. Am. Chem. Soc.* **133**, 18280–18288 (2011).
7. Deyle, K. M. *et al.* A protein-targeting strategy used to develop a selective inhibitor of the E17K point mutation in the PH domain of Akt1. *Nat. Chem.* **7**, 455–462 (2015).
8. Yang, J. *et al.* Crystal structure of an activated Akt/Protein Kinase B ternary complex with GSK3-peptide and AMP-PNP. *Nat. Struct. Mol. Biol.* **9**, 940–944 (2002).
9. Chu, Q. *et al.* Towards understanding cell penetration by stapled peptides. *MedChemComm* **6**, 111–119 (2015).

10. Hassane, F. S., Saleh, A. F., Abes, R., Gait, M. J. & Lebleu, B. Cell penetrating peptides: overview and applications to the delivery of oligonucleotides. *Cell. Mol. Life Sci.* **67**, 715–726 (2009).
11. Heitz, F., Morris, M. C. & Divita, G. Twenty years of cell-penetrating peptides: from molecular mechanisms to therapeutics. *Br. J. Pharmacol.* **157**, 195–206 (2009).
12. Camphausen, K. *et al.* Influence of in vivo growth on human glioma cell line gene expression: Convergent profiles under orthotopic conditions. *Proc. Natl. Acad. Sci. U. S. A.* **102**, 8287–8292 (2005).
13. Engelman, J. A. Targeting PI3K signalling in cancer: opportunities, challenges and limitations. *Nat. Rev. Cancer* **9**, 550–562 (2009).
14. Xu, N., Lao, Y., Zhang, Y. & Gillespie, D. A. Akt: A Double-Edged Sword in Cell Proliferation and Genome Stability. *J. Oncol.* **2012**, e951724 (2012).
15. Berridge, M. V., Herst, P. M. & Tan, A. S. in *Biotechnology Annual Review* (ed. M.R. El-Gewely) **Volume 11**, 127–152 (Elsevier, 2005).
16. Scudiero, D. A. *et al.* Evaluation of a Soluble Tetrazolium/Formazan Assay for Cell Growth and Drug Sensitivity in Culture Using Human and Other Tumor Cell Lines. *Cancer Res.* **48**, 4827–4833 (1988).
17. Kandel, E. S. *et al.* Activation of Akt/Protein Kinase B Overcomes a G2/M Cell Cycle Checkpoint Induced by DNA Damage. *Mol. Cell. Biol.* **22**, 7831–7841 (2002).
18. Ramaswamy, S. *et al.* Regulation of G1 progression by the PTEN tumor suppressor protein is linked to inhibition of the phosphatidylinositol 3-kinase/Akt pathway. *Proc. Natl. Acad. Sci.* **96**, 2110–2115 (1999).

19. Datta, S. R. *et al.* Akt Phosphorylation of BAD Couples Survival Signals to the Cell-Intrinsic Death Machinery. *Cell* **91**, 231–241 (1997).
20. Peso, L. del, González-García, M., Page, C., Herrera, R. & Nuñez, G. Interleukin-3-Induced Phosphorylation of BAD Through the Protein Kinase Akt. *Science* **278**, 687–689 (1997).
21. Arden, K. C. FoxO: Linking New Signaling Pathways. *Mol. Cell* **14**, 416–418 (2004).
22. Zhu, J., Blenis, J. & Yuan, J. Activation of PI3K/Akt and MAPK pathways regulates Myc-mediated transcription by phosphorylating and promoting the degradation of Mad1. *Proc. Natl. Acad. Sci.* **105**, 6584–6589 (2008).
23. Mattson, M. P. & Sherman, M. Perturbed signal transduction in neurodegenerative disorders involving aberrant protein aggregation. *NeuroMolecular Med.* **4**, 109–131 (2003).
24. Jo, H. *et al.* Small molecule-induced cytosolic activation of protein kinase Akt rescues ischemia-elicited neuronal death. *Proc. Natl. Acad. Sci.* **109**, 10581–10586 (2012).
25. Buckley, D. L. & Crews, C. M. Small-Molecule Control of Intracellular Protein Levels through Modulation of the Ubiquitin Proteasome System. *Angew. Chem. Int. Ed.* **53**, 2312–2330 (2014).
26. Sakamoto, K. M. *et al.* Protacs: Chimeric molecules that target proteins to the Skp1–Cullin–F box complex for ubiquitination and degradation. *Proc. Natl. Acad. Sci.* **98**, 8554–8559 (2001).
27. Hines, J., Gough, J. D., Corson, T. W. & Crews, C. M. Posttranslational protein knockdown coupled to receptor tyrosine kinase activation with phosphoPROTACs. *Proc. Natl. Acad. Sci.* **110**, 8942–8947 (2013).

28. Rodriguez-Gonzalez, A. *et al.* Targeting steroid hormone receptors for ubiquitination and degradation in breast and prostate cancer. *Oncogene* **27**, 7201–7211 (2008).
29. Gustafson, J. L. *et al.* Small-Molecule-Mediated Degradation of the Androgen Receptor Through Hydrophobic Tagging. *Angew. Chem. Int. Ed.* **54**, 9659–9662 (2015).
30. Long, M. J. C., Gollapalli, D. R. & Hedstrom, L. Inhibitor Mediated Protein Degradation. *Chem. Biol.* **19**, 629–637 (2012).
31. Neklesa, T. K. & Crews, C. M. Chemical biology: Greasy tags for protein removal. *Nature* **487**, 308–309 (2012).
32. Hewitt, W. M. *et al.* Cell-Permeable Cyclic Peptides from Synthetic Libraries Inspired by Natural Products. *J. Am. Chem. Soc.* **137**, 715–721 (2015).
33. Walensky, L. D. & Bird, G. H. Hydrocarbon-Stapled Peptides: Principles, Practice, and Progress. *J. Med. Chem.* **57**, 6275–6288 (2014).
34. Bock, J. E., Gavenonis, J. & Kritzer, J. A. Getting in Shape: Controlling Peptide Bioactivity and Bioavailability Using Conformational Constraints. *ACS Chem. Biol.* **8**, 488–499 (2013).
35. Bartlett, J. B., Dredge, K. & Dalglish, A. G. The evolution of thalidomide and its IMiD derivatives as anticancer agents. *Nat. Rev. Cancer* **4**, 314–322 (2004).
36. Ito, T. *et al.* Identification of a Primary Target of Thalidomide Teratogenicity. *Science* **327**, 1345–1350 (2010).
37. Lu, J. *et al.* Hijacking the E3 Ubiquitin Ligase Cereblon to Efficiently Target BRD4. *Chem. Biol.* **22**, 1–9 (2015).

38. Winter, G. E. *et al.* Phthalimide conjugation as a strategy for in vivo target protein degradation. *Science* **348**, 1376–1381 (2015).
39. Todorovski, T., Fedorova, M. & Hoffmann, R. Mass spectrometric characterization of peptides containing different oxidized tryptophan residues. *J. Mass Spectrom.* **46**, 1030–1038 (2011).
40. Perdivara, I., Deterding, L. J., Przybylski, M. & Tomer, K. B. Mass spectrometric identification of oxidative modifications of tryptophan residues in proteins: chemical artifact or post-translational modification? *J. Am. Soc. Mass Spectrom.* **21**, 1114–1117 (2010).
41. Krishnamurthy, V. R. *et al.* Chemoselective Immobilization of Peptides on Abiotic and Cell Surfaces at Controlled Densities. *Langmuir* **26**, 7675–7678 (2010).

DISCOVERY OF THE FIRST SELECTIVE LIGANDS AGAINST THE MUTANT ONCOPROTEIN K-RAS^{G12D}

4.1 Summary of Contributions

I have worked independently on this project for the majority of its existence. I identified the target and the degradation strategy and have conducted the majority of the experiments myself. However, I did greatly benefit from several technical advances to the screening platform that were made by my colleagues such as the epitope targeting strategy and the macrocyclic peptide libraries. I also received help from several amazing summer students over the years. This work has not yet been published but a patent application is currently pending.

4.2 Introduction

The *KRAS* oncogene is a member of the Ras family of GTPases that are involved in numerous cellular signaling processes.¹ The Ras protein can act as a molecular switch by adopting two distinct conformations, depending on the nucleotide that is bound to the protein. When bound to GTP Ras is in the active state and sends downstream signals that result in cell division. Ras is inactivated upon GTP hydrolysis to GDP and cells can then enter a resting state.² Activating Ras mutations are present in up to 30% of all tumors, including as many as 90% of pancreatic cancers.³ K-Ras is the Ras family member that most often associated with tumorigenesis. Ras mutations tend to abrogate the enzymatic activity and render the protein constitutively active due to the persistent GTP-bound state - active Ras will then result in increased cell proliferation due to upregulation of the MAPK and PI3K pathways, respectively.⁴ Due to the clinical significance of this protein, many attempts have been made to develop Ras inhibitors but no targeted therapy has been developed thus far. This is largely due to the difficulty in outcompeting GTP for the K-Ras binding pocket in cells, and the lack of known allosteric regulatory sites.⁵

A recent study presented the first compounds that specifically target a mutant form of K-Ras.⁶ Non-small cell lung cancer often presents a K-Ras^{G12C} mutation that is associated with poor prognosis.⁷ The nucleophilicity of the cysteine thiol group can be targeted with electrophilic compounds and screening K-Ras^{G12C} against such a chemical library yielded promising hits that could inhibit the mutant protein – efforts are now underway to optimize

these compounds towards potential clinical candidates.⁸ However, this strategy is not applicable to targeting other more common Ras mutations.

The most common K-Ras mutation is glycine 12 to aspartic acid (G12D) – this mutation accounts for nearly half of all K-Ras oncoproteins.⁹ We recently used an *in situ* click chemistry screen to identify PCC agents that are the first known compounds that bind K-Ras with preference for the oncogenic G12D mutation. Our compounds are capable of binding to the surface of K-Ras, thus circumventing difficulties encountered in previous research where a binding pocket was needed.

4.3 Results and discussion

Epitope targeting screen. To develop these new compounds we used the epitope-targeting PCC agent platform to target the specific region of interest.¹⁰ First, the non-cancerous wild-type K-Ras epitope encompassing the glycine 12 residue was synthesized (Figure 4.1A). The leucine residue near glycine 12 was replaced with propargylglycine in order to provide a click handle where members of an azide library could then bind. This azide library was a macrocyclic one-bead-one-compound (OBOC) peptide library with 1.4×10^6 unique members (Figure 4.2).¹¹ Approximately 200 hits clicked to the wild-type K-Ras fragment, and were removed from the screen in order to avoid selecting hits that bind to the wild-type protein (Figure 4.3). The remaining beads were then incubated with another propargylglycine-functionalized fragment – this time containing the oncogenic G12D mutation (Figure 4.1B) – and seven hit beads were identified. The seven hits yielded nine

potential compounds due to ambiguity in some of the sequencing results (Table 4.1). The nine sequences were then synthesized and tested for binding to the full-length K-Ras^{G12D} protein by ELISA assays (Figure 4.4, Appendix A). The best binder was also tested for selectivity to wild type or G12D K-Ras and showed a preference for K-Ras^{G12D}. Hit seven demonstrated the best performance in the single point ELISA assays and the variable region was identified as LRGDR. Hit 7b, which was subsequently renamed 7b1 after a second series of compounds was generated, has an affinity for K-Ras^{G12D} of 33 μ M and approximately 4:1 selectivity over the wild type protein (Figure 4.5). The mutant selectivity of hit 7b1 makes this compound an extremely promising initial candidate given the significance of this oncoprotein and the fact that no K-Ras^{G12D}-selective compounds have been reported to date.

Second generation hits. In order to optimize hit 7b1 a second generation of compounds was synthesized based on rational modifications to the 7b1 variable region (Appendix A) – the sequences of the new compounds are listed in Table 4.2. The new PCC agent candidates were tested via single point ELISA assays and two new compounds of particular interest emerged – the compounds were identified as hits 7b5 and 7b10 (Figure 4.6).

Characterization of ligand 7b10. From the single point ELISA assay of the new compounds hit 7b10 showed the greatest signal for K-Ras^{G12D} binding – this compound was therefore chosen for further characterization. Hit 7b10 was generated by replacing the arginine at position 5 in the variable region of 7b1 with the unnatural amino acid 4-guanidine phenylalanine (Gnf),¹² resulting in a new sequence of LRGD-Gnf. Hit 7b10

showed improved affinity of 17.5 μM for K-RasG12D and maintained 3:1 selectivity for the mutation over the wild type protein (Figure 4.7).

In addition to assessing the binding properties of 7b10 we also sought to investigate any potential effects this compound may have on the GTPase activity of K-Ras. Ras sends downstream signals for cell growth and division when it is in the GTP-bound state. A potential Ras inhibitor would stimulate Ras enzymatic activity in order to promote GTP hydrolysis to GDP resulting in attenuation of the downstream signaling cascade. Indeed, when K-RasG12D complexed with a GTPase Activating Protein (GAP) was treated with 7b10 the rate of GTP hydrolysis increased seven-fold relative to the wild type K-Ras-GAP complex (Figure 4.7C). Basal levels of K-Ras GTPase are very low so a GAP was added to enhance the signal to noise in the GTPase assay format. In addition to the novel mutant binding selectivity, 7b10 is also unique in its ability to restore Ras enzymatic activity as no such compounds has been reported. One possible explanation for the restoration of RAS/GAP GTPase activity is that the Gnf residue could be mimicking the GAP arginine finger that promotes the hydrolysis reaction. Normally GAPs stimulate Ras GTP hydrolysis by inserting an arginine residue, termed the arginine finger, near the GTP terminal phosphate that stabilizes the transition state of the hydrolysis reaction. Oncogenic Ras mutations at codons 12 and 13 are known to occlude the arginine finger from interacting with GTP through steric hindrance and thus render the protein GAP-insensitive.¹ Perhaps the planar structure of the benzyl group in the Gnf side chain allows for insertion of the guanidium moiety into a productive GTPase-activating orientation. This important result warrants further investigation into the chemical mechanism of GTPase activation and

potential downstream K-Ras pathway inhibition in cells treated with 7b10. Stimulation of oncogenic K-Ras GTPase activity is expected to inhibit K-Ras signaling and validation of this result would demonstrate that 7b10 is a useful tool compound for perturbing oncogenic K-Ras signaling in cells.

Understanding the binding of our PCC agent with K-Ras^{G12D} can provide guidance for rationally optimizing the PCC agent to improve its binding and functional properties. We next sought to identify the key interacting residues in 7b10 by conducting an alanine scan. A set of five new variants of 7b10 were synthesized with each compound presenting an alanine substitution to one of residues in the variable region (Figure 4.8). If an alanine substitution abrogates the affinity for K-Ras that would identify a potentially critical interacting residue. Conversely, if a residue can tolerate an alanine substitution and maintain its affinity for the target protein then that residue is likely not involved in binding. Indeed, the results from the alanine scan indicate that the only tolerable alanine substitution is at aspartic acid at position four in the variable region. This result provides a logical path for 7b10 optimization. The aspartic acid at position four can potentially be replaced with another residue that does contribute to binding and improve the overall performance of the ligand. Alternatively, position four may also be a suitable branch point to screen for a secondary ligand in an additional *in situ* click screen.

Characterization of ligand 7b5. Another interesting ligand identified in the second generation of hits was 7b5. This compound was generated by substituting the aspartic acid at position four of 7b1 with a proline resulting in a variable region of LRGDR (Figure 4.9).

However, this sequence did not stimulate K-Ras enzymatic activity when used in the GTPase assay — on the other hand, 7b5 appears to inhibit K-Ras (Figure 4.7C), which is the opposite of what is required for a potential K-Ras inhibitor. We hypothesized that substituting the anionic aspartic acid to the more hydrophobic proline residue could yield a cell-penetrant PCC agent — it is believed that peptides are more likely to be cell penetrant with cationic and/or hydrophobic residues.¹³ Compound 7b5 maintained an affinity of 56.6 μ M for K-Ras^{G12D} in spite of the proline substitution. Despite the lack of influence on Ras enzymatic activity (Figure 4.7C) this peptide could potentially be utilized as targeting ligand for PROTAC development, and indeed appears to reduce K-Ras^{G12D} expression on its own through an unknown mechanism (Figure 4.12).¹⁴ 7b5 was synthesized with the HIF-1 α degradation signal¹⁵ with and without a cell penetrating peptide (CPP) in order to test its performance as a potential K-Ras-PROTAC (Figures 4.10 and 4.11). The compounds were tested in the pancreatic carcinoma cell line Panc 08.13 because this cell line is known to be *KRAS*^{G12D} homozygous.¹⁶ When the cells were treated with the 7b5-PROTACs a marked decrease in Ras protein was observed via western blot analysis. In order to test if the Ras degradation was mediated by the proteasome the experiment was repeated with an additional control. In the next experiment the cells were also pre-treated with the proteasome inhibitor MG13 before addition of the 7b5 PROTACs and the Ras degradation no longer occurred, supporting the notion that the 7b5-PROTAC is inducing proteasomal degradation of K-Ras^{G12D} (Figure 4.12). Surprisingly, in the second experiment unmodified 7b5 without the degradation tag appears to also decrease Ras expression (Figure 4.12B, lane 4). Speculatively, perhaps the hydrophobic glycine-proline sequence in 7b5 is causing the protein to misfold and undergo non-specific proteasomal

degradation. Destabilization of the protein could be tested via a thermal denaturation assay to determine the melting temperature with and without the compound.

4.4 Conclusion

This work demonstrates the capacity of the PCC agent screening platform to develop ligands against difficult protein targets. Oncogenic K-Ras proteins were considered undruggable for many years and they still remain among the holy grails of cancer therapeutic targets.¹⁷ The epitope targeting strategy combined with the macrocyclic peptide library resulted in multiple ligands with previously undiscovered properties. Until now no ligand has been presented with selectivity for K-Ras^{G12D} oncoprotein but a single PCC agent screen has produced at least three such potential ligands. In addition, compound 7b10 is the first known molecule to stimulate mutant K-Ras GTPase activity in *in vitro* biochemical assays. A future step towards characterizing compound 7b10 would be to test this result in cells through a RAS-GTP binding assay as well assessing downstream signaling pathway modulation. Finally, 7b5-PROTAC development is a promising approach to induced degradation of K-Ras^{G12D} in carcinoma cells. Unexpectedly, unmodified 7b5 also reduced K-Ras protein expression and it will be important to determine the mechanism of action in order to confirm the specificity of the compound towards K-Ras. While significant work must still be done to develop the first efficacious Ras inhibitors, this study presents proof of concept for two potential new strategies to target this difficult protein: enzymatic activation and targeted degradation.

4.5 Material and Methods

Solid phase peptide synthesis general protocol

Peptides were synthesized on Rink Amide MBHA or Biotin Novatag either by hand, on a Liberty1 Microwave Peptide Synthesizer (CEM), or on a Titan 357 Automatic Peptide Synthesizer (AAPPTec). Peptide coupling reactions were done in NMP with 2 equivalents of amino acid, 2 equivalents of HATU, and 6 equivalents of N,N-Diisopropylethylamine (Sigma). For removal of N α -Fmoc protecting groups, a solution of 20% piperidine in NMP was used.

Synthesis of K-Ras synthetic epitopes

Modified K-Ras wild type and G12D epitopes were synthesized with acetylene-functionalized amino acids for use in the *in situ* click screen (Figure 4.1). The epitopes were derived from amino acids 2-22 from the K-Ras protein sequence with valine14 substituted with propargylglycine (Pra). Additionally, an 11-unit polyethylene glycol (PEG) spacer and biotin were added to the C-terminus of the synthesized fragments for detection with streptavidin during the screen. The sequence of the wild type K-Ras epitope fragment was NH₂-TEYKLVVVGAGG[Pra]GK-PEG₁₁-Biotin. The sequence of the G12D fragment was NH₂-TEYKLVVVGADG[Pra]GKSALTIQ-PEG₁₁-Biotin. The epitopes were synthesized by solid phase peptide synthesis (SPPS) on biotin novatag resin according to standard protocols. The peptides were removed from the resin and deprotected in a TFA cleavage solution of 95% TFA, 2.5% H₂O, and 2.5% triethylsilane for two hours at room temperature. The cleavage solution was filtered to remove the resin and added

dropwise to an ice-cooled solution of diethyl ether to precipitate the crude peptide. Crude peptides were then purified via HPLC.

Synthesis of macrocyclic peptides

The macrocyclic peptides, including the library and hit sequences, were made by first synthesizing the linear sequence H₂N-Pra-X₁X₂X₃X₄X₅-Az₄ via SPPS. On-bead Cu catalyzed click reactions were then performed to cyclize the peptide through the Pra and Az₄ side chains. The resin was treated with 1.5 equivalents of CuI (Sigma) and 2.5 equivalents of ascorbic acid (Sigma), in a solution of 20% piperidine in DMF. The reaction was performed overnight at room temperature. Excess copper was removed from the resin by washing with a Cu chelating solution (5% (w/v) sodium diethyl dithiocarbamate, 5% (v/v) DIEA in DMF).

Synthesis of 7b5 PROTACs

7b5-Hif and 7b5-Hif-TAT PROTACs that were used in the cell assays were made from previously-synthesized 7b5 peptide. After the 7b5 macrocycle was synthesized on resin Ahx was coupled to the N-terminus as a linker followed by the addition of the Hif-1 α degradation sequence ALAPYIP using standard SPPS. The peptide was then either cleaved from the resin as 7b5-Hif (Figure 4.10) or the HIV-TAT sequence was added to create 7b5-Hif-TAT (Figure 4.11).

HPLC purification of peptides

All peptides were purified using a preparative or semi-preparative scale HPLC with a C18 reverse phase column. A gradient of double distilled water and HPLC grade acetonitrile and 0.1% TFA was used for all purifications.

Mass spectrometry analysis

All intermediate and final peptides were analyzed via MALDI-TOF-MS using a Voyager DE-PRO MALDI TOF-MS system (Applied Biosystems). Peptides were dissolved in 50:50 water/acetonitrile with 0.1% trifluoroacetic acid at a final concentration of 10 pmol/ μ L. 1 μ L of the peptide sample was then added to 10 μ L of a saturated solution of MALDI matrix, either α -cyano-4-hydroxycinnamic acid or Sinapinic Acid, in 50:50 water/acetonitrile with 0.1% trifluoroacetic acid and analyzed via MALDI-TOF MS.

Screening of KRAS Fragments to Identify Cyclic Anchors

Preclear: Approximately 500 mg (~1,400,000) beads of 5-mer macrocyclic peptide library (Figure 4.2) was obtained. The library sequence was Az4-[Pra]-X₁X₂X₃X₄X₅-[Az4]-M-TG where X = 18 amino acids (excluding Cys and Met) while [Pra] and [Az4] are connected via a 1,4-triazole linkage on tentagel resin (TG).

Library was allowed to swell in TBS for 6 hours and then blocked overnight at 4 °C with 1% BSA in TBS + 0.1% Tween 20 (= Blocking Buffer). The following day the library was washed with fresh blocking buffer and then incubated with 1:10,000 anti-Biotin-AP Antibody (Sigma Aldrich) in Blocking Buffer for 1 h at RT. Beads were then washed five

times with Blocking Buffer, five times with Wash 1 buffer (0.1% BSA in TBS + 0.1% Tween 20), and then five times with 3 mL Wash 2 buffer (TBS + 0.1% Tween 20). The preclear was then developed with BCIP: NBT (Promega #S3771). The purple hit beads represent false hits that bind non-specifically to the anti-Biotin antibody and were thus removed.

The remaining clear beads were washed with 7.5 M guanidine hydrochloride, pH 2.0 for 30 min, then rinsed with water ten times. To remove residual purple color the clear beads were then incubated in NMP for two hours. After washing with water to remove the NMP the beads were blocked overnight at 4 °C with Blocking Buffer.

Anti-screen against wild type K-Ras polypeptide target: The next day the precleared library was incubated with 50 μ M (2% DMSO, v/v) wild type K-Ras fragment in blocking buffer for 5 hours at room temperature to allow the *in situ* click reaction to occur. The screen then proceeded as in the preclear above. Briefly, the beads were washed, stripped in 7.5 M guanidine hydrochloride, washed, blocked, probed with anti-Biotin-AP, and developed with BCIP/NBT. Approximately 200 purple hits were identified that represent library elements that bound to the wild type K-Ras fragment. After removal of the purple beads the library was again decolorized and blocked overnight in preparation for the target screen with the G12D epitope.

Product screen against the mutant K-Ras^{G12D} fragment: The next day the precleared and anti-screened library was incubated with the mutant polypeptide target. 25 μ M G12D

fragment was incubated with the library to undergo a second *in situ* click reaction, this time against the desired target. The library was then probed and developed as before and 7 hit beads were identified. Hit beads were then sequenced via Edman degradation and the results are shown in Table 4.1.

Protein expression and purification.

His-tagged human K-Ras^{G12D} (isoform 4B) GTPase domain (residues 1-169) was transformed into E. coli BL21(DE3) cells. Bacterial cultures were grown in LB broth with ampicillin until the OD₆₀₀ reached approximately 0.5. Expression was induced with 0.5 mM IPTG at 18°C for about 18 hours overnight and cells were harvested by centrifugation and pellets were stored at -80°C.

Cell pellets were suspended in 20 mM Tris, pH 8.0 with 500 mM NaCl, 5 mM imidazole and 1 mM DTT. Cells were then lysed by microfluidizer and cellular debris was removed by ultracentrifugation. Crude lysate was then passed through a 0.22 µm filter and purified with a Ni-NTA column and eluted with an imidazole gradient. K-Ras^{G12D} fractions were then pooled and then buffer exchanged into 20 mM HEPES, pH 7.5, 150 mM NaCl, and 1 mM DTT using a HiTrap desalting column. Protein was then purified by gel filtration with a Superdex 75 column and pure protein was aliquoted and flash frozen in liquid nitrogen and thawed as needed.

ELISA of hit peptides against full-length K-Ras protein

1 μ M of the biotinylated hit peptides were first immobilized onto 96-well Neutravidin ELISA plates (Pierce) for 2 hours at room temperature in binding buffer: Tris-buffered saline TBS with 0.1% Tween-20 (TBST) and 0.1% BSA. The plates were then blocked with 5% BSA in TBST for 1 hour, followed by incubating with full-length K-Ras protein in binding buffer for 30 minutes. For single point ELISA assays 100 nM K-Ras protein was added per well. For EC₅₀ determination the protein was added at various concentrations. After washing three times with TBST the plate was then treated with a 1:1000 dilution of the anti-RAS rabbit mAb (Cell Signaling Technology) in binding buffer for thirty minutes, washed three times with TBST, incubated with anti-Rabbit-HRP secondary antibody (Cell Signaling Technology) for thirty minutes, and developed with TMB substrate (KPL) for five to ten minutes. The absorbance of samples at 450 nm wavelength was measured using a FlexStation 3 microplate reader (Molecular Devices).

K-Ras GTPase assay

To assess the effects of compound 7b10 and 7b5 on K-Ras enzymatic activity a GTPase assay kit (Sigma #MAK113-1KT) was used. Recombinant K-Ras protein was combined with the recombinant human protein RAS GTPase Activating Protein Protein 1 (MyBiosource #MBS951091) to enhance the activity to detectable levels. In a 96-well plate 20 μ L of 0.7 mg/mL K-Ras protein (0.6 nmol) was combined with 1 μ L of 0.1 mg/mL RasGAP1, 5 μ L of 100 μ M peptide (7b5 or 7b10), 20 μ L reaction buffer (20 mM HEPES pH = 7.5, 150 mM NaCl, 1 mM DTT, 20 mM MgCl₂), and 10 μ L of 4 mM GTP and the reaction was allowed to proceed at room temperature for 30 minutes followed by the

addition of the 200 μ L malachite green reagent (Sigma) and the absorbance was measured at 620 nm.

Cell Culture

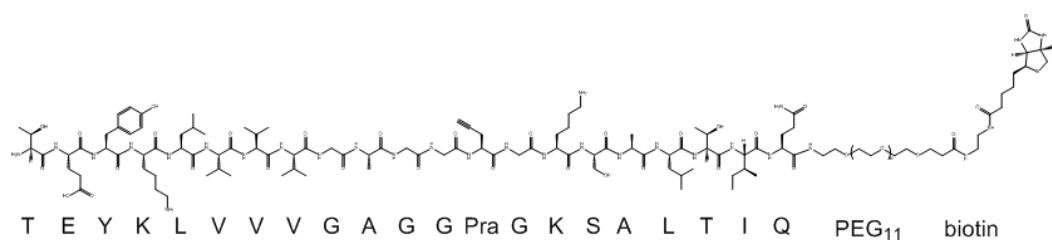
Panc 08.13 cells were purchased from American Type Culture collection (Manassas, VA, USA) and cultured under conditions specified by the provider.

Immunoblotting

Western blots were performed according to standard protocols. Briefly, cells were lysed with cell lysis buffer (Cell Signaling Technology) containing protease and phosphatase inhibitors (Cell Signaling Technology). Cell lysates were quantified with a Bradford protein assay (Thermo Scientific, Waltham, MA, USA) and prepared for gel electrophoresis in Laemmli sample buffer and reducing agent. Twenty micrograms of cell lysate were added to precast polyacrylamide gels (Bio-Rad Laboratories, Inc., Hercules, CA, USA), and proteins were separated by electrophoresis followed by transfer to PVDF membrane. Membranes were then blocked and probed with primary antibodies followed by horseradish peroxidase-conjugated secondary antibodies. The bands were visualized via a chemiluminescent substrate (Thermo Scientific). Ras and tubulin antibodies were from Cell Signaling Technology and used according to manufacturer protocol.

4.6 Figures

A



B

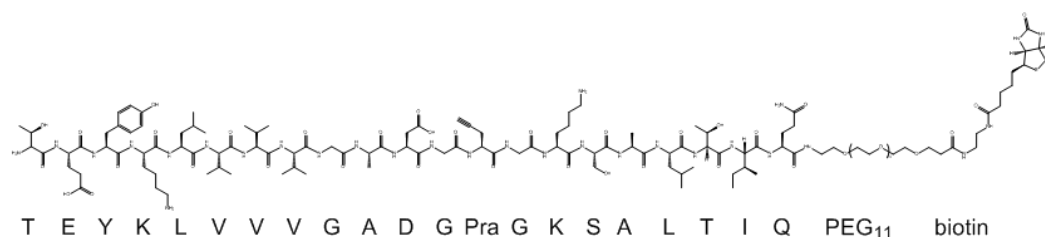


Figure 4.1 – Structure of K-Ras synthetic epitopes. (A) The structure of the wild type K-Ras epitope that was used in the anti-screen. The epitope consists of K-Ras residues 2-20 with a V14Pra substitution for the *in situ* click reaction. (B) The molecular structure of the K-Ras^{G12D} epitope used in the target screen. The epitope consists of K-Ras residues 2-20 with the G12D mutation and V14Pra substitution for the *in situ* click reaction.

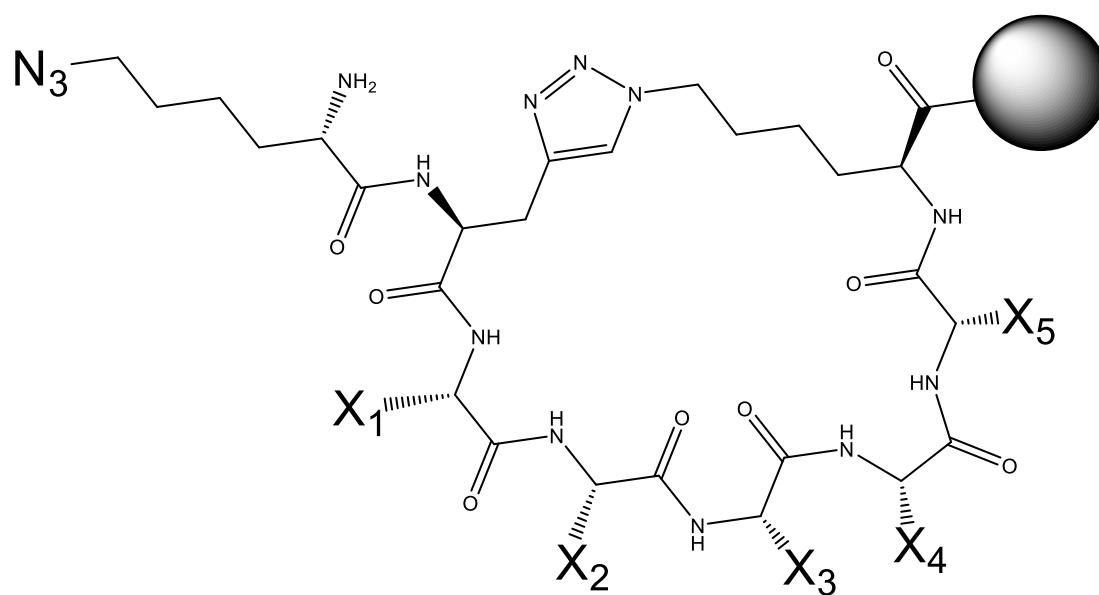


Figure 4.2 – Structure of the macrocyclic peptide library.

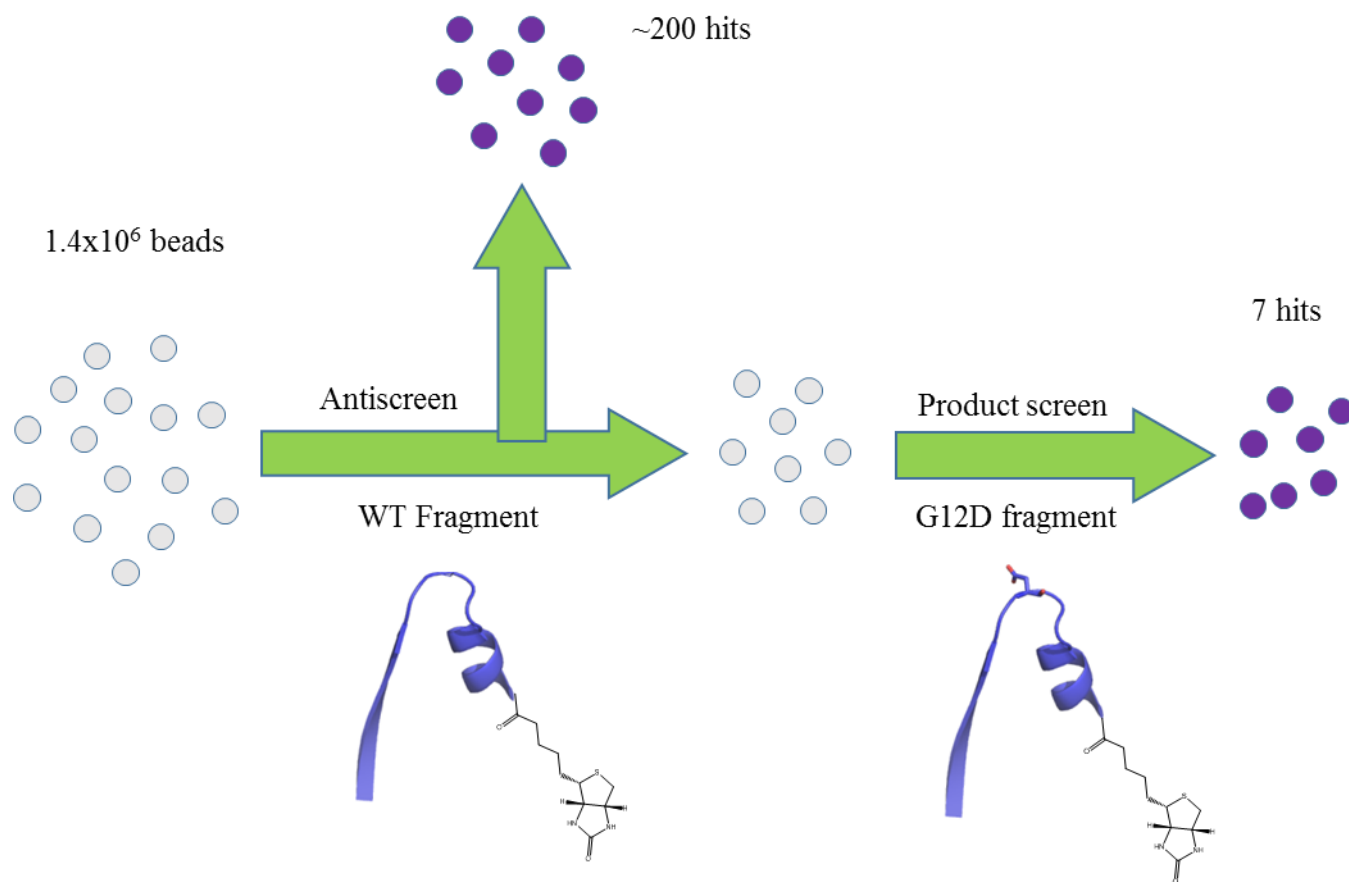


Figure 4.3 – Layout of the K-Ras epitope-targeted PCC agent screen. A 1.4×10^6 member macrocyclic library was first anti-screened against the wild type K-Ras sequence corresponding to residues 2-20. Approximately 200 hit peptides reacted with the wild type epitope and were removed. The remaining beads were then incubated with the G12D fragment, resulting in 7 hit beads.

Variable region

Sequence	X ₁	X ₂	X ₃	X ₄	X ₅
1	N	D	E	T	Y
2	P	S	E	E	G
3	S	E	E	G	G
4	E	G	T	G	T
5	Y	E	Q	G	E
6	Y	G	E	Q	E
7	L	R	G	D	R
8	Q	E	K	P	P
9	E	L	T	F	G

Table 4.1 – Hit sequences from K-Ras^{G12D} epitope-targeted anchor screen. The seven hit beads produced nine possible sequences. Sequences 2 and 3, as well as 5 and 6, represent multiple possible sequences from a single hit bead.

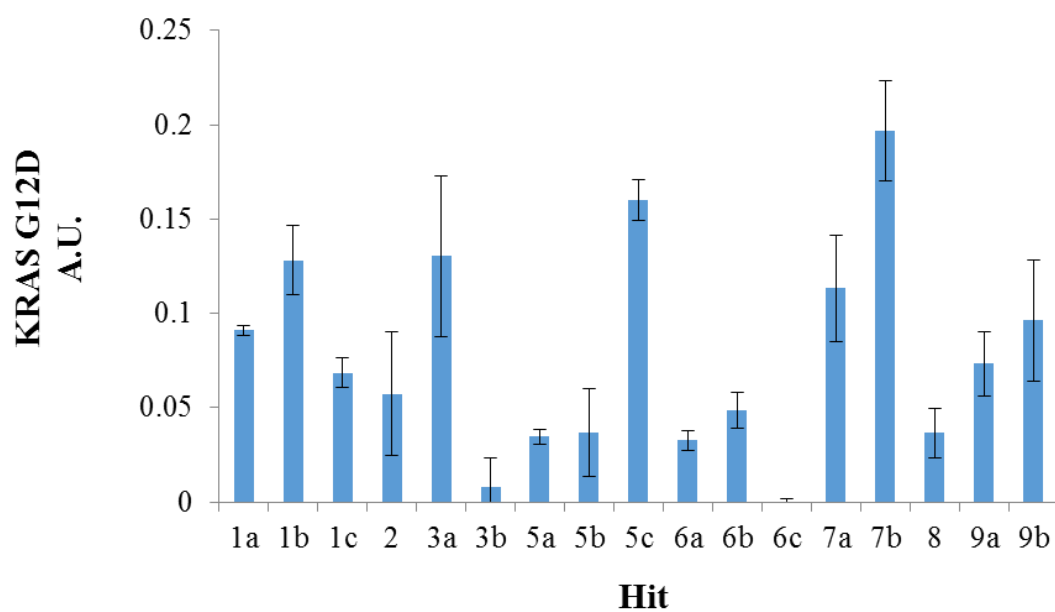


Figure 4.4 – Single point ELISA of hit peptides against K-Ras^{G12D} protein. The hit peptides were tested against the full-length mutant protein. Several sequences produced multiple isobaric fractions after HPLC purification.

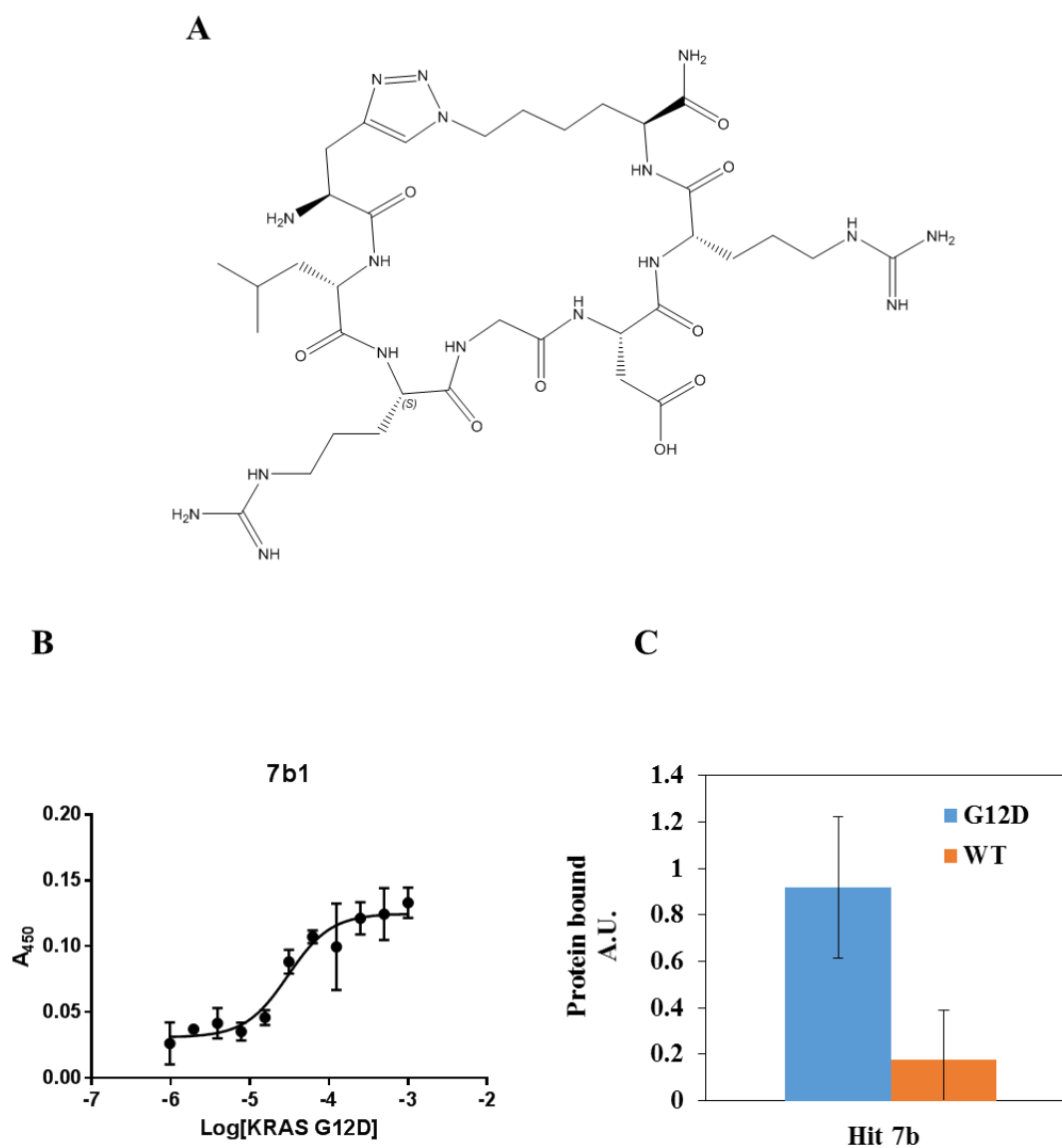


Figure 4.5 – Characterization of hit 7b1. (A) Molecular structure of hit 7b1 from the initial anchor screen. (B) Binding curve between hit 7b1 and K-Ras^{G12D} obtained via ELISA assay. (C) A single point ELISA assay assessing the selectivity of 7b1 for wild type vs. G12D K-Ras. The peptide shows an approximately 4:1 selectivity for the mutant protein.

Sequence							
Peptide		X ₁	X ₂	X ₃	X ₄	X ₅	
7b1	Pra	L	R	G	D	R	Az4
7b2	Az4	L	R	G	D	R	Pra
7b3	Pra	L	R	G	D	R	Az3
7b4	Pra	V	R	G	D	R	Az4
7b5	Pra	L	R	G	P	R	Az4
7b6	Pra	L	R	G	E	R	Az4
7b7	Pra	L	homo-Arg	G	D	R	Az4
7b8	Pra	L	R	G	D	homo-Arg	Az4
7b9	Pra	L	Gnf	G	D	R	Az4
7b10	Pra	L	R	G	D	Gnf	Az4
7b11	Pra	L	R	G	N	R	Az4
7b12	Pra	L	R	G	Q	R	Az4

Table 4.2 – Sequences of second generation of hits designed from hit 7b1. Members of the new series of compounds contained the unnatural amino acids homoarginine (homo-Arg) or 4-guanidine phenylalanine (Gnf).

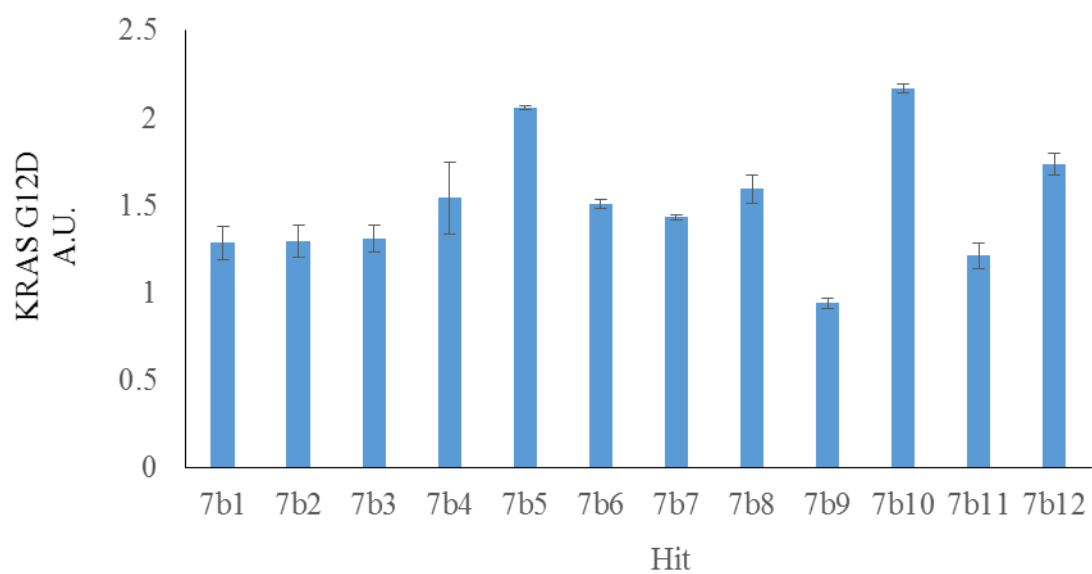


Figure 4.6 – Single point ELISA of second generation hits K-Ras^{G12D}.

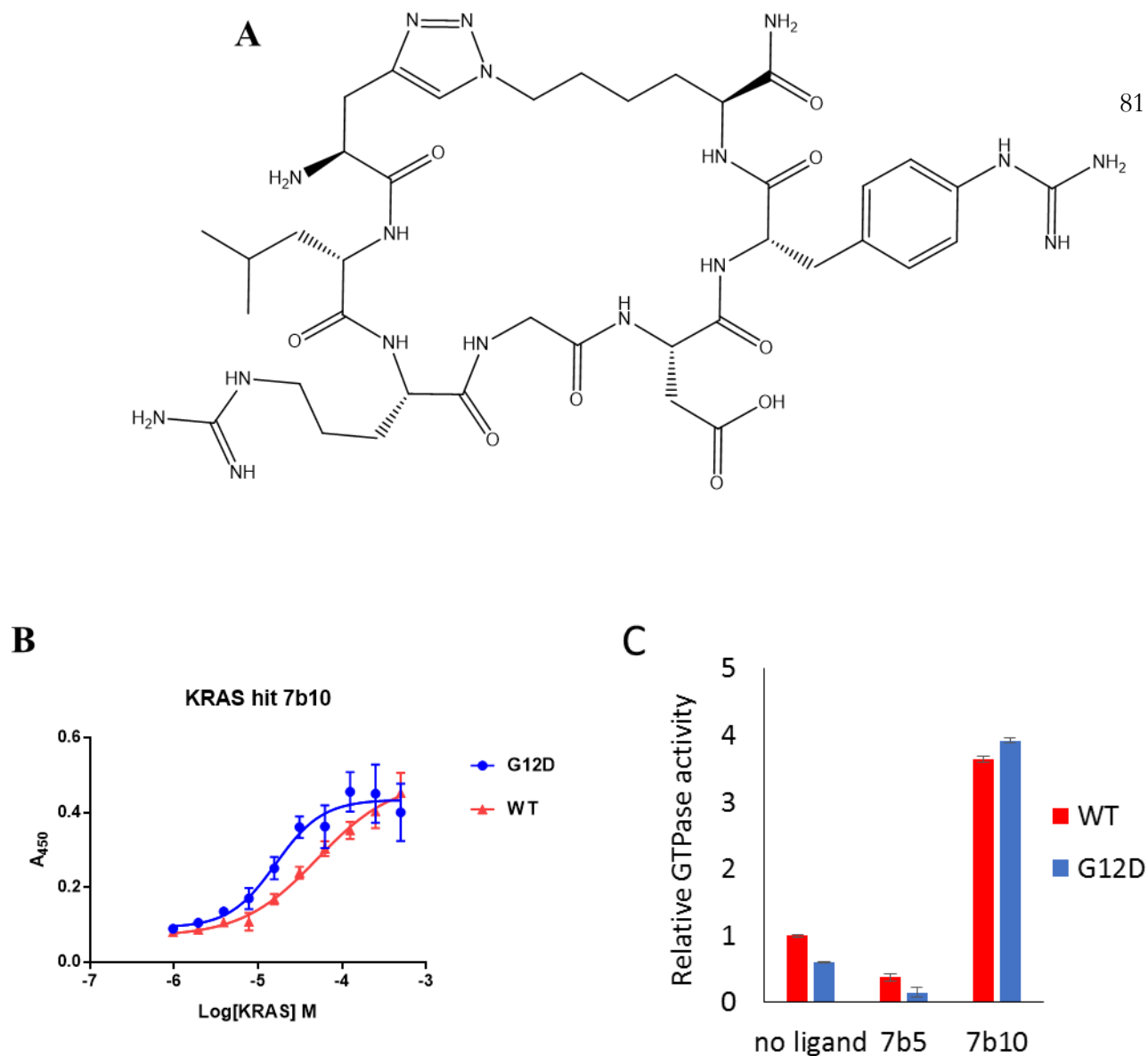


Figure 4.7 – Characterization of hit 7b10. (A) Molecular structure of hit 7b10. (B) Binding curve between hit 7b10 and K-Ras wild type and G12D obtained via ELISA assay. The peptide $EC_{50} = 17.5 \mu\text{M}$ for K-Ras^{G12D} and $EC_{50} = 55.6 \mu\text{M}$ for wild type K-Ras. (C) 7b10 increases wild type and G12D K-Ras GTPase activity nearly seven-fold.

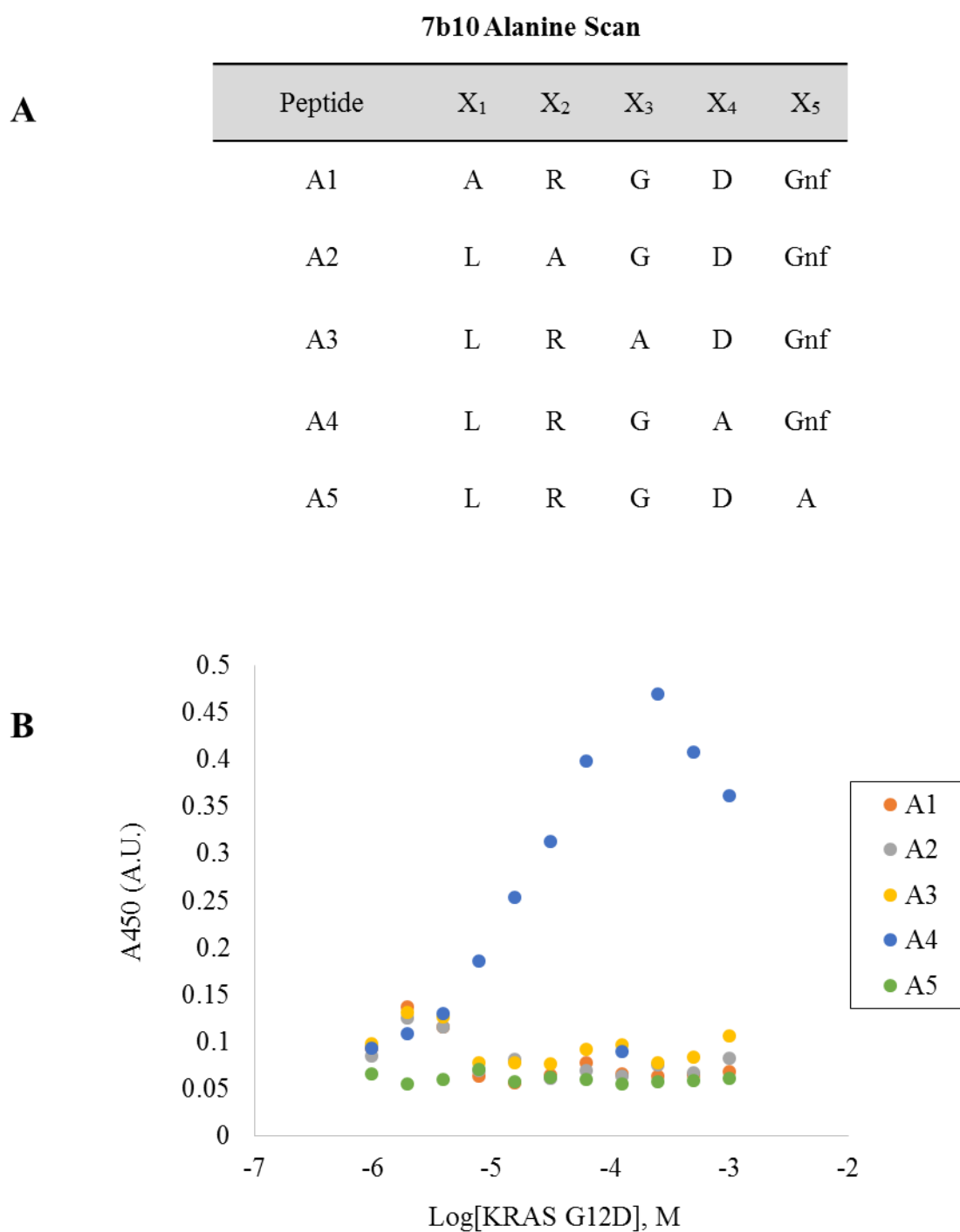


Figure 4.8 – 7b10 alanine scan. (A) Sequences of alanine-substituted peptide series (B) Binding curves between alanine scan peptides and K-Ras^{G12D} obtained via ELISA assay. Only peptide A4 maintains binding affinity for K-Ras^{G12D}.

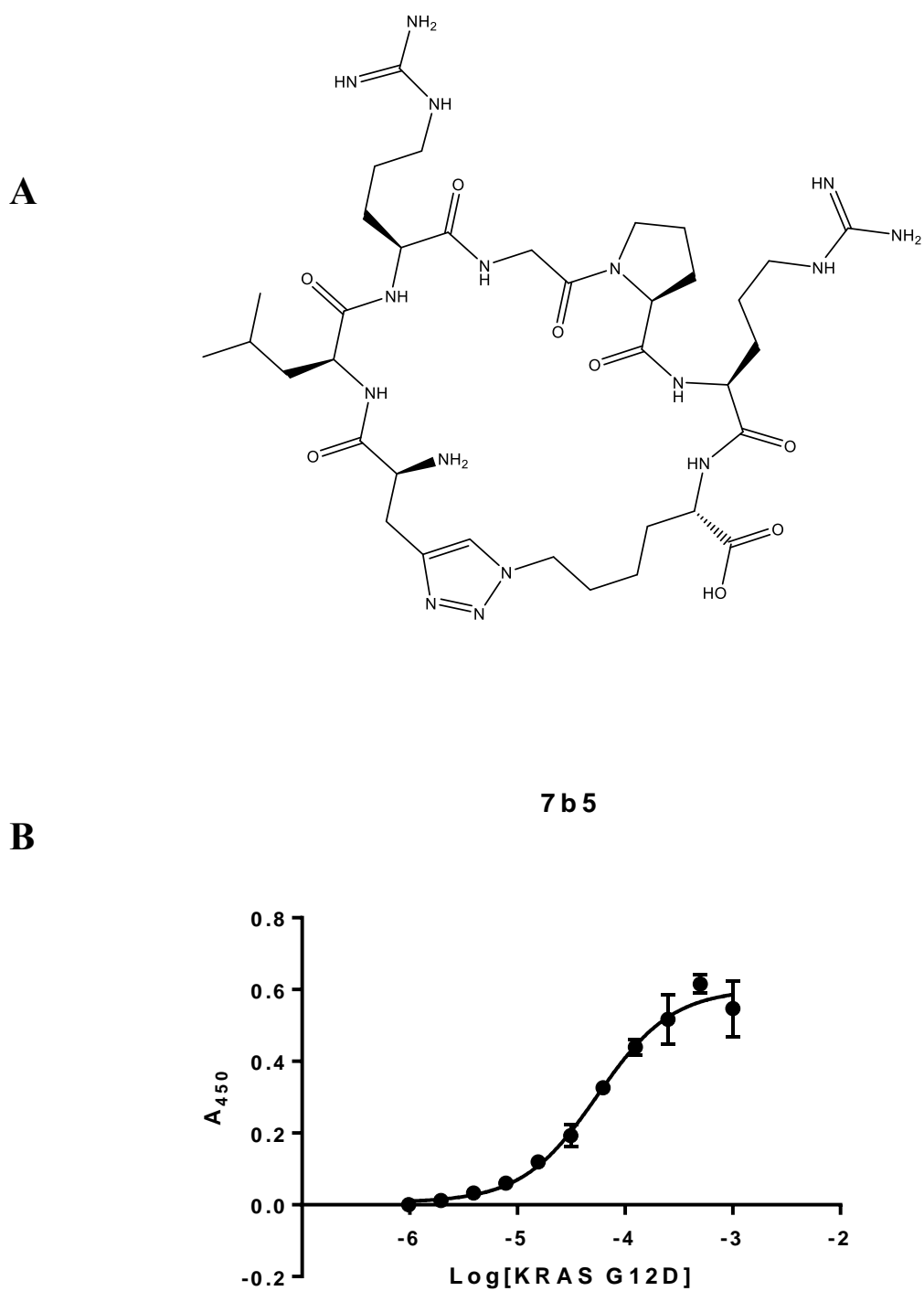


Figure 4.9 – Characterization of hit 7b5. (A) Molecular structure of hit 7b5. (B) Binding curve between hit 7b5 and K-Ras^{G12D} obtained via ELISA assay. The peptide EC₅₀ = 56.6 μM for K-Ras^{G12D}.

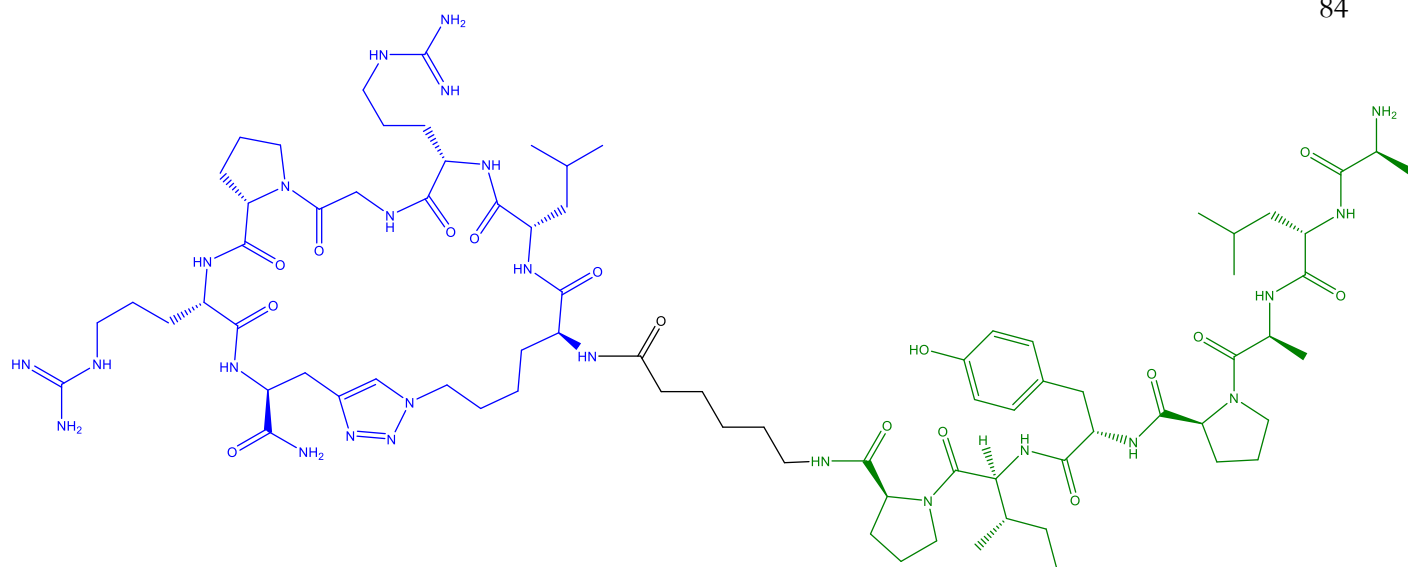


Figure 4.10 – Structure of 7b5-Hif PROTAC.

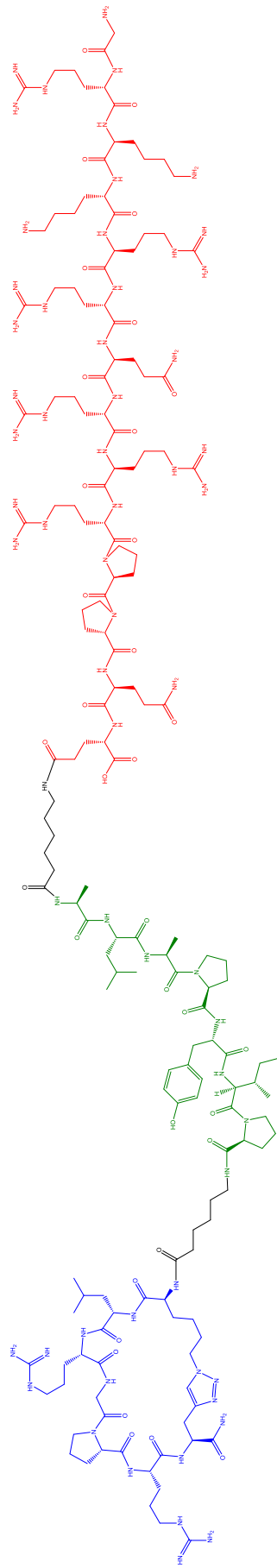


Figure 4.11 – Structure of 7b5-Hif-TAT PROTAC

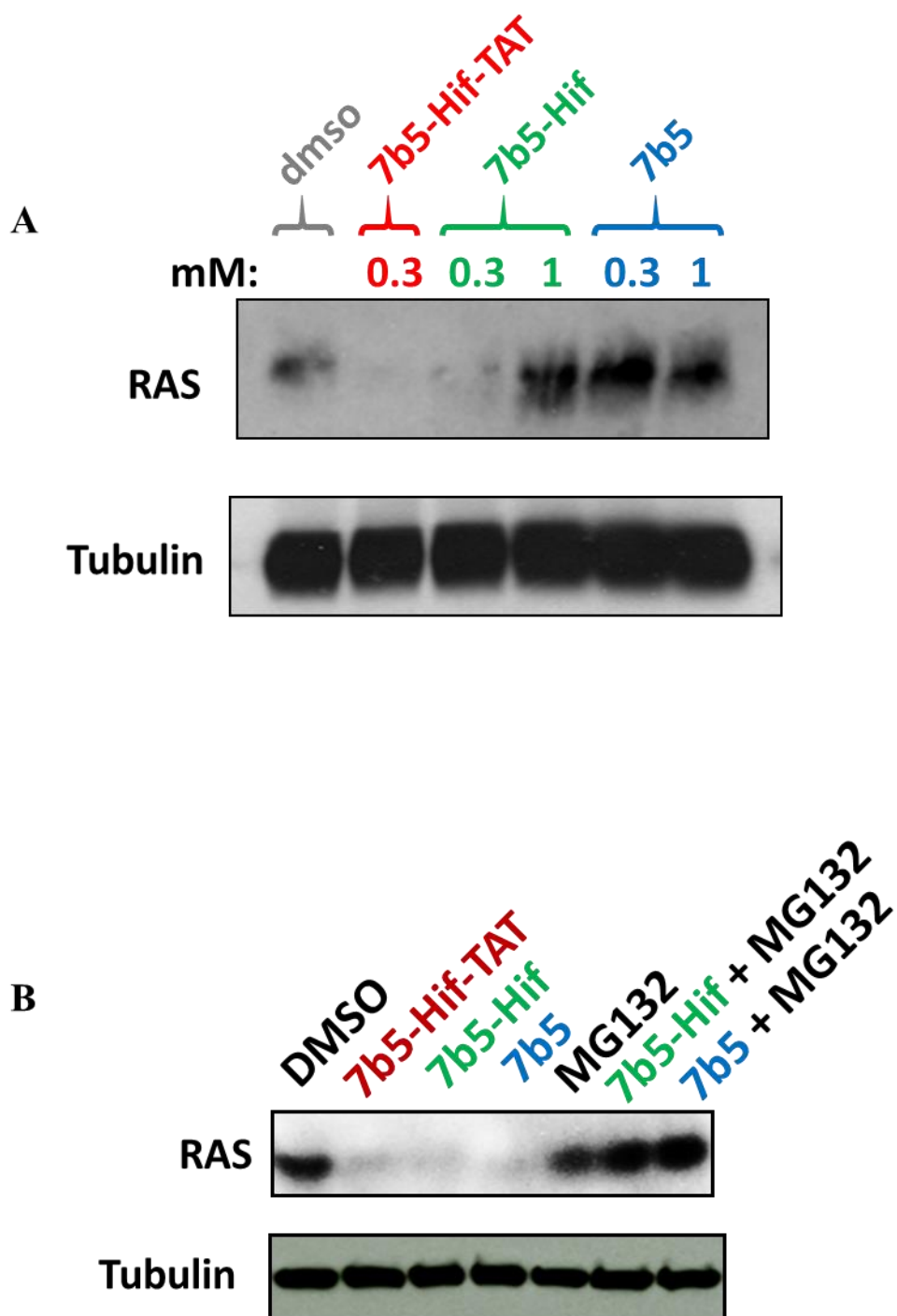


Figure 4.12 – 7b5 PROTACs induce proteasomal degradation of K-Ras^{G12D}. (A) Western blot of lysates from Panc 08.13 cells treated with either 7b5, 7b5-Hif, or 7b5-Hif-TAT. Cells were treated for 4 hours prior to lysis. (B) Western blot of lysates from Panc 08.13 cells treated with 0.3 mM 7b5, 7b5-Hif, or 7b5-Hif-TAT. Cells were also pretreated with the proteasome inhibitor MG132 and the Ras degradation was reversed.

4.7 References

1. Schubbert, S., Shannon, K. & Bollag, G. Hyperactive Ras in developmental disorders and cancer. *Nat. Rev. Cancer* **7**, 295–308 (2007).
2. Filchtinski, D. *et al.* What makes Ras an efficient molecular switch: a computational, biophysical, and structural study of Ras-GDP interactions with mutants of Raf. *J. Mol. Biol.* **399**, 422–435 (2010).
3. Downward, J. Targeting RAS signalling pathways in cancer therapy. *Nat. Rev. Cancer* **3**, 11–22 (2003).
4. Pylayeva-Gupta, Y., Grabocka, E. & Bar-Sagi, D. RAS oncogenes: weaving a tumorigenic web. *Nat. Rev. Cancer* **11**, 761–774 (2011).
5. Baines, A. T., Xu, D. & Der, C. J. Inhibition of Ras for cancer treatment: the search continues. *Future Med. Chem.* **3**, 1787–1808 (2011).
6. Ostrem, J. M., Peters, U., Sos, M. L., Wells, J. A. & Shokat, K. M. K-Ras(G12C) inhibitors allosterically control GTP affinity and effector interactions. *Nature* **503**, 548–551 (2013).
7. McCormick, F. The potential of targeting Ras proteins in lung cancer. *Expert Opin. Ther. Targets* **19**, 451–454 (2015).
8. Lito, P., Solomon, M., Li, L.-S., Hansen, R. & Rosen, N. Allele-specific inhibitors inactivate mutant KRAS G12C by a trapping mechanism. *Science* aad6204 (2016). doi:10.1126/science.aad6204
9. Bamford, S. *et al.* The COSMIC (Catalogue of Somatic Mutations in Cancer) database and website. *Br. J. Cancer* (2004). doi:10.1038/sj.bjc.6601894

10. Nag, A. *et al.* A Chemical Epitope-Targeting Strategy for Protein Capture Agents: The Serine 474 Epitope of the Kinase Akt2. *Angew. Chem. Int. Ed.* **52**, 13975–13979 (2013).
11. Das, S. *et al.* A General Synthetic Approach for Designing Epitope Targeted Macrocyclic Peptide Ligands. *Angew. Chem. Int. Ed.* **54**, 13219–13224 (2015).
12. Melo, R. L. *et al.* Human Tissue Kallikrein S1 Subsite Recognition of Non-Natural Basic Amino Acids. *Biochemistry (Mosc.)* **40**, 5226–5232 (2001).
13. Bechara, C. & Sagan, S. Cell-penetrating peptides: 20 years later, where do we stand? *FEBS Lett.* **587**, 1693–1702 (2013).
14. Crunkhorn, S. Anticancer drugs: Selectively targeting proteins for degradation. *Nat. Rev. Drug Discov.* **14**, 459–459 (2015).
15. Hines, J., Gough, J. D., Corson, T. W. & Crews, C. M. Posttranslational protein knockdown coupled to receptor tyrosine kinase activation with phosphoPROTACs. *Proc. Natl. Acad. Sci.* **110**, 8942–8947 (2013).
16. Bamford, S. *et al.* The COSMIC (Catalogue of Somatic Mutations in Cancer) database and website. *Br. J. Cancer* **91**, 355–358 (2004).
17. Targeting KRAS in GI Cancers: The Hunt for the Holy Grail in Cancer Research - The ASCO Post. Available at: <http://www.ascopost.com/issues/april-15-2012/targeting-kras-in-gi-cancers-the-hunt-for-the-holy-grail-in-cancer-research.aspx>. (Accessed: 1st May 2016)

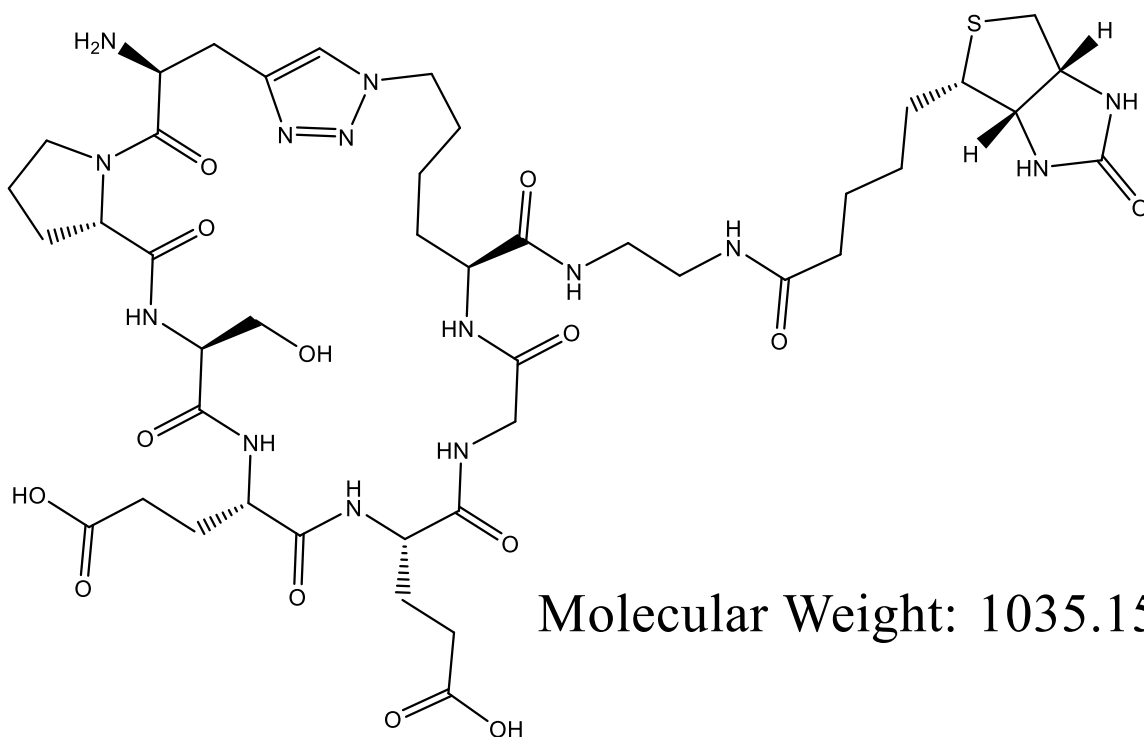
Appendix A

SUPPLEMENTARY INFORMATION FOR CHAPTER 4

A.1 Structure and Characterization of Synthetic Epitopes used in Anchor Screen

Hit 2: Pra-PSEEG-Az4-Biotin

93



Molecular Weight: 1035.15

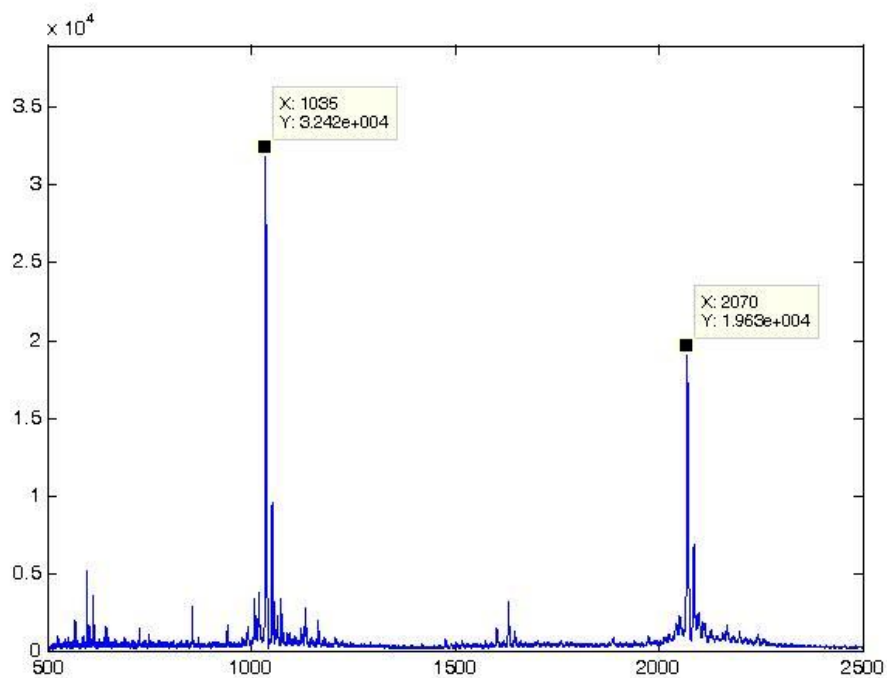


Figure A4 – Structure and characterization of hit 2: PSEEG. MALDI-TOF MS:
Expected [M+H]⁺ = 1036.15, Observed [M+H]⁺ = 1035.

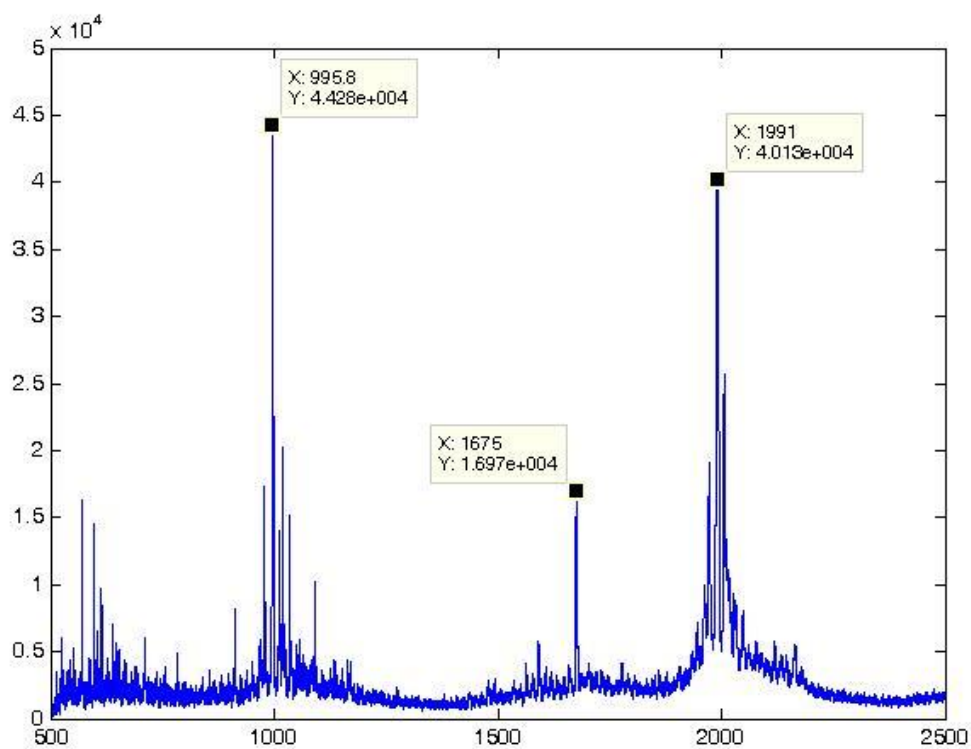
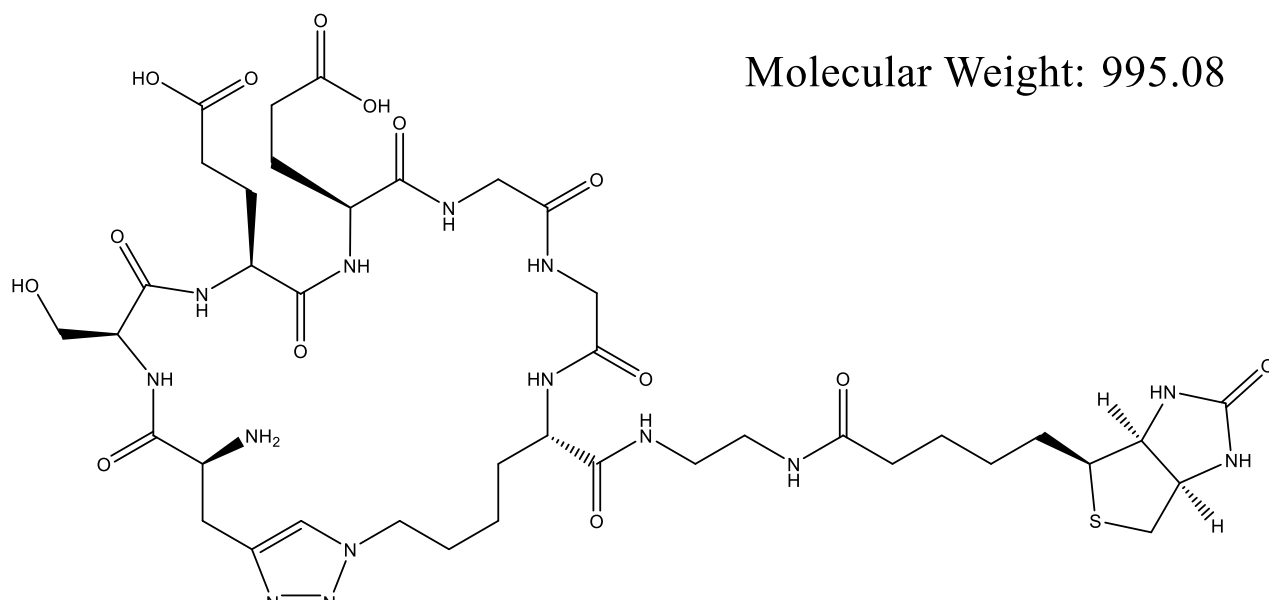
Hit 3: Pra-SEEGG-Az4-Biotin

Figure A5 – Structure and characterization of hit 3: SEEGG. MALDI-TOF MS:
Expected $[M+H]^+$ = 996.08, Observed $[M+H]^+$ = 995.8.

Hit 5: Pra-YEQGE-Az4-Biotin

Molecular Weight: 1142.26

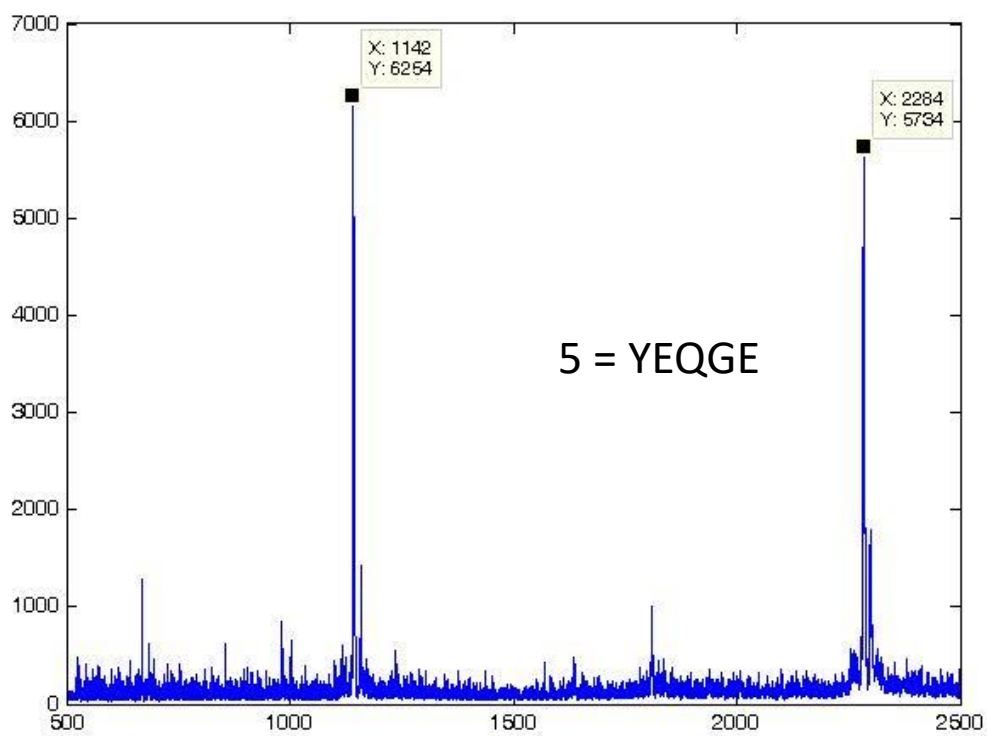
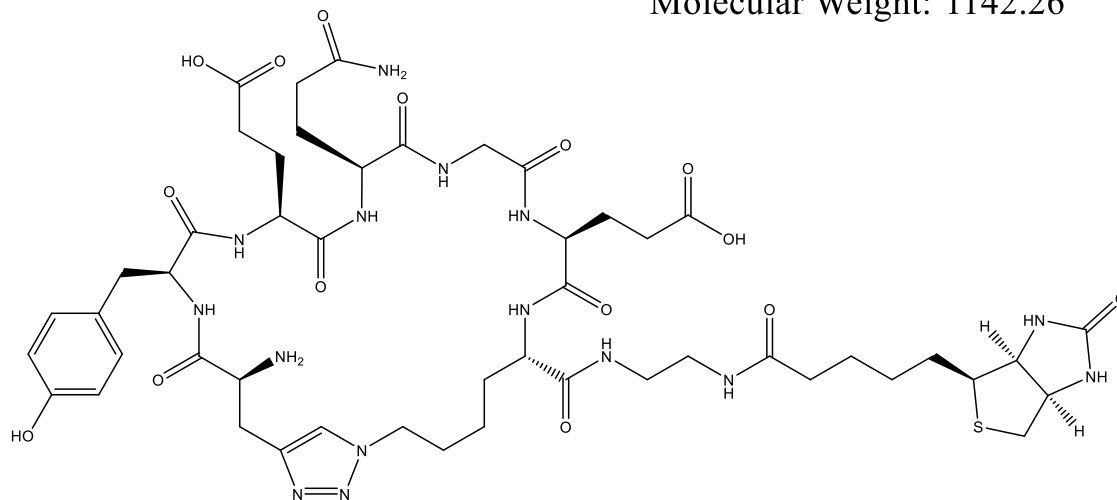


Figure A6 – Structure and characterization of hit 5: YEQGE. MALDI-TOF MS: Expected $[M+H]^+ = 1143.26$, Observed $[M+H]^+ = 1142$.

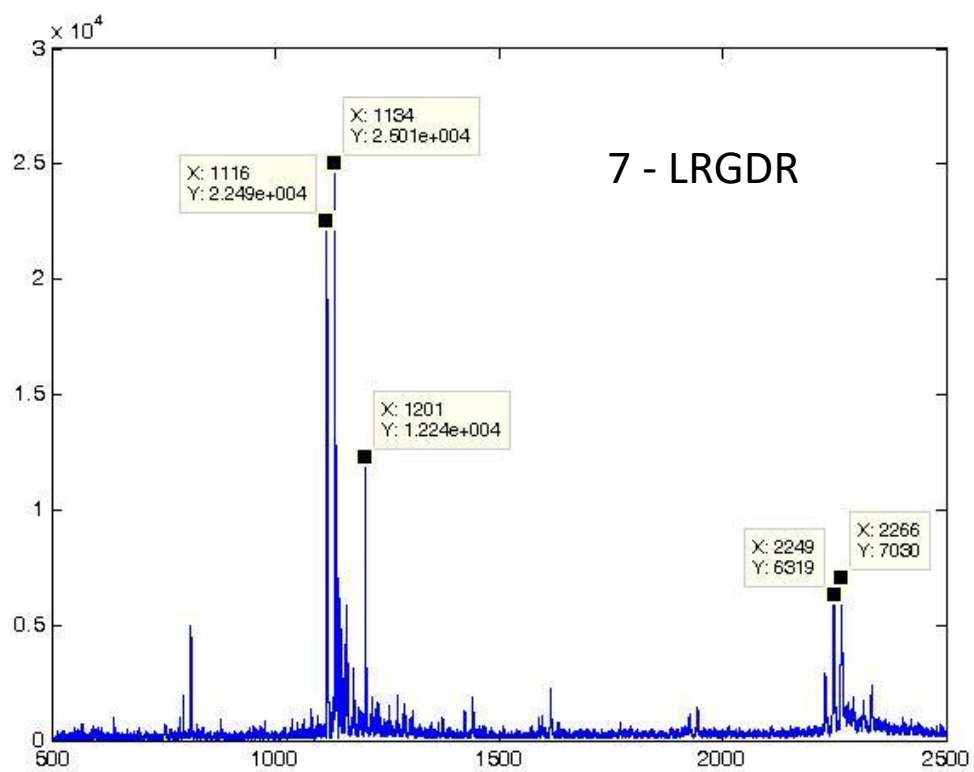
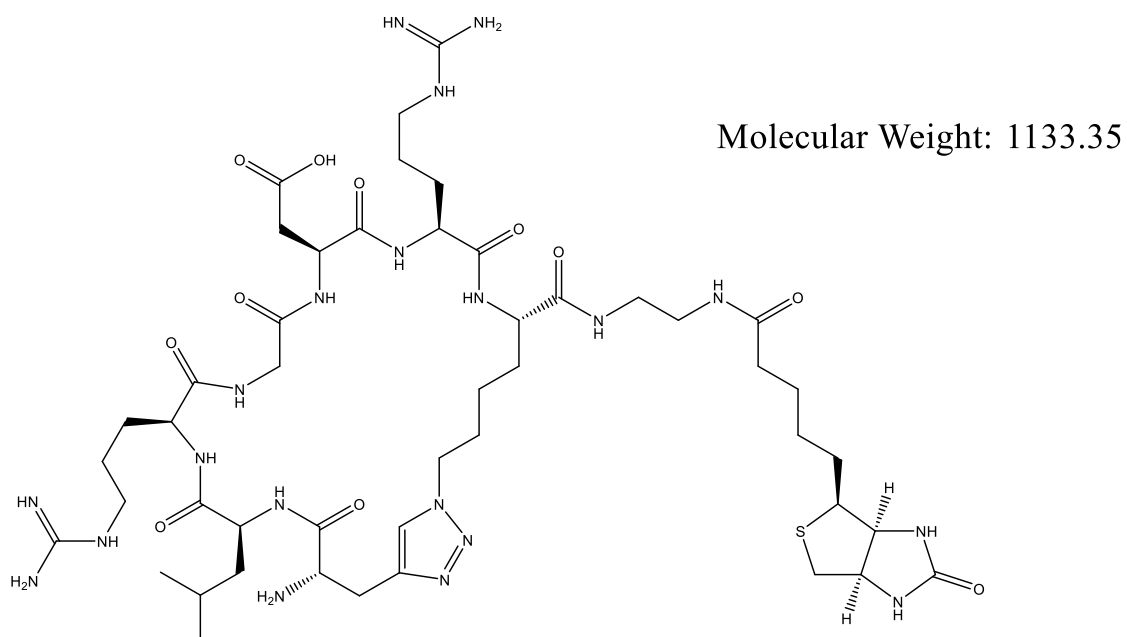
Hit 7: Pra-LRGDR-Az4-Biotin

Figure A8 – Structure and characterization of hit 7: LRGDR. MALDI-TOF MS: Expected $[M+H]^+ = 1134.35$, Observed $[M+H]^+ = 1134$.

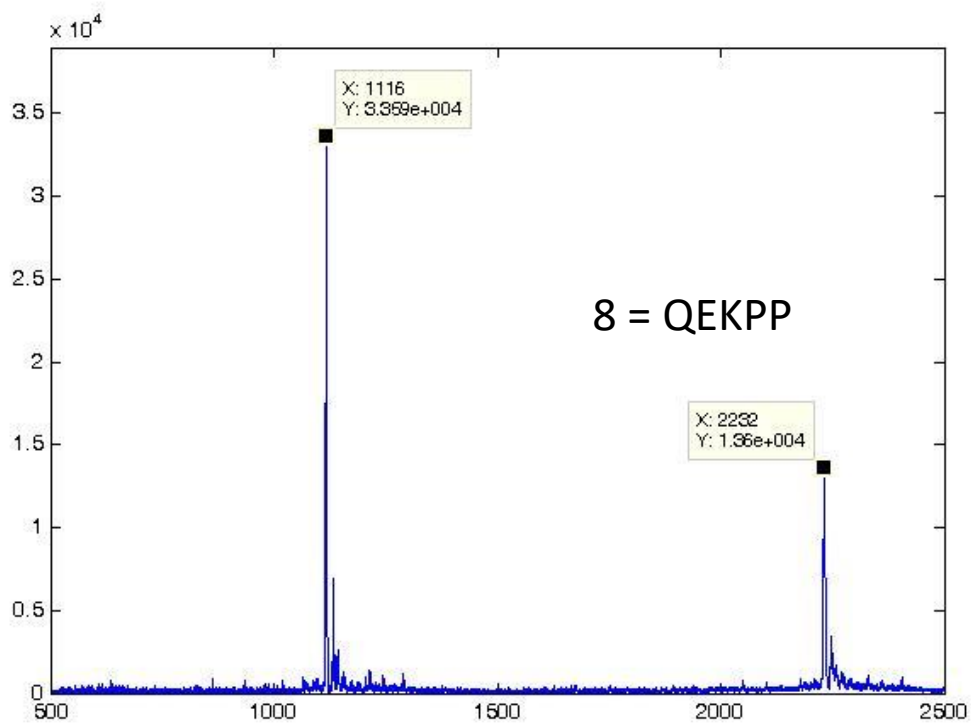
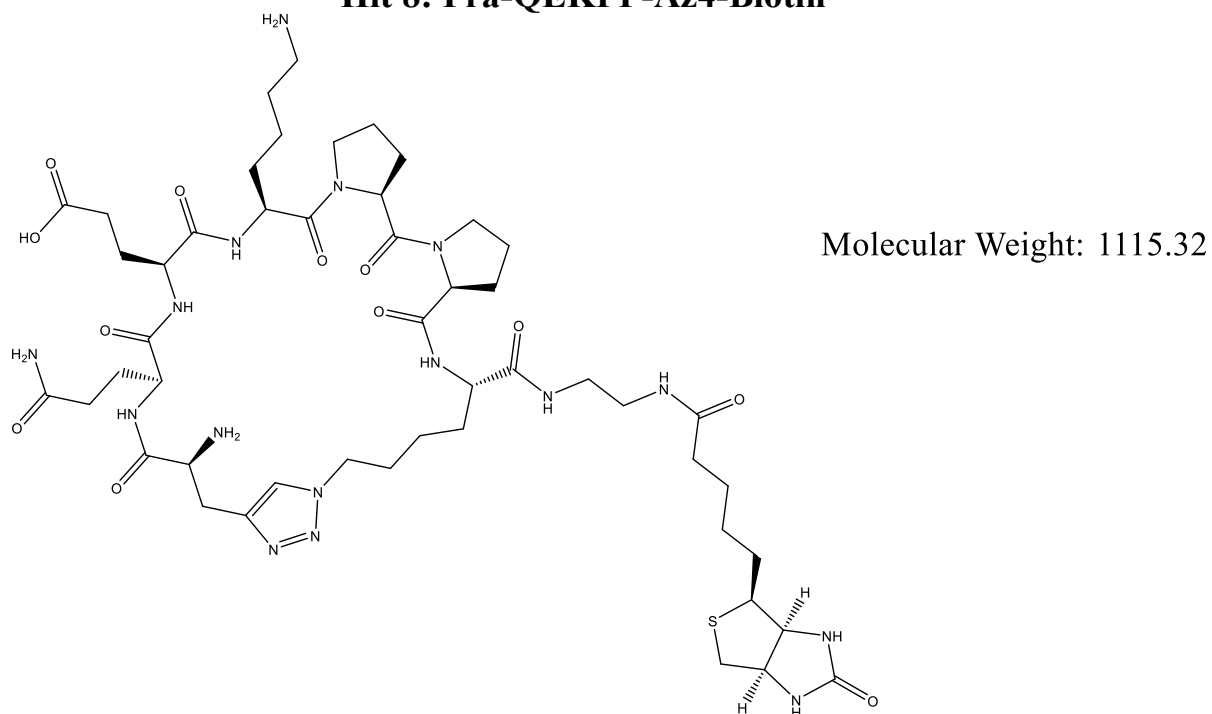
Hit 8: Pra-QEKPP-Az4-Biotin

Figure A9 – Structure and characterization of hit 8: QEKPP. MALDI-TOF MS:
Expected $[M+H]^+ = 1116.32$, Observed $[M+H]^+ = 1116$.

Hit 9: Pra-ELTFG-Az4-Biotin

Molecular Weight: 1083.28

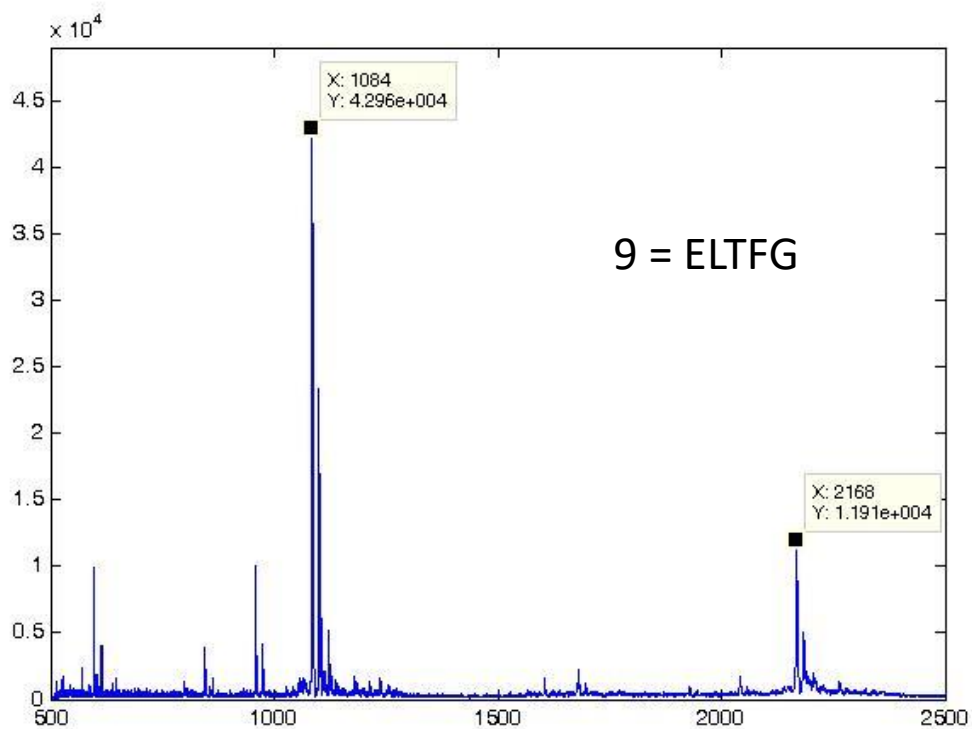
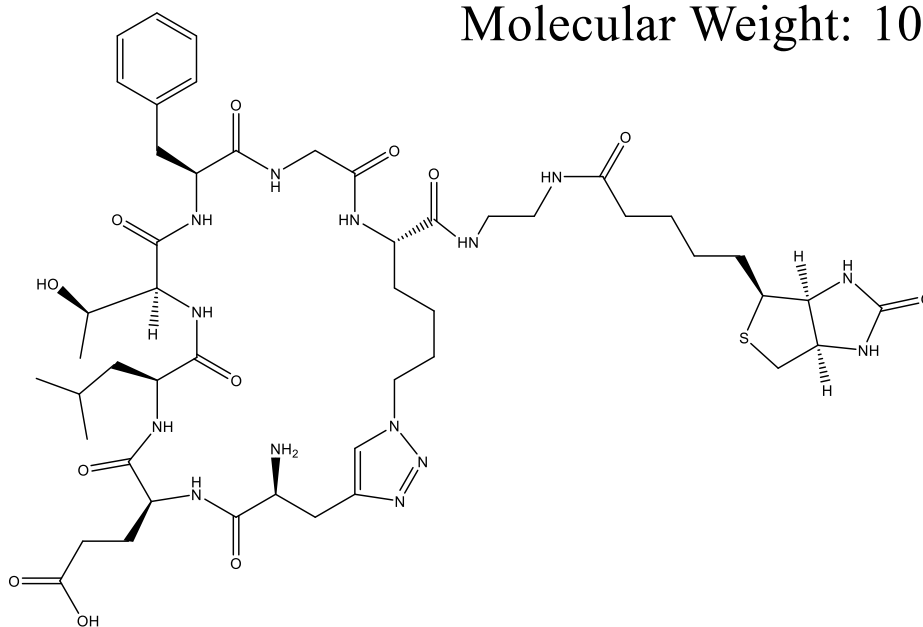


Figure A10 – Structure and characterization of hit 9: ELTFG. MALDI-TOF MS:
Expected $[M+H]^+ = 1084.28$, Observed $[M+H]^+ = 1084$.

A.3 STRUCTURE AND CHARACTERIZATION OF SECOND GENERATION HIT PEPTIDES

7b1: Pra-LRGDR-Az4-PEG₅-Biotin

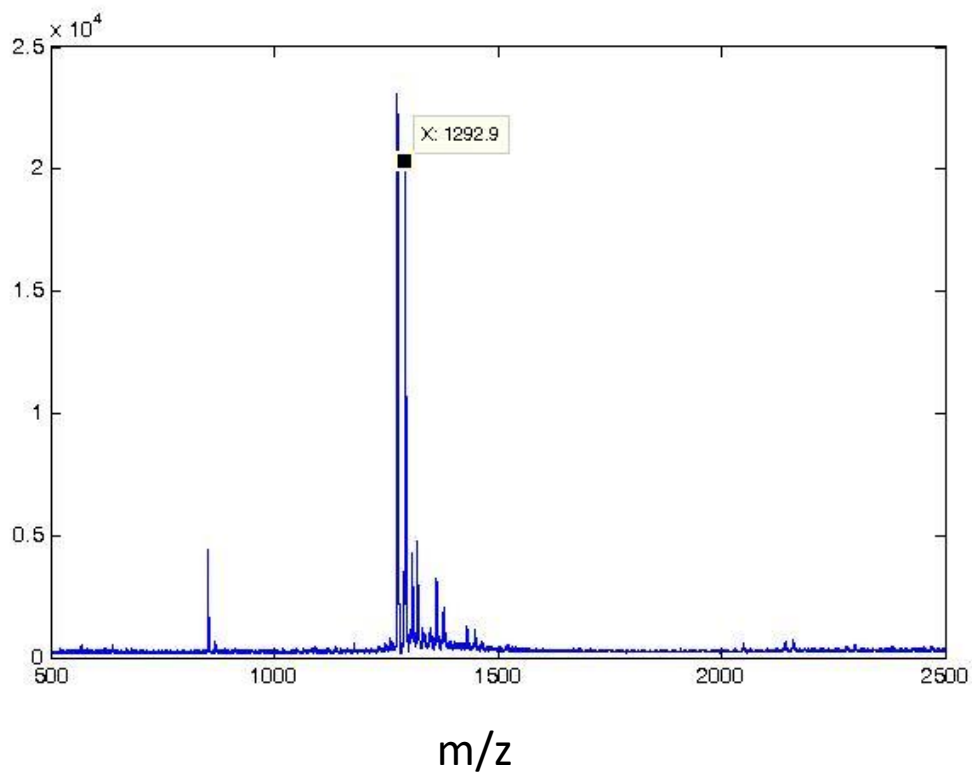
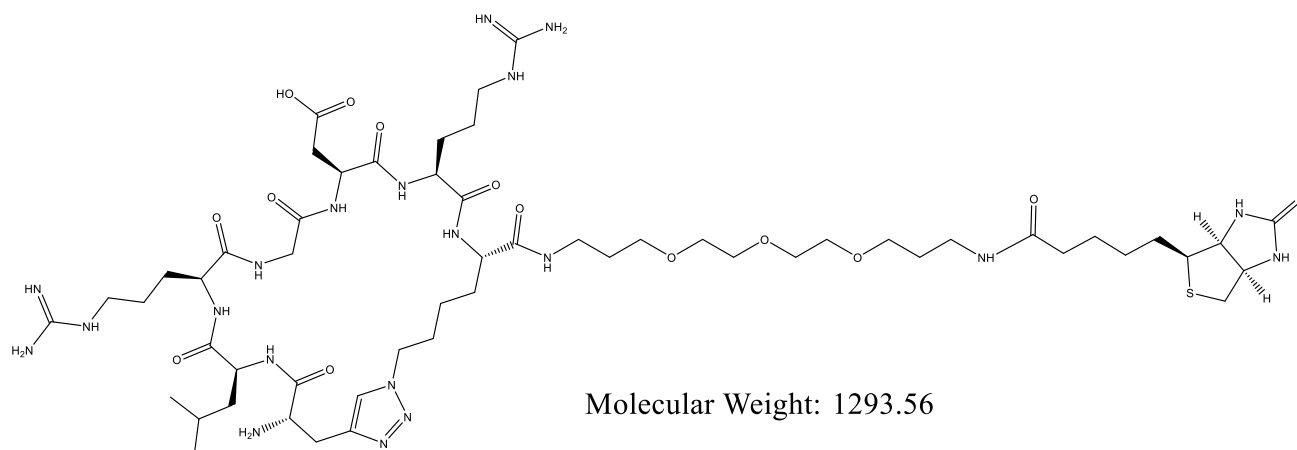


Figure A11 - Structure and characterization of peptide 7b1. The peptide sequence is Pra-LRGDR-Az4-PEG₅-Biotin with a 1,4-triazole linkage between Pra and Az4. MALDI-TOF MS: Expected $[M+H]^+$ = 1294.6, Observed $[M+H]^+$ = 1292.9

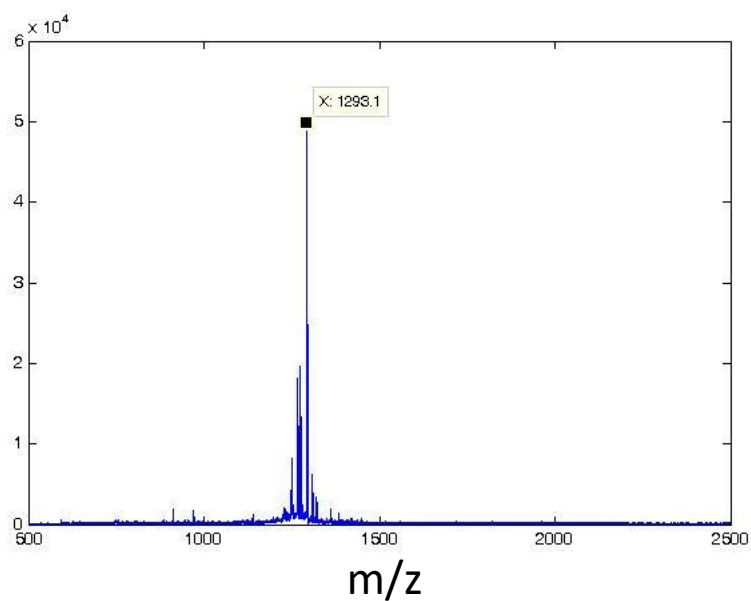
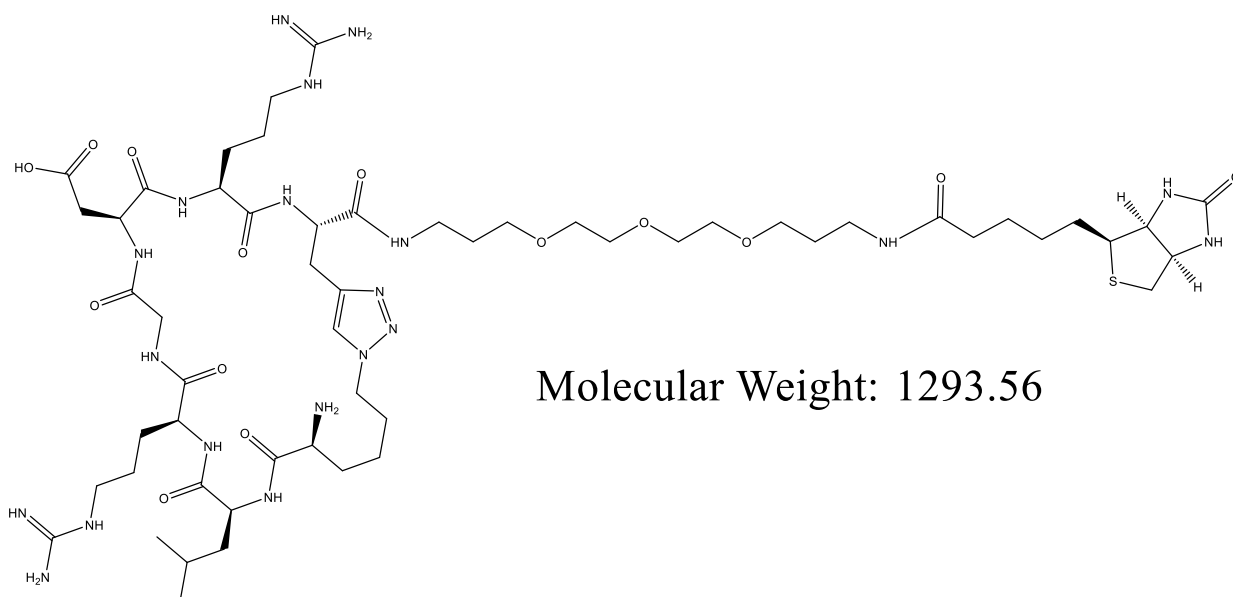
7b2: Az4-LRGDR-Pra-PEG₅-Biotin

Figure A12 - Structure and characterization of peptide 7b2. The peptide sequence is Az4-LRGDR-Pra-PEG₅-Biotin with a 1,4-triazole linkage between Az4 and Pra. MALDI-TOF MS: Expected $[M+H]^+ = 1294.6$, Observed $[M+H]^+ = 1293.1$

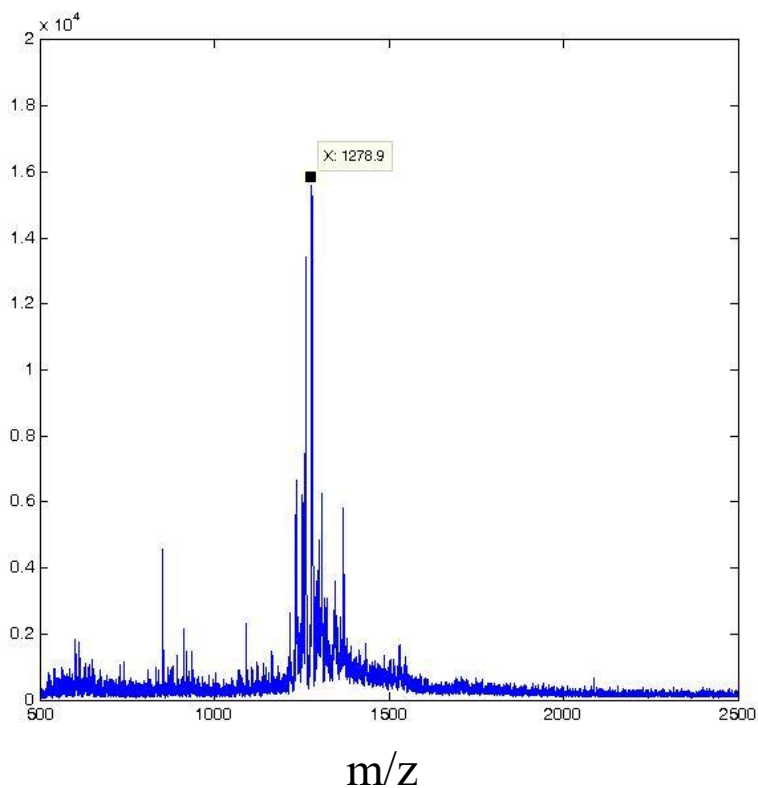
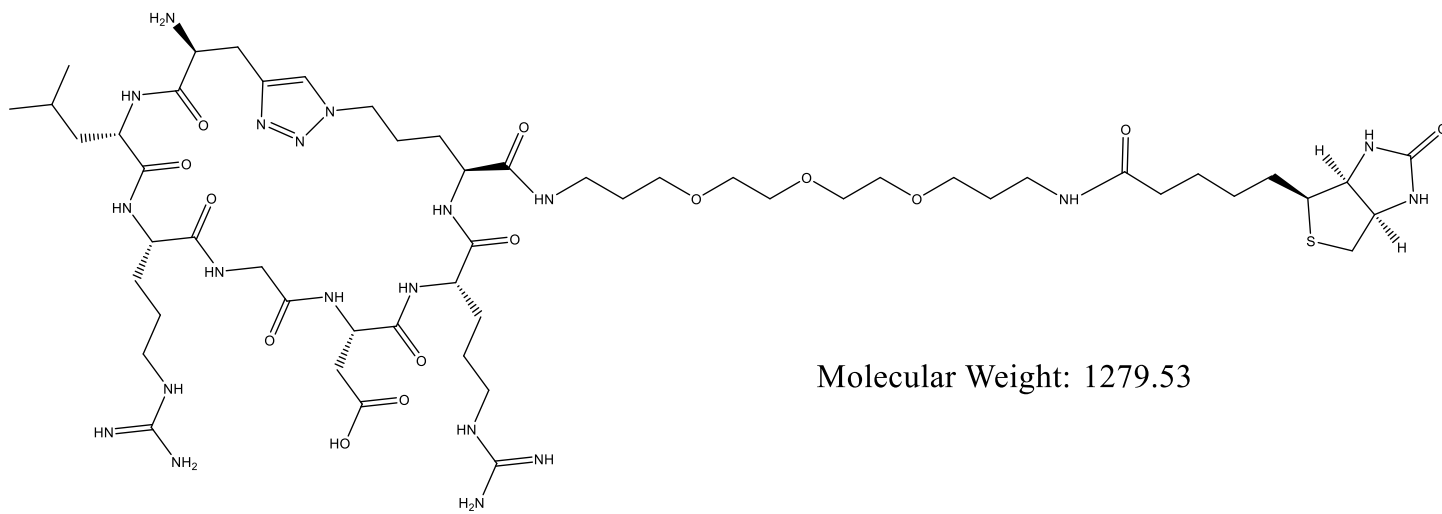
7b3: Pra-LRGDR-Az3-PEG₅-Biotin

Figure A13 - Structure and characterization of peptide 7b3. The peptide sequence is Pra-LRGDR-Az3-PEG₅-Biotin with a 1,4-triazole linkage between Pra and Az3. MALDI-TOF MS: Expected $[M+H]^+ = 1280.5$, Observed $[M+H]^+ = 1278.9$

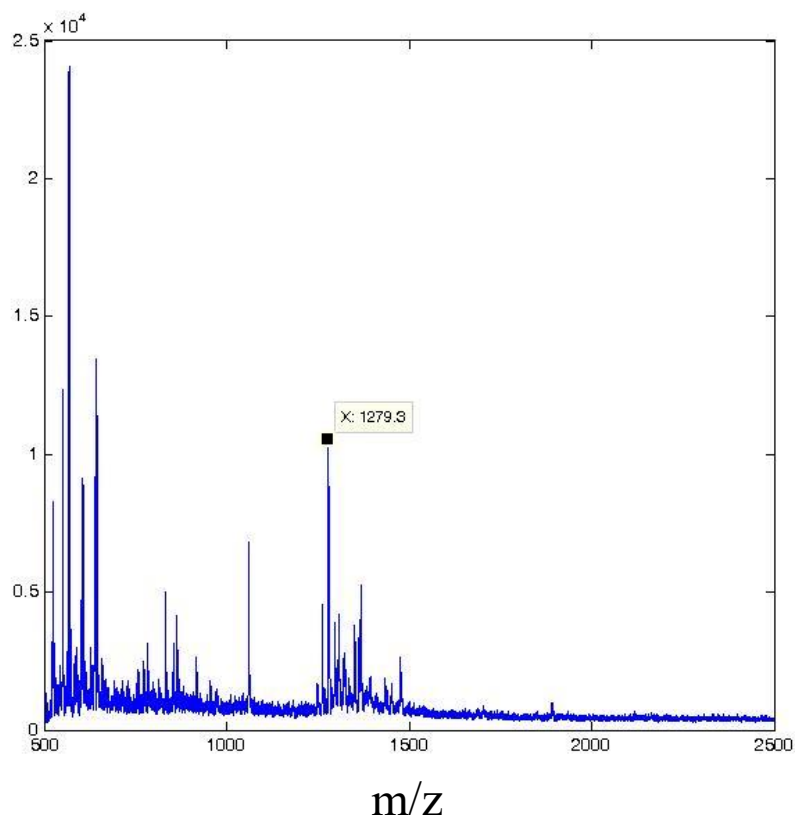
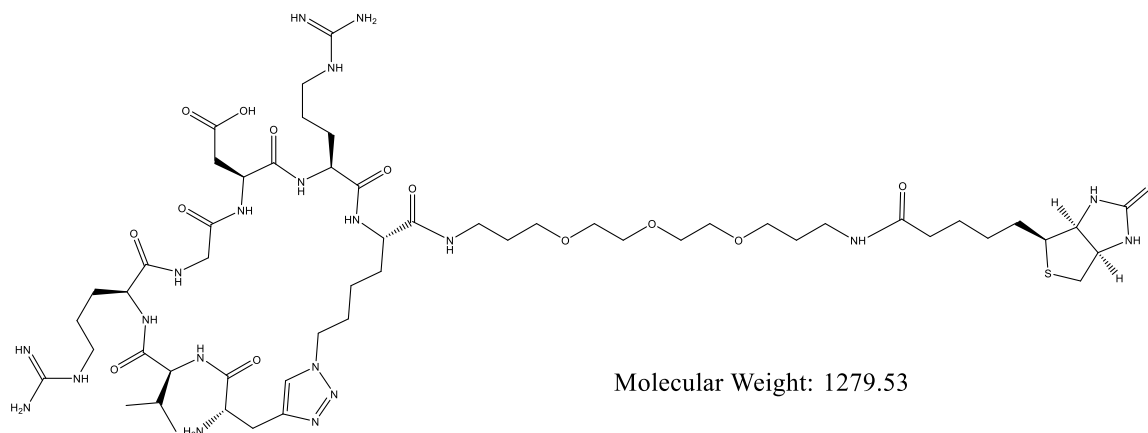
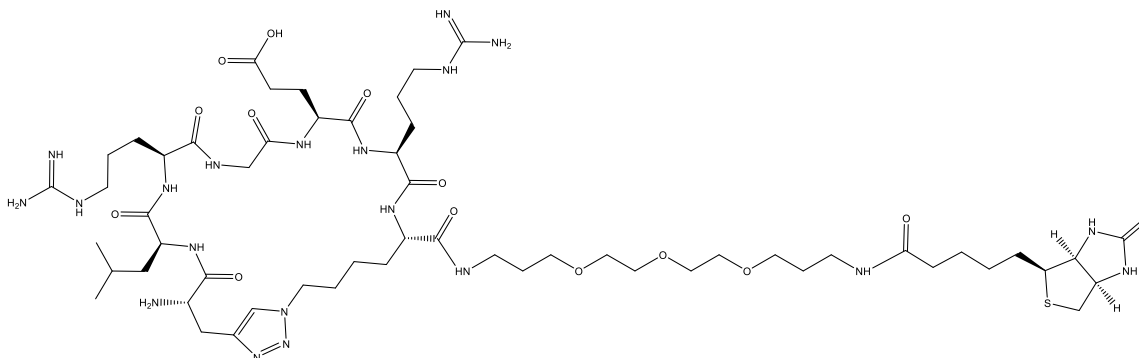
7b4: Pra-VRGDR-Az4-PEG₅-Biotin

Figure A14 - Structure and characterization of peptide 7b4. The peptide sequence is Pra-VRGDR-Az4-PEG₅-Biotin with a 1,4-triazole linkage between Pra and Az4. MALDI-TOF MS: Expected $[M+H]^+ = 1280.5$, Observed $[M+H]^+ = 1279.3$

7b6: Pra-LRGER-Az4-PEG₅-Biotin

Molecular Weight: 1307.59

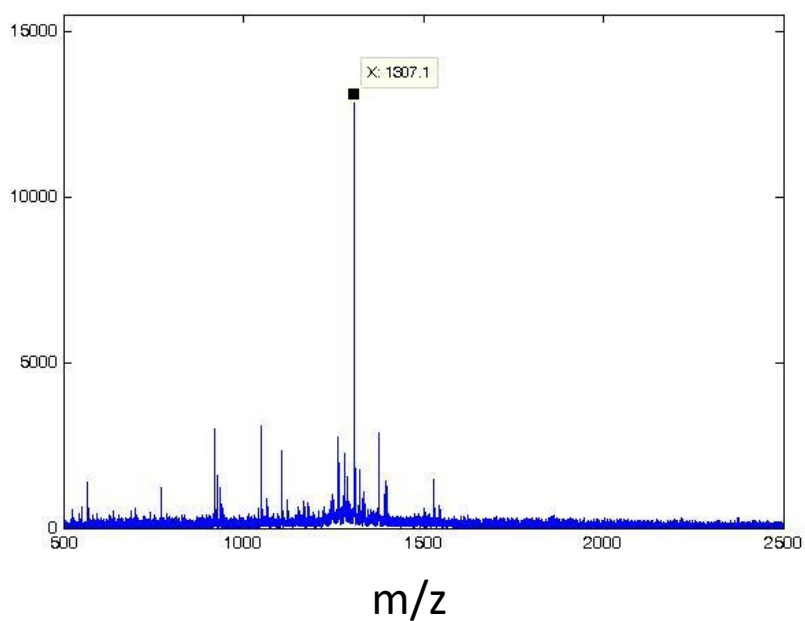


Figure A16 - Structure and characterization of peptide 7b6. The peptide sequence is Pra-LRGER-Az4-PEG₅-Biotin with a 1,4-triazole linkage between Pra and Az4. MALDI-TOF MS: Expected $[M+H]^+ = 1308.6$, Observed $[M+H]^+ = 1307.1$

7b7: Pra-Leu-Homoarginine-Gly-Asp-Arg-Az4-PEG₅-Biotin

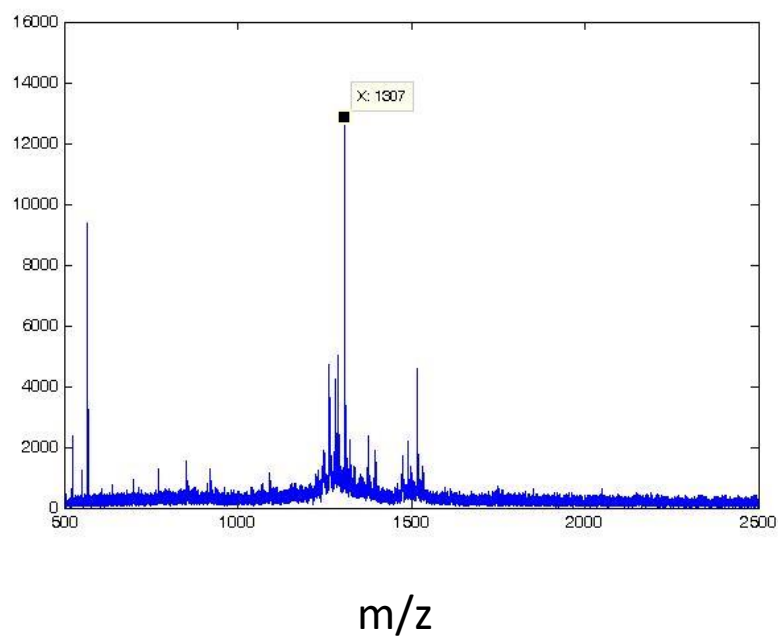
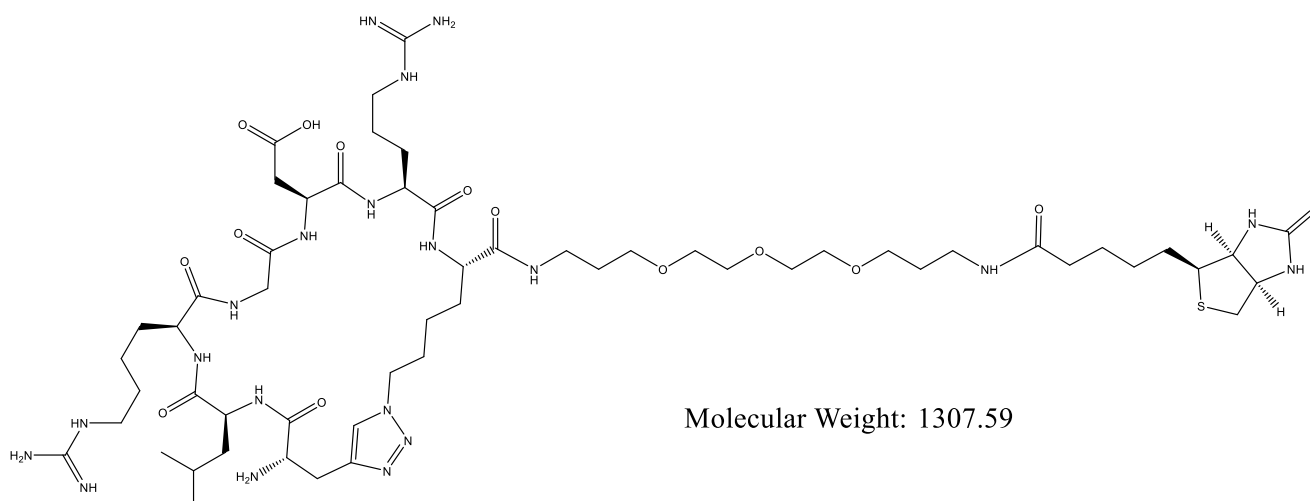
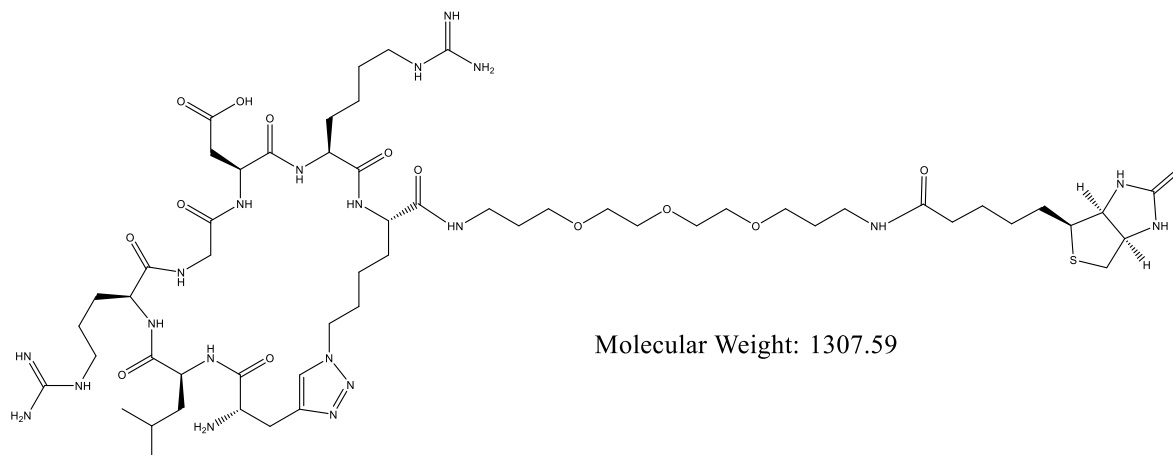


Figure A17 - Structure and characterization of peptide 7b7. The peptide sequence is Pra-L[Homoarginine]GDR-Az4-PEG₅-Biotin with a 1,4-triazole linkage between Pra and Az4. MALDI-TOF MS: Expected $[M+H]^+ = 1308.6$, Observed $[M+H]^+ = 1307.0$

7b8: Pra-Leu-Arg-Gly-Asp-Homoarginine-Az4-PEG₅-Biotin

Molecular Weight: 1307.59

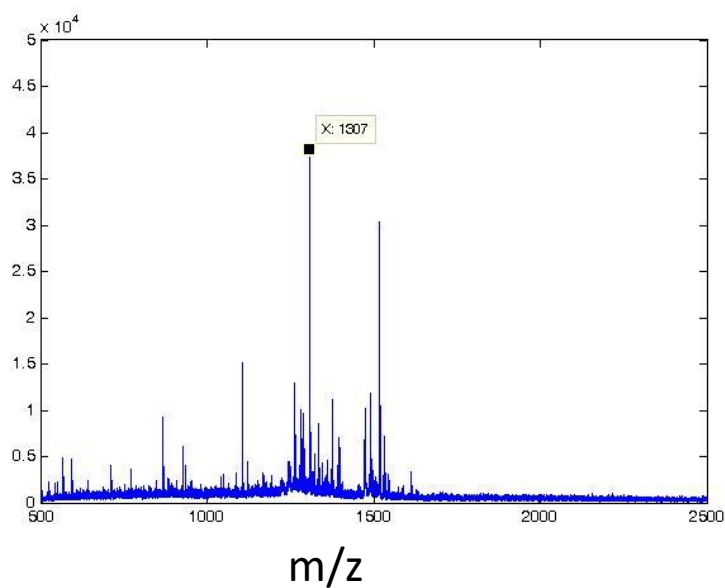


Figure A18 - Structure and characterization of peptide 7b8. The peptide sequence is Pra-LRGD[Homoarginine]-Az4-PEG₅-Biotin with a 1,4-triazole linkage between Pra and Az4. MALDI-TOF MS: Expected $[M+H]^+ = 1308.6$, Observed $[M+H]^+ = 1307.0$

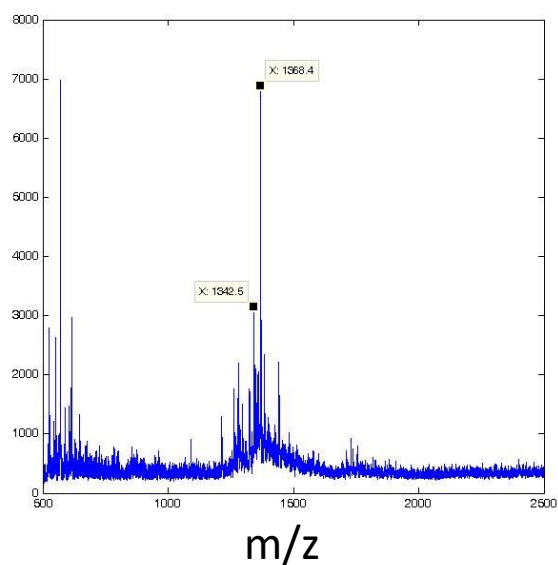
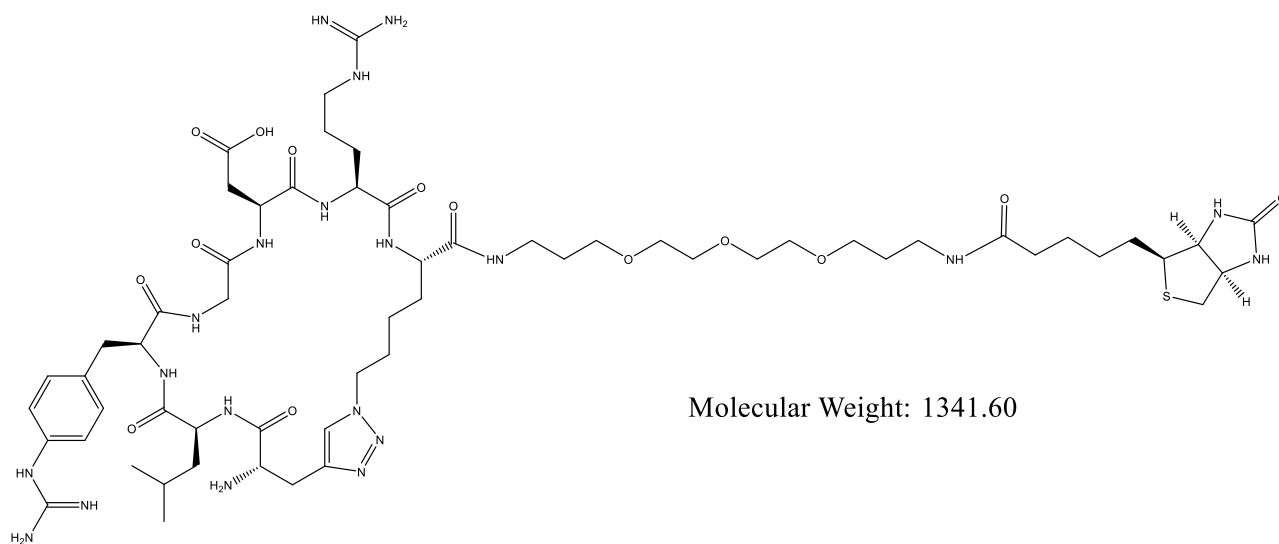
7b9: Pra-Leu-Guanidinophenylalanine-Glv-Asn-Arg-Az4-PEG₅-Biotin

Figure A19 - Structure and characterization of peptide 7b9. The peptide sequence is Pra-L[Guanidinophenylalanine]GDR-Az4-PEG₅-Biotin with a 1,4-triazole linkage between Pra and Az4. MALDI-TOF MS: Expected [M+H]⁺ = 1342.6, Observed [M+H]⁺ = 1342.5

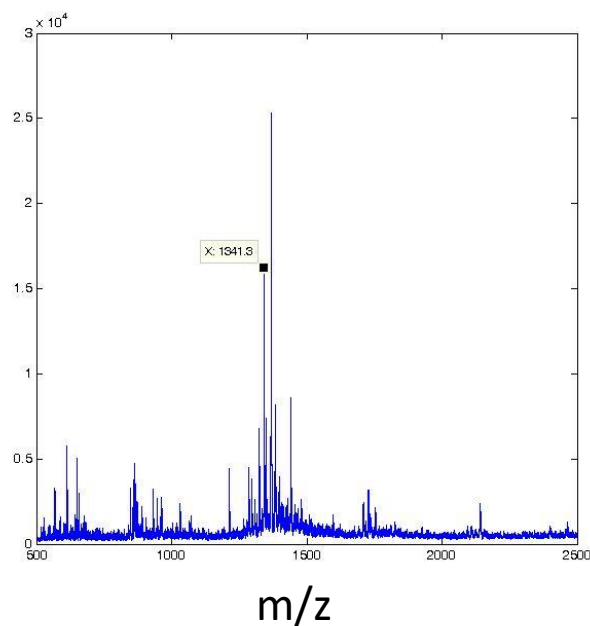
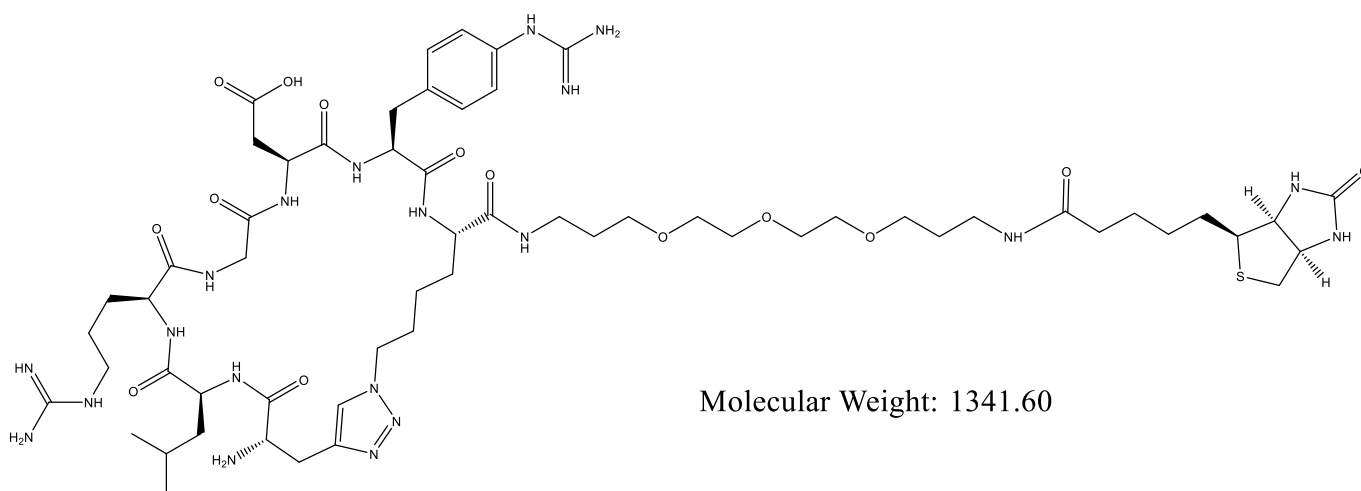
7b10: Pra-Leu-Arg-Gly-Asp-Guanidionphenylalanine-Az4-PEG₅-Biotin

Figure A20 - Structure and characterization of peptide 7b10 .The peptide sequence is Pra-LRGD[Guanidinophenylalanine] -Az4-PEG₅-Biotin with a 1,4-triazole linkage between Pra and Az4. MALDI-TOF MS: Expected $[M+H]^+$ = 1342.6, Observed $[M+H]^+$ = 1341.3

7b11: Pra-LRGNR-Az4-PEG₅-Biotin

110

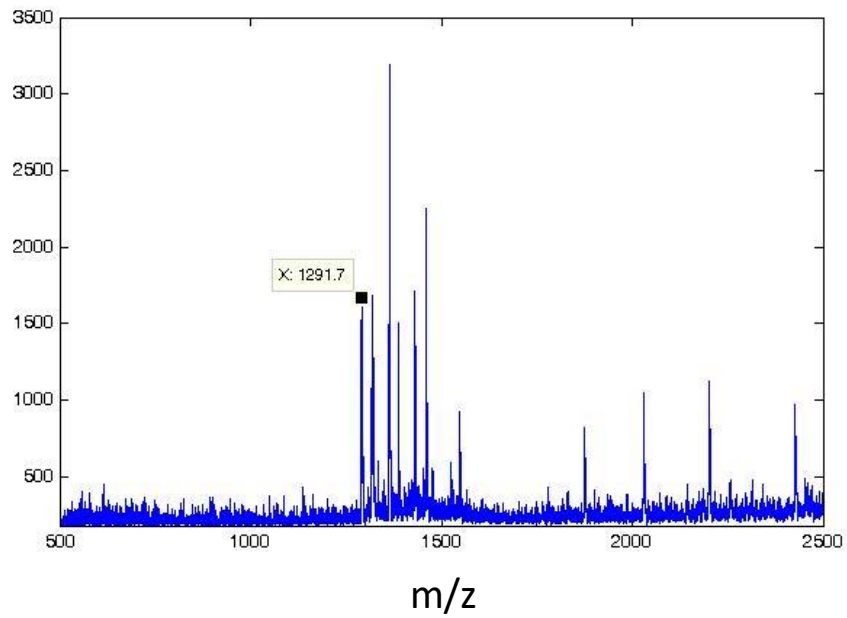
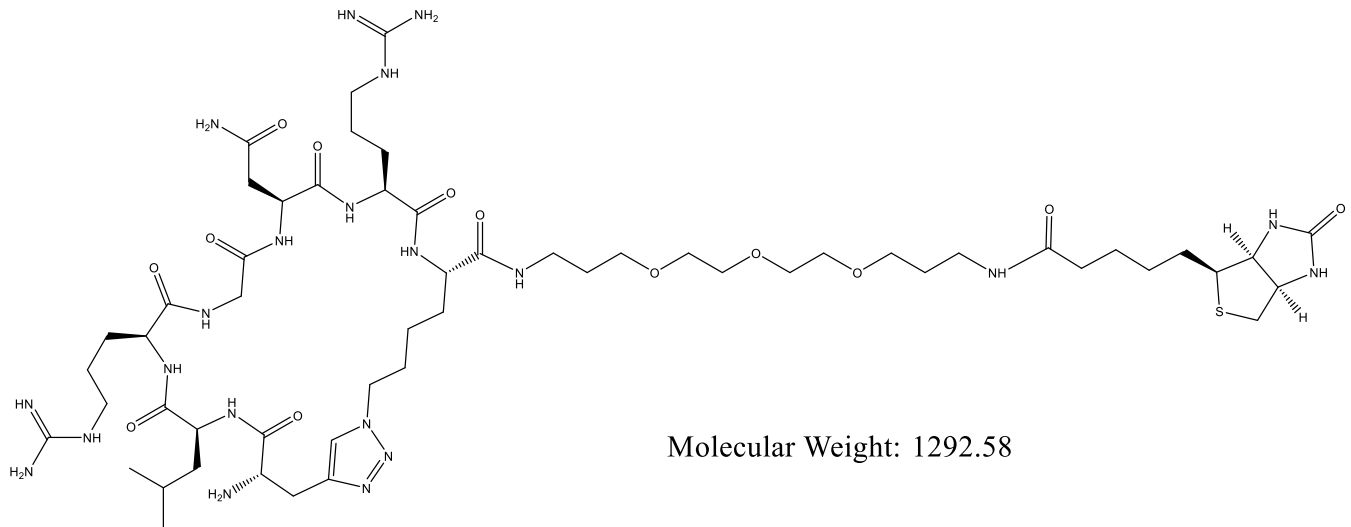


Figure A21 - Structure and characterization of peptide 7b11. The peptide sequence is Pra-LRGNR-Az4-PEG₅-Biotin with a 1,4-triazole linkage between Pra and Az4. MALDI-TOF MS: Expected $[M+H]^+ = 1293.6$, Observed $[M+H]^+ = 1291.7$

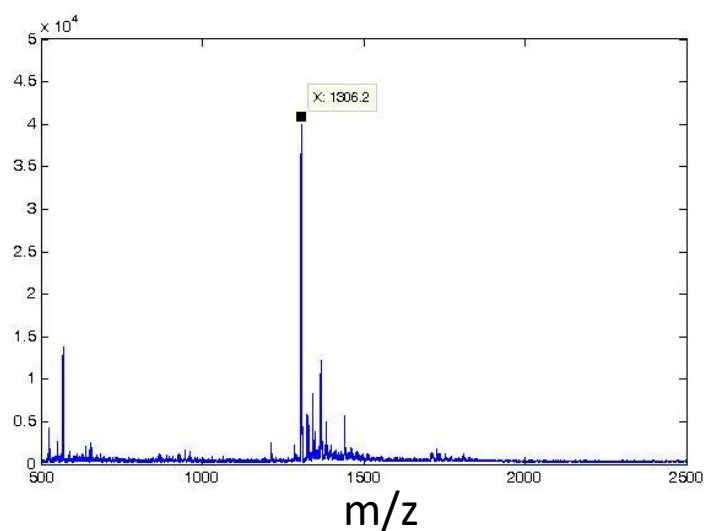
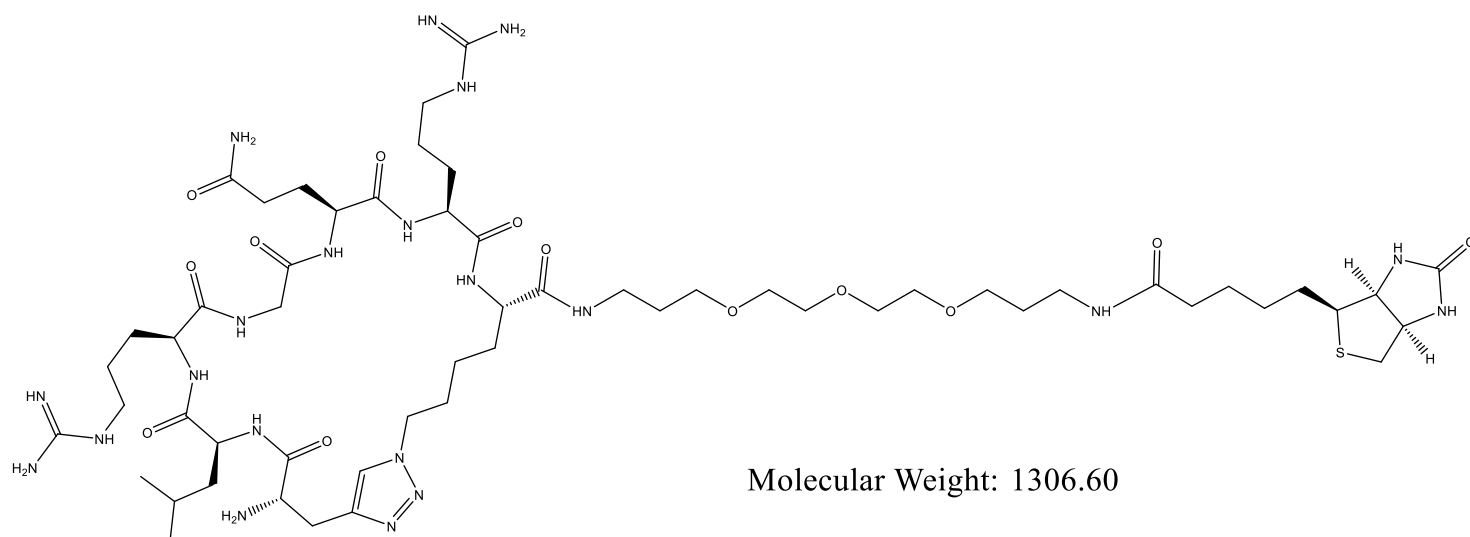
7b12: Pra-LRGQR-Az4-PEG₅-Biotin

Figure A22 - Structure and characterization of peptide 7b12. The peptide sequence is Pra-LRGQR-Az4-PEG₅-Biotin with a 1,4-triazole linkage between Pra and Az4. MALDI-TOF MS: Expected $[M+H]^+ = 1307.6$, Observed $[M+H]^+ = 1306.2$